JIMMA UNIVERSITY

SCHOOL OF GRADUATE STUDIES

JIMMA INSTITUTE OF TECHNOLOGY

FACULTY OF MECHANICAL ENGINEERING

Post Graduate Program

(MSc Thermal System Engineering)

Design, Performance Analysis, Optimization and CFD Simulation of Indirect Type Forced Solar Coffee Dryer

BY

GADISA DESA

A RESEARCH PROPOSAL SUBMITTED TO THE FACULTY OF MECHANICAL ENGINEERING, JIMMA INSTITUTE OF TECHNOLOGY, JIMMA UNIVERSITY.

September, 2017

JIMMA, ETHIOPIA

JIMMA UNIVERSITY

SCHOOL OF GRADUATE STUDIES

JIMMA INSTITUTE OF TECHNOLOGY

FACULTY OF MECHANICAL ENGINEERING

Post Graduate Program

(MSc Thermal System Engineering)

Design, Performance Analysis, Optimization and CFD Simulation of Indirect Type Forced Solar Coffee Dryer

By:

GADISA DESA

ADVISOR: prof.Dr.A.Venkata Ramayya (Ph.D.)

CO-ADVISOR: Debala Genat. (MSc)

September, 2017

JIMMA, ETHIOPIA

JIMMA UNIVERSITY

SCHOOL OF GRADUATE STUDIES

JIMMA INSTITUTE OF TECHNOLOGY

FACULTY OF MECHANICAL ENGINEERING

Design, Performance Analysis, Optimization and CFD Simulation of Indirect Type Forced Solar Coffee Dryer

By: Gadisa Desa

Approved by Board of Examiners:-

---	---	---
Chairman, Department of Graduate Committee	Signature	Date
Prof.Dr.A.Venkata Ramayya (Ph.D)	---	---
Advisor	Signature	Date
---	---	---
Internal Examiner	Signature	Date
---	---	---
External Examiner	Signature	Date

DECLARATION

Here to declare this thesis entitled "design, performance analysis, optimization and CFD simulation of indirect type forced solar coffee dryer at Jimma Institute of Technology " is the original work done under the supervisor of prof.Dr.A.Venkata Ramayya (Ph.D.) at Jimma Institute of Technology during the year 2017 as part of Masters of Science Mechanical Engineering in thermal system engineering and has not been presented for a degree in any other university.

Name	Signature	Date
Gadisa Desa	_____	_____
(Student)		

Approved by:	**Signature**	**Date**
Prof.Dr.A.Venkata Ramayya (Ph.D)	_____	_____
(Advisor)		
Debala. Genat (MSc)	_____	_____
(**Co- advisor**)		

Acknowledgment

First and foremost I would like to thank God. This work could not have been possible without the help of many people who supported my work.

I would like to express my whole hearted deep sense of gratitude to my advisor Prof.Dr.A.Venkata Ramayya (Ph.D) for giving me the opportunity to work on this thesis and for this guidance and encouragement without which this work could have not been completed. He has been a constant source of inspiration throughout my study period.

I am also grate full to my co-advisor Debala Genet for his kind help on different occasions.

Last but not least, I would like to my family and friends who were always besides me and played great role in completion of my work.

Abstract

Solar drying is the methods by using solar energy to dry coffee beans; since improve the quality, while reducing wastes producing and traditional drying thus improving the quality of life. The objective of this thesis to design, optimize and performance analysis of the indirect forced solar dryer for coffee parchment with CFD simulation. In this study mathematical modeling of solar dryer and drying chamber was described and the analysis of heat transfer coefficient (losses) through the flat plate collector was discussed and the techniques that used to reduces these losses also mentioned. From the simulation results; the effect of air mass flow rate on different type of collector, temperature rise and pressure drop were characterized including the variation of turbulence intensity using CFD approach. Optimized different types of duct shape dryer based pressure drop and airflow of with uniform velocity, a smooth curve with collector diffuser duct has low pressure drop and smooth curve with guide vanes has uniform air flow. The effect of different air gap on the temperature outlet and pressure drop of different air flow rate for flat plate collector has been conducted. The turbulence intensity effect on temperature outlet of the air and pressure drop was simulated using the 2%, 5% and 10% with in the same flow rate of air and dryer profile. The direction of air flow through the collector was evaluated based on temperature outlet and pressure drop. When flow was below absorber plate collector, it is more acceptable. In addition, thermal performance of solar air heater was simulated at different airflow rates on a collector with v-grooved absorber plate and another three absorber collector plate. High collector outlet temperature and efficiency were observed in a collector with v-grooved absorber plate. The effect of try's arrangement of dryer chamber with air flow. A good agreement has been observed between the experimental results and the CFD collector efficiency predicted output with a deviation of 9%.

Key words: solar coffee dryer, CFD simulation, performance analysis, indirect forced solar dryer

TABLE CONTENTS

LIST OF TABLES

LIST OF FIGURES

Nomenclature

Symbols	Description
T_a	Temperature of Ambient Air, ^{O}C
T_p	Temperature of absorber plate, ^{O}C
T_{ai0}	Temperature of air inlet, ^{O}C
T_g	Temperature of Glass Cover, $_{O}C$
T_{ao0}	Temperature of air out let, ^{O}C
T_{sky}	Temperature of sky, ^{O}C
I_N	Solar Intensity, W/m^2
NU	Nusselt number
K	Thermal conductivity of absorber plate
L	Length of absorber plate, m
h_{1c}	Convective heat transfer coefficient from plate to glass, W/m^2
β	Tilt angle
Ra	Rayleigh number
Pr	Prandetell number
h_{2c}	Convective heat transfer coefficient from glass to ambient,w/m^2
G_{rl}	grashof number
V	Wind velocity, m/s
h_1	Total heat transfer coefficient from the plate to cover
h_2	Total heat transfer coefficient from the cover to ambient
U_t	Overall top heat loss coefficient
U_b	Overall bottom heat loss coefficient
K_{in}	Thermal conductivity of insulation
L_{in}	Insulation thickness
A_c	Collector plate area, m^2
A_c	surface area dryer chamber, m^2
A_e	Collector edge area, m^2

U_e	Edge loss coefficient
U_L	Overall heat loss coefficient
q_u	Useful energy gained by the collector per unit area
Q_u	Useful energy gained by the collector
Q_g	The heat gained by the air
q_L	Overall heat lost by the absorber to the ambient per unit area
δ	Declination angle
ω	Hour angle
τ	Transmittance
α	Solar absorbance
η_c	Overall collector efficiencies
ν	Dynamic viscosity of air.
hl	The layer drying bed thickness,
ρ	The bulk density of the crop on wet basis
K a	Thermal conductivity of air.
Mw	Mass of water evaporated from the food item (kg /s).
h_{fg}	Latent heat of vaporization of water (kJ/kg)
M_f	Final moisture content (Kg)
M_i	Initial moisture content (Kg)
η_d	Overall drying efficiencies(%)
m_a	Mass flow rate of air [Kg/s]
E_{mc}	Equilibrium moisture content
ε_g	Glass emissivity
ε_p	Plate emissivity
ε_{eff}	Effective emissivity of plate-glazing

CHAPTER ONE

INTRODUCTION

1.1 General Introduction

Drying is the removal of moisture to a safe level to maintain quality during storage. Solar radiation in the form of solar thermal energy, is an alternative source of energy for drying especially to dry coffee fruits, vegetables, agricultural grains and other kinds of material, such as wood. This procedure is especially applicable in the so-called “sunny belt” world-wide, i.e. in the regions where the intensity of solar radiation is high and sunshine duration is long. It is estimated that in developing countries there exist significant postharvest losses of agricultural products, due to lack of other preservation means. Drying by solar energy is a rather economical procedure for agricultural products, especially for medium to small amounts of products. It is still used from domestic up to small commercial size drying of crops, agricultural products and foodstuff, such as fruits, vegetables, aromatic herbs, wood, etc. contributing thus significantly to the economy of small agricultural communities and farms [2].

Sun drying is still the most common method used to preserve agricultural products in most tropical and subtropical countries. However, being unprotected from rain, wind-borne dirt and dust, infestation by insects, rodents and other animal, products may be seriously degraded to the extent that sometimes become inedible and the resulted loss of food quality in the dried products may have adverse economic effects on domestics and international markets. Some of the problems associated with open-air sun drying can be solved through the use of a solar dryer which comprises of collector, a drying chamber and sometimes a chimney. The conditions in tropical countries make the use of solar energy for drying food practically attractive and environmentally sound [1].

Dryers have been developed and used to dry agricultural products in order to improve shelf life. Most of these either use an expensive source of energy such as electricity or a combination of solar energy and some other form of energy. Most projects of these nature have not been adopted by the small farmers, either because the final design and data collection procedures are frequently inappropriate or the cost has remained inaccessible and the subsequent transfer of technology from researcher to the end user has been anything but effective [3].

Coffee drying is one of the major steps in coffee processing, and has a significant effect on the quality (flavor and aroma) of coffee beans after processing. It is not in any way a trivial processing step, regardless of the degree of technology employed, and quality can easily be lost by drying that is too slow, too fast or otherwise inappropriate. Depending on the processing method employed, the whole fruit, the crushed fruit, parchments (bean enclosed by the inner integument), or naked beans dried [10].

1.2. Statement of problem

Energy is limited but energy demand is unlimited. All our activities such as transportation and communication need to use energy. The most important advantage of the solar dryers is that they work on renewable energy and are pollution free. Also, solar dryers can be easily constructed from local materials. It is successfully proved how solar dryer technology is key element to climatic and environmental protection as well as sustainable development [13].

Direct solar drying is the easiest method of solar drying; however, it has many disadvantages such as: Direct exposure to solar radiation reduces the quality of the products and reduces the vitamins and nutrients from them, Drying rate is very slow, No control over rate of drying, Products are directly exposed to uneven climatic changes and poor solar conditions. The speed of drying especially in open sun drying which is solar radiation exposed directly to the products will cause the product's surface becomes hard before the moisture inside has a chance to evaporate and it will affect the quality of dried product due to over drying. Those disadvantages which came by direct solar and open sun dryer are solves by indirect type solar dryers. In this thesis, modeling and CFD simulation to investigate the design and optimization of the indirect forced solar dryer. The effects of the location of trays and use of different type's designs of collector of which improved performance of indirect forced solar dryer analyses using simulation. The improvement of air flow in the collector drying for the performance improvement of the collector dryer and the recirculation of the drying air to improve the thermal efficiency of the dryer analysis using CFD simulation.

1.3. Objectives

1.3.1. General Objective

The general objective of this thesis is design, performance analysis, optimization and CFD simulation of indirect type forced solar coffee dryer in order to reduce the moisture content of the coffee beans to reach the desired standard moisture content.

1.3.2 Specific Objective

The specific objective of this study are, therefore:

- ❖ To design and size of the collector need to cover the energy demand for drying coffee.
- ❖ To perform heat and mass transfer from air heater to coffee dryer parchment
- ❖ To perform CFD simulation of solar coffee dryer design using ANSYS FULENT software.
- ❖ To improve the performance of design coffee dryer.
- ❖ To optimize efficiency of the design solar indirect type forced solar coffee dryer

1.4. Methodology and materials

The methods and materials which used to full fill the specific objective the thesis.

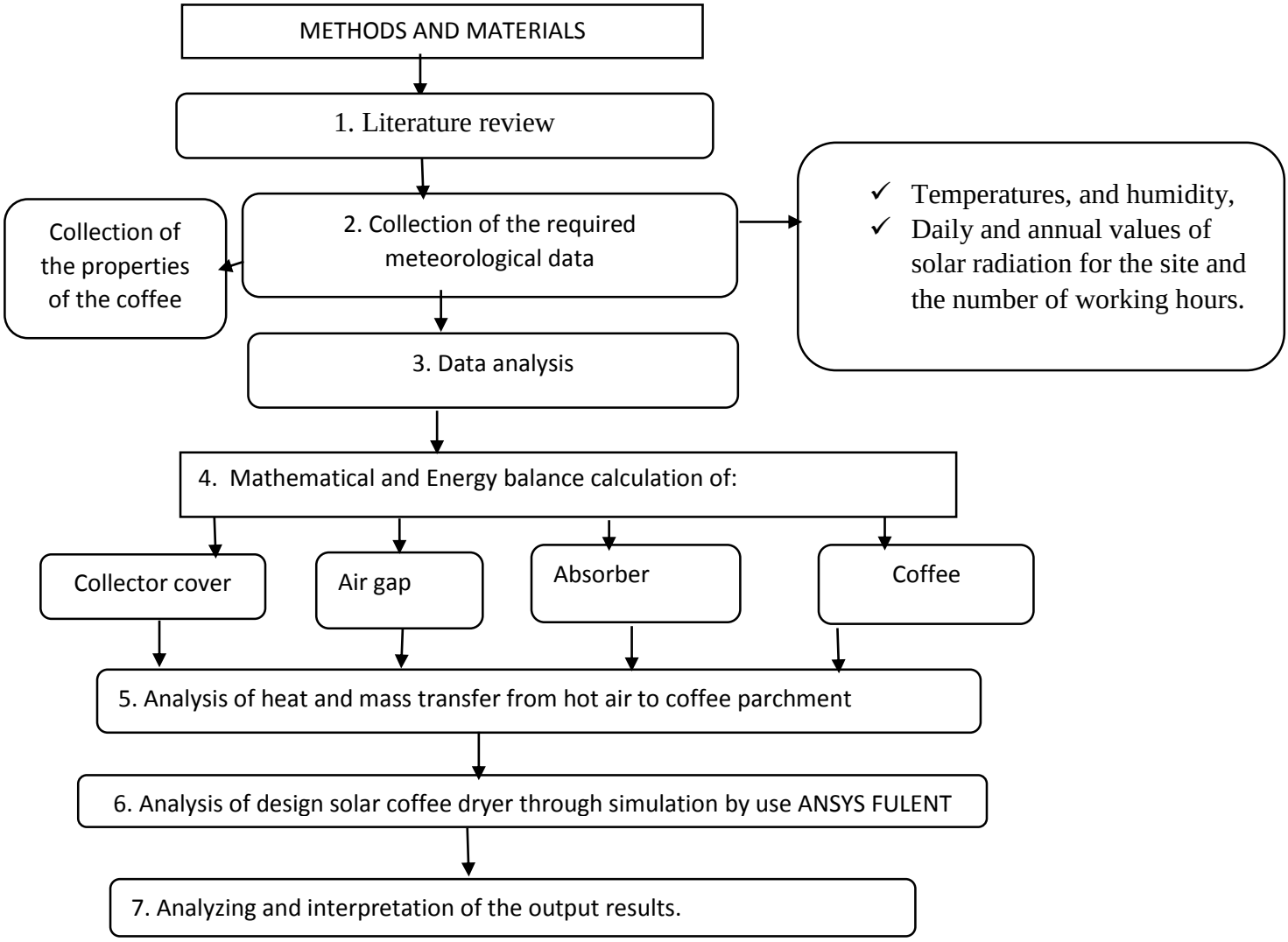

Figure 1.1: methodology

1.5 Significance of the Study

Crop drying is the most energy consuming process in all processes on the farm. The purpose of drying is to remove moisture from the agricultural produce so that it can be processed safely and stored for increased periods of time. Crops are also dried before storage or, during storage, by forced circulation of air, to prevent spontaneous combustion by inhibiting fermentation.

This Solar dryer design benefits for farms which crops coffee:

- ✓ Improvement in product quality (colour, texture and taste).
- ✓ No contamination by insects, microorganism and mycotoxin.
- ✓ Reduction in drying time.
- ✓ Reduction of drying and storage losses.
- ✓ Considerable increase in shelf life of dried products

CHAPTER TWO

LITERATURE REVIEW

2.1 General Review

Crop drying is the most energy consuming process in all processes on the farm. The purpose of drying is to remove moisture from the agricultural produce so that it can be processed safely and stored for increased periods of time. Crops are also dried before storage or, during storage, by forced circulation of air, to prevent spontaneous combustion by inhibiting fermentation. It is estimated that 20% of the world‘s grain production is lost after harvest because of inefficient handling and poor implementation of post-harvest technology [3].

Energy is important for the existence and development of human kind and is a key issue in international politics, the economy, military preparedness, and diplomacy. To reduce the impact of conventional energy sources on the environment, much attention should be paid to the development of new energy and renewable energy resources. Solar energy, which is environment friendly, is renewable and can serve as a sustainable energy source.

Hence, it will certainly become an important part of the future energy structure with the increasingly drying up of the terrestrial fossil fuel. However, the lower energy density and seasonal doing with geographical dependence are the major challenges in identifying suitable applications using solar energy as the heat source. Consequently, exploring high efficiency solar energy concentration technology is necessary and realistic [8].

Solar energy is free, environmentally clean, and therefore is recognized as one of the most promising alternative energy recourses options. In near future, the large-scale introduction of solar energy systems, directly converting solar radiation into heat, can be looked forward. However, solar energy is intermittent by its nature; there is no sun at night. Its total available value is seasonal and is dependent on the meteorological conditions of the location. Unreliability is the biggest retarding factor for extensive solar energy utilization. Of course, reliability of solar energy can be increased by storing its portion when it is in excess of the load and using the stored energy whenever needed. Solar drying is a potential decentralized thermal application of solar energy particularly in developing countries [9].

This section provides an overview of previous studies that have been conducted by researchers in the fields of Thermal Engineering. Different sources were reviewed in order to understand the techniques and key studies that have been conducted.

2.2 Research Related Studies

A lot of research work has been carried out throughout the world to investigate and analyze the solar dryer and thermal performance of air heaters. A brief review of literature is presented here.

Table 2.1. Summary of literature review

Authors	Tasks performed	Methodology used	Results obtained	Validation
Tesfaye [2]	Study on Solar Tunnel Dryer Mathematical Modeling and Simulation for Coffee Drying in Harar.	mathematical modeling and simulation	The parchment coffee exposed to the drying air gets dried faster than the parchment coffee found at the center.	Analytical with simulation
Tiruwork .B [5]	Design, construction and evaluation of performance of solar dryer for drying fruit.	Experimental testing	The moisture content of pineapple and mango was reduced from 87 % and 85 % to 16 % and 13 %, respectively, within two to three days. The collector efficiency was found to be 31.7 %. Drying efficiency was also found to be 9.7 %, 7.5 % and 8.7 % for solar	Experimental
Feyza .A [6]	The available solar dryer's systems and new technologies.	comparison of drying	properly designed forced convection (active) solar dryers are agreed generally to be more effective and more controllable than the natural-circulation (passive) types	Analytical

Umesh .T [7]	Review of the research paper is state that, the solar dryer is beneficial than the sun drying techniques.	Review	Solar dryers involve an initial expense, they produce better looking, better tasting, and more nutritious foods, enhancing both their food value -and their marketability. They also are faster, safer, and more efficient than traditional sun drying techniques	
R.VidyaSagarRaju, [8]	Design and Fabrication of Efficient Solar Dryer.	Experimental testing	The designed dryer with a collector area of $1m^2$ is expected to dry 20kg fresh vegetables from 89.6% to 13% wet basis in two days under ambient conditions during harvesting period from February to March.	Experimental
Baloraj [12]	Design, Construction and Calibration of Low Cost Solar Cabinet Dryer.	Experimental testing	The dryer removed a maximum of 49% moisture content from inside drying chamber for drying low moisture content food products	Experimental
Tefera[13]	Simulation and Experimental Investigation on Active Solar Coffee Dryer	Mathematical, Experimental testing and ANASYS Simulation model	The moisture content of the coffee was reduced from 29% to 12.3% after 5h for clear sunshine day and average thermal efficiency of the dryer was determined to be 50.5% for clear sunshine day.	Analytical with ANASYS simulation and Experimental
Aklilu[27]	Experimental analysis for performance evaluation of solar dryer	Experimental testing	For all the test conditions, the material gets dried with system's efficiency of 15.9%. The drying time compared to sun drying was reducing by about 19%.	Experimental

S.Vijayan [22]	Performance Study of an Indirect Forced Convection Solar Dryer for Potato	Experimental testing	The drying experiments have been carried out simultaneously in solar dryer with 0.058 kg/s mass flow rate of air and open sun drying. The result indicates that the moisture content of potato was reduced from 85 % to 14 % in 4 hours and 5 hours respectively in solar dryer and open sun drying.	Experiments with analytical
Chabane. F [23]	Experimental study of heat transfer and thermal performance with longitudinal fins of solar air heater.	Experimental testing	Experiments were performed for two air mass flow rates of 0.012 and 0.016 kg/s. Moreover, the maximum efficiency values obtained for the 0.012 and 0.016 kg/s with and without fins were 40.02%, 51.50% and 34.92%, 43.94%, respectively	Experimental with simulation

2.3 Types of Solar Dryer

Dryer is to supply more heat to the product than that available naturally under ambient conditions, thus increasing sufficiently the vapour pressure of the crop moisture. Therefore, moisture migration from the crop is improved. The dryer also significantly decreases the relative humidity of the drying air, and by doing so, its moisture-carrying capability increases, thus ensuring sufficiently low equilibrium moisture content.

Solar energy drying systems are classified primarily according to their ways of drying and the manner in which the solar heat is utilized.

A. Solar dryer:

The process which involves deliberate removal of moisture from a product is termed as drying. Various agricultural products such as vegetables, fruits, fish, coffee, cocoa and tobacco are being dried using open-air drying technique. But in open-air drying, since there is little control over drying rates, crops can either be over-dried or under-dried. Over-drying the crops in the sun can cause discoloration, bleaching and scorching, loss of germination power, and reduction in

nutritional value. On the contrary, under-drying leads to the development of bacteria and fungi. Thus, drying under controlled conditions of temperature and humidity helps the crop to dry reasonably rapidly to a safe moisture content level and ensure a superior quality of the product [4].

Solar drying is a continuous process where moisture content, air and product temperature, and the humidity of air all change simultaneously along with the two basic inputs to the system: the solar insolation and the ambient temperature. The drying rate is affected by ambient climatic conditions.

B. **Solar tunnel dryer:**

Tunnel dryer is a direct continuous type of dryer. It is a largest scale dryer. In this dryer, the materials to be dried are sent to the air heated tunnel for drying purpose. The material is entered at one end and the dried material is collected at the other end of the tunnel. The outgoing material met the incoming air to ensure maximum drying and the outgoing air contacted the wettest material so that the air was as nearly saturated as possible.

Mechanism of action: one of the doors of the tunnel is opened and the material to be dried are placed to the trolleys and trucks are pushed slowly in the tunnel and then door is closed. Hot air is circulated and passed through the rail truck and perforated trolleys. The hot air then followed are recirculated with the help of fans and the material becoming dried. The moist air is passed out through the exhaust after completion of drying. The door is opened and the trolleys are taken out of the funnel and some new trolleys with the wet materials are introduced into the trucks and the process is repeated [21].

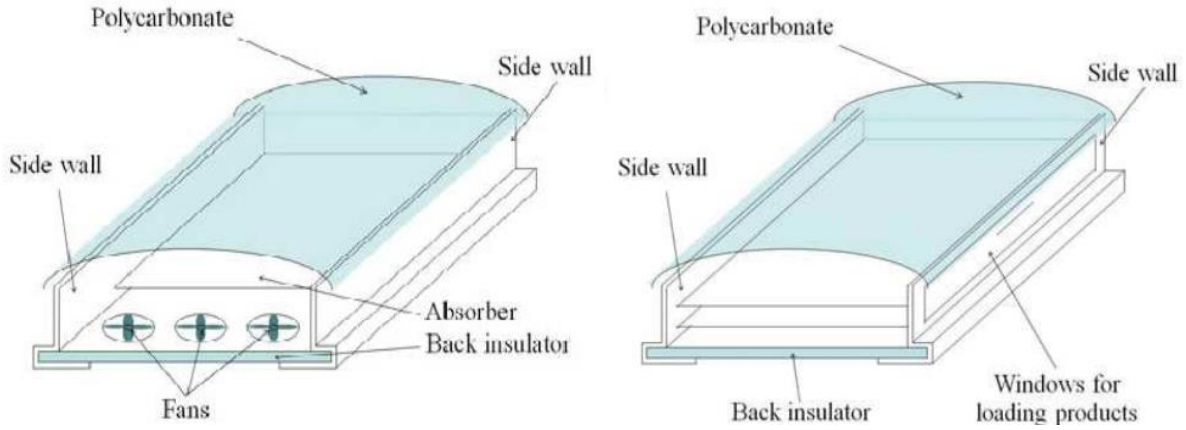

a) b)

Figure 2.1. The characteristics of solar tunnel dryer (a) Solar collector and (b) Product container [21].

C. Solar Bubble Dryer

The Solar Bubble Dryer (SBD) is the latest low-cost drying technology that aims to provide a simple and flexible alternative to sun drying. The SBD is mobile and completely independent of fuel or the power grid, and is therefore very cheap to operate. It comes in different sizes, with current models having a 0.5- or 1-ton batch capacity.

The Solar Bubble Dryer uses solar energy from the sun in two ways. First, the drying tunnel serves as a solar collector to convert energy from the sun's rays (entering through the transparent top of the drying tunnel) to heat, therefore increasing the temperature of the air for faster drying. Second, the SBD is equipped with a photovoltaic system that consists of solar panels for generating electricity - a rechargeable deep cycle beery for use at night and one or two small blowers to inflate the drying tunnel and move air through it. The air also removes water evaporating from the grains inside the tunnel. A simple roller with ropes an ached to both of its ends is periodically dragged underneath to mix the grains without the need to open the tunnel. A rake for internal mixing is also available [20].

Figure 2.2. Solar bubble dryer [20].

Table 2.2.Advantages and dis advantages of type of solar dryer [4, 14, 20, and 21]

Types of dryer	Advantages	Dis advantages
Solar dryer	It gives better quality of drying product.	More expensive.
	It reduces losses and bacterial contamination.	It may requires some parts material to be import.
	Requires less area for drying.	
	May reduce labor required.	
	Drying time reduces.	
Solar tunnel dryer	In research laboratories and QC department for drying glass wires and small apparatus.	High labor cost for loading and unloading.
	In drying of packing materials plastic caps, spoons injectable vials, glass containers, etc.	Thermo labile substance can't be dried.

	Used for drying of paraffin wax, gelatin, soap, pottery, etc.	Drying rage is low, so time consuming.
		It is not suitable for small scale production.
		It is a non-agitated process.
		Drying of liquid material is not possible.
		There is a chance of accident when doors are opened before stopping the hot air circulation.
Solar bubble dryer	Improves the traditional sun-drying process and eliminates all losses due to spillage, running over the rains, Animals, the weather, and vehicles	High labor cost for rotating mixing
	More flexible,	
	Requires lower investment, and	
	Does not need fuel for heating the air or for running the blower.	
Sun dryer	The process is independent of any other source of energy except sunlight.	Damage to the crop by rodents, birds, and animals.
	The cheapest method.	Degradation through exposure to direct irradiation of the sun and to rain, storm, and dew.
	Less skill labor required	Contamination by dirt dust, wind-blown debris, and environmental pollution,
		Loss due to over drying.
		Insect infestation Growth of microorganisms.
		Additional losses during storage due to insufficient or no uniform drying

Then based on the above table in the thesis select solar dryer that means solar dryer has more quality of drying product and takes less time drying than the others.

2.4 Classification of Solar-Energy Drying Systems

To classify the various types of solar dryers, it is necessary to simplify the complex constructions and various modes of operation to the basic principles. Solar-energy drying systems are classified primarily according to their heating modes and the manner in which the solar heat is utilized.

In broad terms; they can be classified into two major groups, namely [14]:

2.4.1 Passive Solar Drying Systems

In a passive solar dryer, air is heated and circulated naturally by buoyancy force or as a result of wind pressure or in combination of both. Normal and reverse absorber cabinet dryer and greenhouse dryer operates in passive mode. Passive drying of crops is still in common practice in

many Mediterranean, tropical and subtropical regions especially in Africa and Asia or in small agricultural communities. These are primitive, inexpensive in construction with locally available materials, easy to install and to operate especially at sites far off from electrical grid. The passive dryers are best suited for drying small batches of fruits and vegetables such as banana, pineapple, mango, potato, carrots [14].

Three distinct sub-classes of passive are:

1. Direct (integral) type solar dryers;
2. Indirect (distributed) type solar dryers; and
3. Mixed model solar dryer.

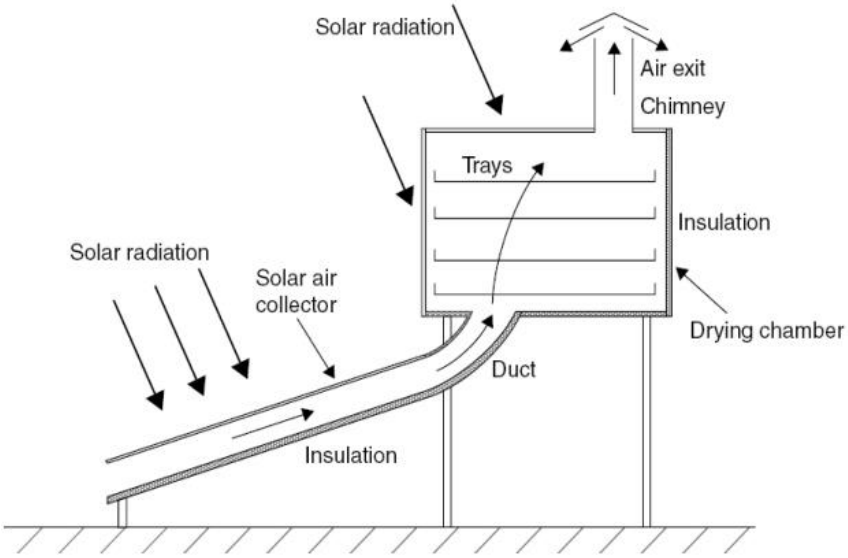

Figure 2.3: schematic diagram of a natural circulation, indirect-mode solar energy dryer [4]

2.4.2 Active Solar Drying Systems

Active solar drying systems depend only partly on solar-energy. They employ solar energy and/or electrical or fossil-fuel based heating systems and motorized fans and/or pumps for air circulation. All active solar dryers are, thus, by their application, forced convection dryers. Major applications of active solar dryers are in large-scale commercial drying operations in which air heating solar-energy collectors supplement conventional fossil-fuel fired dehydrators, thus reducing the overall conventional energy consumption, while maintaining control of the drying conditions. If warm enough, the solar-heated air could be used directly for the drying process; otherwise the fossil-fuel fired dehydrator would be used to raise the drying air temperature to the required level, thus

avoiding the effects of fluctuating energy output from the solar collector, since the fossil-fuel system can be controlled automatically to provide the required optimum drying conditions. These active solar dryer types that incorporate dehydrators for supplemental heating are commonly known as ``hybrid solar dryers'' [4].

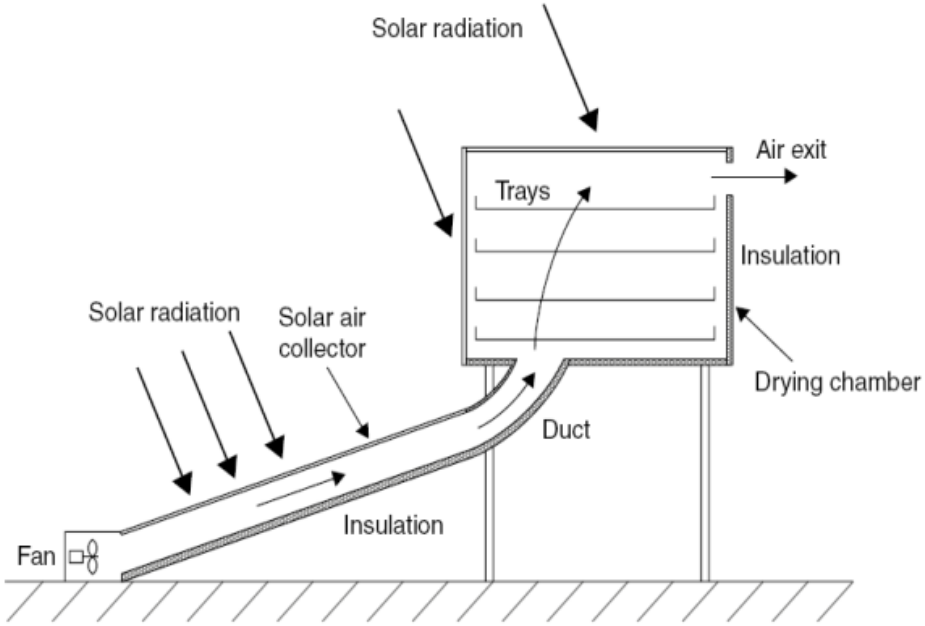

Figure 2.4: schematic diagram of a forced circulation, mixed-mode solar energy dryer [4]

Similarly like passive solar drying system there three distinct sub-classes of the passive solar drying systems can be identified which vary mainly in the design arrangement of system components and the mode of utilization of the solar heat, namely:

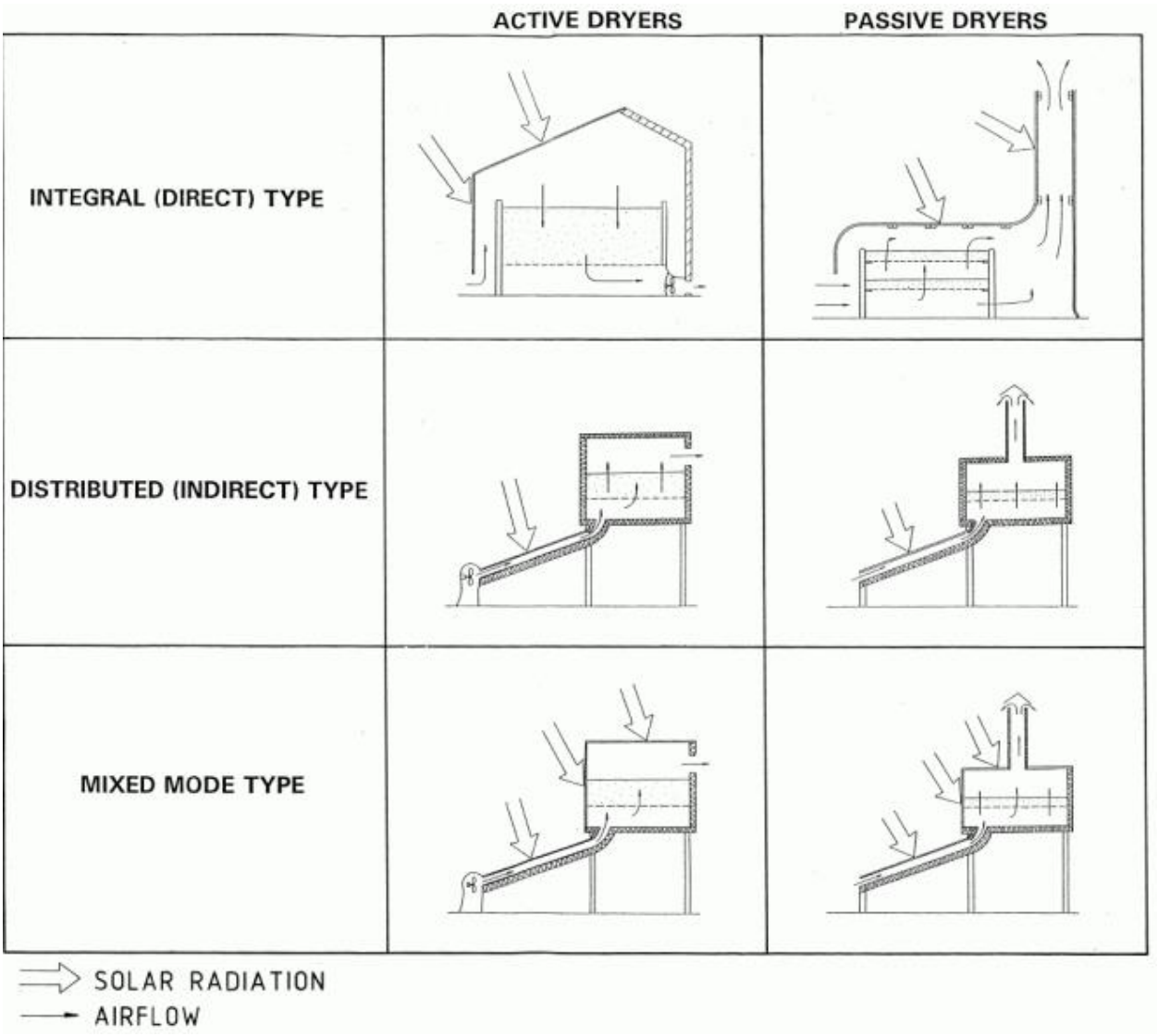

Figure 2.5. Typical solar energy dryer designs [4].

2.4.2.1 Indirect-Type Active Solar Drying System

These are often termed indirect active solar dryers. These differ from direct dryers with respect to heat transfer and vapor removal. Here the crops in these indirect solar dryers are located in trays or shelves inside an opaque drying cabinet and a separate unit termed as solar collector is used for heating of the entering air into the cabinet. The heated air is allowed to flow through/over the wet crop that provides the heat for moisture evaporation by convective heat transfer between the hot air and the wet crop. Drying takes place due to the difference in moisture concentration between the drying air and the air in the vicinity of crop surface.

However as the efficiency of collector decreases at higher temperature operation, an optimum temperature and airflow rate has to be determined to have a cost effective design. While most solar collectors are made up of metal or wood absorbers with appropriate coatings, materials like black polythene are also used as they form an economic substitute.

The efficiency of the indirect-type active solar dryer also depends on the location of the fan, though not so significantly in small batches. The prime objective of the fan is to maintain a desired flow-rate in the drying cabinet causing uniform evaporation of moisture from the wet material and in the collector is the collection of heat maintaining a negative pressure, reducing the heat losses [15].

A typical distributed natural-circulation solar-energy dryer would be comprised of the following basic units:

1. An air-heating solar-energy collector;
2. A drying chamber;
3. A fan for air circulation and
4. A chimney.

2.4.2.2 Direct-Type Active Solar-Energy Drying Systems

The direct-type active solar dryers are designed with an integrated solar energy collection unit. In integral-type active-circulation solar-energy dryers (often termed direct solar dryers), the product is placed in a drying chamber with transparent walls that allow the insulation necessary for the drying process to be transmitted. Thus, solar radiation impinges directly on the product. The heat extracts the moisture from the product and concomitantly (alongside) lowers the relative humidity of the resident air, thereby increasing its moisture carrying capability. In addition, it expands the air in the chamber, generating its circulation and the subsequent removal of moisture along with the warm air [15].

However, convective and evaporative losses occur inside the chamber from the heated material. The moisture is taken away by the air entering into the chamber from below and escaping through another opening provide at the top as shown in Fig below. A direct solar dryer is one in which the material is directly exposed to the sun‘s rays. This dryer comprises of a drying chamber that is covered by a transparent cover made of glass or plastic. The drying chamber is usually a shallow,

insulated box with air-holes in it to allow air to enter and exit the box. The product samples are placed on a perforated tray that allows the air to flow through it and the material [15].

2.4.2.3 Hybrid-Type Active Solar-Energy Dryers

The hybrid solar dryers combine the features of the direct and indirect by type active circulation solar energy dryers. Here the combined action of incident direct solar radiation on the product to be dried and air pre-heated in a solar collector heater produces the necessary heat required for the drying process. A hybrid type active solar-energy dryer would have the same typical structural features as the indirect-type and direct-type (i.e. a solar air heater, a separate drying chamber and a chimney), and in addition has glazed walls inside the drying chamber so that the solar radiation impinges directly on the product as in the direct-type dryers. These dryers generally are medium to large installations operating in the range of 50-60%, and compensate the temperature fluctuations induced by the climatic uncertainties [15].

Table 2.3. Advantages and disadvantages of sub-classes the active solar drying systems [25].

Types	Advantages	Dis advantages
Direct solar dryer	Contamination of product due to enclosure with transparent cover is less	Drying rate is very slow
	Product quality obtained is higher than open to the sun drying.	Direct exposure to solar radiation reduces the quality of the products and reduces the vitamins and nutrients from them.
		Products are directly exposed to uneven climatic changes and poor solar conditions
		No control over rate of drying.
Indirect solar dryer	This technique avoids contamination of final product.	Requires more initial cost
	It is very efficient method than the direct type of solar drying.	Need maintenance after particular period of time.
	Maintain the quality of product by avoiding direct exposure in solar radiations	
	Time required for drying some product is less.	
	Final conditions of product are avoided on the circumstances of natural phenomenon.	

Mixed mode solar dryer	Rapid rate of drying with safe moisture level in product.	Quality of dry grain obtained over a year is less than indirect type of dryer.
	Time required for drying is less than other drying techniques.	Cost required for maintenance.
		Capital cost required is higher.

These disadvantages direct and mixed mode are taken care of indirect type solar dryers. Indirect solar drying is the new and more effective technique of product drying. In this type of drying, the products are not directly exposed to the sun but, the solar radiation is used to heat the air which then flows through the product to be dried. Thus, moisture from the product may be lost by convection and diffusion, and so on the thesis indirect type solar dryer was preferable and selected.

2.5. Open Sun Drying

In open sun drying, there is a considerable loss due to various reasons such as rodents, birds, insects and micro-organisms. The unexpected rain or storm further worsens the situation. Further, over drying, insufficient drying, contamination by foreign material like dust dirt, insects, and micro-organism as well discoloring by UV radiation are characteristic for open sun drying. In general, open sun drying does not fulfill the intern9ational quality standards and therefore it cannot be sold in the international market. [15].

Figure 2.6: working principle of open sun drying [4].

2.7 Applications of Solar Technology

Solar energy refers primarily to the use of solar radiation for practical ends. All other renewable energies other than geothermal and tidal derive their energy from the sun. The applications of solar energy which are enjoying most success to-day, some of its thermal applications are as follows [14].

- Water heating; Space heating; Power generation; Space cooling and refrigeration; Distillation; Drying, and Cooking.

2.8 Drying Mechanism

In the process of drying, heat is necessary to evaporate moisture from the material and a flow of air helps in carrying away the evaporated moisture. There are two basic mechanisms involved in the drying process: the migration of moisture from the interior of an individual material to the surface, and the evaporation of moisture from the surface to the surrounding air.

The drying of a product is a complex heat and mass transfer process which depends on external variables such as temperature, humidity and velocity of the air stream and internal variables which depend on parameters like surface characteristics (rough or smooth surface), chemical composition (sugars, starches, etc.), physical structure(porosity, density, etc.), and size and shape of products. The rate of moisture movement from the product inside to the air outside differs from one product to another and depends very much on whether the material is hygroscopic or non-hygroscopic [15].

CHAPTER THREE

SOLAR DRYERS

Solar dryers are mainly made up of three parts. These are flat plate solar collector, drying chamber and connecting duct.

3.1 Solar Collector

Solar collectors are used to convert direct and diffuse radiation from the sun into thermal energy. It is a special kind of heat exchanger that transforms solar energy to heat. Energy is transferred from a distant source of radiant energy to a fluid.

Flat-plate collectors can be designed for applications requiring energy delivery at moderate temperatures, up to perhaps 100^{o}C above ambient temperature. They use both beam and diffuse solar radiation, do not require tracking of the sun, and require little maintenance. They are mechanically simpler than concentrating collectors [11].

Generally, flat plate collector designs consist of three major parts. These are transparent cover, absorber plate and insulation. The transparent cover also called glazing is where the solar energy passes through the collector. Translucent (transmitting light only), low iron glass is a common glazing material for flat-plate collectors because low iron glass transmits a high percentage of the available solar energy. Glass is the common transparent cover for collectors, but some plastics have also desirable characteristics. Although plastics can transmit as much solar radiation as glass and resist impact stress better than glass, it allows more thermal energy loss than glass.

The roles of glazing in a solar collector are:

- To transmit as much solar energy as possible to the absorber plate;
- To minimize heat loss from the absorber plate to the environment;
- To shield the absorber plate from direct exposure to weathering.

Absorber plate is made from a material which can rapidly absorb heat from the sun's rays. It is usually made from black painted metal sheet. Insulation should be used at the back side of the absorber to minimize heat loss. The material chosen as insulator should be stable at high temperatures, i.e. it should not break down at high temperatures. In order to reduce heat loss from

the sides of the collector, it should be incorporated into a box. Collector boxes should be strong enough to resist loads imposed by wind and need to be sealed to exclude water.

3.2 Drying Chamber

The drying chamber where the material to be dried comes in direct contact with the hot air from the collector and reduces its moisture. It will consist of trays for putting in the produce to be dried. At the drying chamber there should be means for loading and removing the material to be dried. This is usually provided by a door at the back side of the dryer. The drying chamber should be insulated and well-sealed in order to contain the heated air without any leaks.

3.3. Transient analysis of solar dryer

3.3.1 Mathematical Model

The transient thermal performance of the solar collector is evaluated by applying energy balance on its components.

3.3.2 Energy Balance on Each Component of Solar Drier

A solar air heater is a flat plate collector with an absorber plate, a transparent cover at the top and insulation at the bottom and on the sides.

3.3.2.1 Absorber Plate

Energy balance on the absorber plate is expressed as:

$$(mCp)_p\frac{dTp}{dt} = A_cI_c - A_cU_{pg}(T_p-T_g) - AcU_a\left[T_p-\left(\frac{Tai+Tao1}{2}\right)\right]$$

$$- A_cU_{pab}(T_p - T_a) - A_1U_{pae}\left[\left(\frac{Tp+Ta}{2}\right) - T_a\right] \quad 3.1$$

Where A1 = p*dE -collector perimeter x depth of the edge.

Then the unknown values in the above equation in the following sections can be determined.

U_{pg} = the overall heat transfer coefficients from the plate to the glass by convection and radiation are given by empirical equation as follows:

The plate temperature T_p at any time Δt can be determined from conditions at time *t* and the energy absorbed by the plate and energy losses.

$$U_{pg} = \left[0.06 - 0.017\frac{\theta}{90}\right]\frac{k_a}{s_{12}}G_{r1}^{1/3} + \epsilon_{pg}\,\delta\,(T_p^2 + T_g^2)(T_p + T_g) \quad 3.2$$

The Grashof number is given by:

$$G_{r1} = [g\Theta\,(T_p - T_g)\,L^3]\,/\nu^2 \quad 3.3$$

Where: g – gravitation force

ν - Kinematic viscosity of the air

The value of Θ is volume expansion coefficient calculated as:

$$\Theta = \frac{2}{Tai+Tao} \quad 3.4$$

Then the overall emittance factor ϵ_{pg} for the absorber plate and the glass cover is obtained from the relation.

$\epsilon_{eff} = (\frac{1}{\epsilon_p} + \frac{1}{\epsilon_g} - 1)^{-1}$ From above chapter

Then the rest are obtained from the standard table by using the equation which is evaluated at the film temperature T_f given by:

T_f = (Tao +Tai)/2 3.5

Then the heat transfer coefficient U_a of the air is defined as:

$$U_a = 0.664\frac{K_a}{L}[\frac{P_r G_{rL}\cos\Theta}{P_r+0.9524}]^{0.25} \quad 3.6$$

Where: $p_r = \frac{\nu_a}{\alpha_a} = \frac{C_p \nu}{K_a}$ 3.7

Then we have to find the value U_{pab} [heat transfer coefficient from collector plate to air heat transfer coefficient in the bottom side.

$$U_{pab} = \frac{K_{in}}{L_{in}}$$

Then find the value of U_{pae} [heat transfer coefficient from the plate to the air through the edge].

$U_{pae} = U_{pab}\{\frac{A_e}{A_c}\}$ Where: $A_e = p*t_{BE}$

Therefore, $dE=t_{BE}$ then results in:-

$A1 = p * dE = p * t_{BE}$

Due to the transient nature of the radiant and convective heat transfer coefficients, absorber plate energy balance equation is a non-linear equation and its solution requires an integration scheme that line arises the given differential equation within a given time step.

The temperature of the plate at time ($t + \Delta\tau$) in terms of the absorbed useful incident radiation on the surface of the plate, the heat losses through the glass cover and the collector edge, the quantity of heat absorbed by the air stream and temperatures of the collector components at time t is obtained from the absorber plate energy balance equation:

$$Tp1 = \frac{AcIc}{(mCp)p}\Delta\tau + \{1-[\frac{A_cU_{pg}}{(mC_P)_P} + \frac{2A_cU_a}{(mC_P)_P} + \frac{A_cU_{pab}}{(mC_P)_P} + \frac{A_cU_{pae}}{2(mC_P)_P}]\Delta\tau\}T_{po} + (\frac{A_cU_{pg}}{(mC_P)_P})\Delta\tau\ T_{go} + (\frac{A_cU_a}{(mC_P)_P})\Delta\tau\ T_{aio} + (\frac{A_cU_a}{2(mC_P)_P})\ \Delta\tau T_{a01} + ([\frac{A_cU_{pab}}{(mC_P)_P} + \frac{A_cU_{pae}}{2(mC_P)_P}]\Delta\tau)T_{a0} \quad 3.8$$

3.3.2.2. For Pass Air Stream

Consider heat transfer from the collector plate to the air steam, heat transfer from the air-stream to the glazing and heat transfer to the air entering the collector, energy balance on the stream yields:

$$(mCp)_a\frac{dTa01}{dt} = AcU_a\ [T_p - (\frac{Tai+Tao1}{2})] - A_cU_a\ [(\frac{Tai+Tao1}{2}) - T_g\ ] - (\ m_{fra}\ C_{pa})_a(T_{pa01} - T_{ai}) \quad 3.9$$

$$\text{Where: } m_{fra} = 1.7 * \rho * \mu * L*(\frac{G_r}{pr2+\ p_r+0.924})^{0.25} \quad 3.10$$

$$T_{a012} = \{1 - \frac{\Delta\tau}{(mC_P)_a}(m_{fra}\ c_{pa} + A_cU_a)\ T_{a01}\} + \frac{\Delta\tau}{(mC_P)_a}(m_{fra}\ c_{pa} - A_cU_a)\ T_{aio} + [\frac{\Delta\tau}{(mC_P)_a}A_cU_a]\ T_{p0} + [\frac{\Delta\tau}{(mC_P)_a}A_cU_a]\ T_{g0} \quad 3.11$$

3.3.2.3 Glass cover
Energy balance on the glass cover yields:

$$(mC_P)_g\frac{dTg}{dt} = A_cI_N\ (1- \tau_g) + A_cU_{pg}\ (T_p-T_g) - AcUg_a\ [T_p-T_a] \quad 3.12$$

The glazing temperature at time t in relation to the absorbed incident radiation on the surface of the glass, the heat losses from the collector plate to the glazing and heat losses from the glazing to the surrounding at time ($t + \Delta\tau$) is given by:

$$T_{g1} = \frac{AcIN\ (1-\tau g)}{(mC_P)_g}\Delta\tau + \{1- \frac{\Delta\tau}{(mC_P)_g}(A_cU_{pg} - A_cU_{ga})\ T_g + [\frac{\Delta\tau}{(mC_P)_g}A_cU_{pg}]\ T_{p0} + [\frac{\Delta\tau}{(mC_P)_a}A_cUg_a]\ T_{a0} \quad 3.13$$

3.4 Energy Balance Equation for the Drying Process

It is needed to find the drop in temperature as the heated air from solar air heater rises through the drying chamber [14].

3.4.1 Heat and Mass Balance on the First Tray of Drying Chamber

$$(m_aC_p)a\ (T_2 - T_1) = M_{w1}h_{fg} \quad 3.14$$

The temperature of the air stream out going from first tray of the drying chamber at the ambient conditions at time ($t + \Delta\tau$) gains energy from the incident radiant energy on the collector plate and black wall of drying chamber in the first tray is determined from:

$$T_2 = T_1 - \frac{M_{w1}\, h_{fg}}{(mC_P)_a}\Delta\tau \quad 3.15$$

Where: m_a = mass of the dry air through the drying bed, [kg]

C_{pa} = Specific heat of the drying air, [J, kg^{-1}, k^{-1}]

T1 = temperature of the air entering to the bed or exit from the collector, [^{0}C]

T2 = temperature of the air entering to the second chamber or exit from the first chamber, [^{0}C]

m_{w1} = mass of water removed per kg of air, [kg]

h_{fg} = latent heat of vaporization, [KJ,kg^{-1}]

3.4.2 Heat and Mass Balance on the Second Tray of Drying Chamber

$$(m_aC_p)_a\ (T_{2d} - T_{1d}) = M_{w2}h_{fg} \quad 3.16$$

The temperature of the air stream out going from second tray of the drying chamber at the ambient conditions at time ($t+\Delta\tau$) gains energy from the incident radiant energy on the collector plate and black wall of drying chamber in the second tray is determined from:

$$T_{2d} = T_{1d} - \frac{M_{w1}\, h_{fg}}{(mC_P)_a}\Delta\tau \quad 3.17$$

3.5. Heat Loss Coefficient of Flat Plate Collector

It is useful to develop the concept of an overall loss coefficient for a solar collector to simplify the mathematics and defied by the equation.

$$Q^{\cdot} = U_L A_C (T_{Pm} - T_a) \quad 3.18$$

Where: U_L = overall loss coefficient

A_C = area of the collector

T_{pm} = average temperature of the absorber plate and

T_a = temperature of surrounding air (assumed to be the same on all sides of the collector).

Heat is lost to the surroundings from the plate through:

The glass cover (referred as top loss), and the insulation (referred as bottom and edge loss). Each of these loses is also expressed in terms of coefficients called the top loss coefficient, the bottom loss coefficient and the edge loss coefficient.

3.5.1 Top Loss Coefficient

The top loss coefficient, Ut is evaluated by considering convection and re-radiation losses from the absorber plate in the upward direction.

i. Convective Heat Transfer Coefficient

1. From the plate to glass cover

For the prediction of the top loss coefficient, the evaluation of natural convection heat transfer between two parallel plates tilted at some angle to the horizontal is of obvious importance. The natural convection heat transfer coefficient h1c is related to three dimensionless parameters, the Nusselt number Nu, the Rayleigh number Ra, and the Prandtl number Pr, that are given by:

$$h_{1c} = N_u \frac{K}{L} \quad 3.19$$

$$R_a = \frac{g\,\beta \Delta\, T L^3}{\alpha\ \nu} \quad 3.20$$

Nu the Nusselt number-the ratio of the convective heat transfer to the conductive heat transfer. The Nu can be obtained from the expression [11].

$$N_U = 1 + 1.44[1 - 1\frac{1708\sin(1.8\beta)^{1.6}}{R_a \cos\beta}]^+ \left(1 - \frac{1708}{R_a \cos\beta}\right)[\frac{(R_a\cos\beta)^{0.33}}{5830} - 1]^+ \quad 3.21$$

Where: L – is the plate spacing,

g – The gravitational constant,

ΔT – Temperature difference between the plate and the glass, and

R_a– is the volumetric coefficient of expansion of air.

V= wind speed, [m, s^{-1}]

K= the thermal conductivity, [W, m^{-1}, ^{0}K]

υ = kinematic viscosity, [m^2, s^{-1}]

α=thermal diffusivity of air

- ✓ "+" exponent means only the positive value of the term in square bracket is to be considered.
- ✓ Zero is to be used for negative values.

2. From Glass Cover to Ambient

The convective heat transfer coefficient (h2c) at the glass cover is calculated from the following empirical correlation.

$$h_{2c} = 2.8 + 3*v \quad 3.22$$

Where: h_{2c} = is in W/m^2 k

v = wind speed in m/s

ii. Radiative Heat Transfer Coefficient

a) From the plate to the cover

- ➢ The radiative heat transfer coefficient from the plate to the glass cover is expressed as:

$$h_{1r} = \epsilon_{eff}\sigma\{\frac{(T_P+273)^4-(T_g+273)^4}{T_P-T_g}\} \quad 3.23$$

- ➢ The effective emissive of plate-glazing system is given by:

$$\epsilon_{eff} = (\frac{1}{\epsilon_p} + \frac{1}{\epsilon_g} - 1)^{-1} \quad 3.24$$

b) From the Glazing Cover to the ambient

Sky Temperature

The effective temperature of the sky is usually calculated from the following simple empirical relation in which temperatures are expressed in Kelvin.

$$T_{sky} = T_a \quad 3.25$$

- The radiative heat transfer coefficient from the glass cover to the ambient is expressed as:

$$h_{2r} = \epsilon_{eff}\sigma\{\frac{(T_P+273)^4-(T_{sky}+273)^4}{T_P-T_g}\} \quad 3.26$$

- The total heat transfer coefficient from collector plate to cover h1 is expressed as:

  $h_1 = h_{1c} + h_{1r}$

- The total heat transfer coefficient from the cover to ambient h2 is expressed as:

  $h_2 = h_{2c} + h_{2r}$

- The effective heat transfer coefficient from plate to ambient (i.e. the top loss coefficient) is given by:

$$U_t = (\frac{1}{h_1} + \frac{1}{h_2})^{-1} \quad 3.27$$

Finally the rate of heat loss from the top per unit area can be given as:

$$q_{losstop} = U_t (T_p - T_a) \quad 3.28$$

3.5.2 Bottom Loss Coefficient

Heat is lost from the plate to ambient by conduction through the insulation and subsequently by convection and radiation from the bottom surface casing. In most cases, the thickness of insulation provided is such that the thermal resistance associated with conduction dominates. Thus, neglecting the convective resistance at the bottom surface of the collector casing, the bottom loss coefficient is given by:

$$U_b = \frac{K_{in}}{L_{in}} \quad 3.29$$

Where: K_{in} = thermal conductivity of the insulation

L_{in} = back insulation thickness

3.5.3 Edge Loss Coefficient

As in the case of the bottom loss coefficient, it will be assumed that the conduction resistance dominates and that the flow of heat is one-dimensional. The one dimensional approximation can be justified on the grounds that the edge loss coefficient is always much smaller than the top loss coefficient, the edge loss is given as:

$$U_e = U_b\{\frac{A_e}{A_c}\} \quad 3.30$$

3.5.4 Overall Heat Loss Coefficient

The overall heat loss coefficient is the sum of the top, bottom and edge loss coefficient. That is:

$$U_L = U_t + U_b + U_e \quad 3.31$$

The overall heat lost by the absorber to the ambient per unit area per unit time can be expressed as:

$$q_L = U_L (T_p - T_a) \quad 3.32$$

The useful energy gained by the collector is expressed as:

$$Q_u = \alpha \tau I_N A_c - A_c U_L (T_{po} - T_{ai}) \quad 3.33$$

Therefore, the energy per unit area (q_u) of the collector is:

$$q_u = \alpha \tau I N - U_L (T_{po} - T_{ai}) \quad 3.34$$

If the heated air leaving the collector is at collector temperature, the heat gained by the air Qg is:

$$Q_g = m * C_{pa} (T_{po} - T_{ai}) \quad 3.35$$

CHAPTER FOUR

4.1 DESIGN OF SOLAR DRYER

Solar drying refers to a technique that utilizes incident solar radiation to convert it into thermal energy required for drying purposes. Most solar dryers use solar air heaters and the heated air is then passed through the drying chamber (containing material) to be dried. The air transfers its energy to the material causing evaporation of moisture of the material [14].

4.1.1 Coffee Property

The following characteristics of coffee were established standards and some of their values were taken from the literature.

Table 4.1 coffee Characteristics and average meteorological data.

Location	Jimma
Product	Coffee
Initial moisture content(%) wet basis	55%
Desired final moisture content(%)wet basis	11.5%
Maximum permissible drying temperature	60 ^{O}C
Wind speed	2.5m/s
Average ambient relative humidity	69%
Average ambient air temperature	22^{o}c
Drying time(sunshine hours)td	9 hours
Incident solar radiation, I	530w/m^2
Vertical distance between two adjacent trays	10cm

Table 4.2. Physical properties of Arabic coffee [18]

Moisture content of parchment ,% w.b	Length (mm)	Width (mm)	Depth (mm)	Thermal conductivity (W/m K)	Thermal diffusivity (x10^{-}7m2/s)	Specific heat (kJ/kg K)	Bulk density (kg/m^3)	True density (kg/m^3)
9.9	11.95	8.45	4.85	0.1	2.36	1.04	410	875
15.1	11.95	8.50	4.90	0.13	2.03	1.5	430	880

The Coefficient of friction, effect of moisture content of the parchment on friction against the various test surfaces, for, aluminum, at moisture content of parchment 11.5%w.b. is 0.25. Porosity of the parchments effect of moisture content on the porosity of the Arabica parchments for moisture content 11.5%w.b is 0.548 [18].

4.1.2 Design Calculation

The performance of a flat-plate solar collector can be described by the useful gain from the collector per unit time of a collector area Ac and it is the difference between the absorbed solar radiation by plate and the thermal loss or the useful energy output of a collector. The heat gained by the dryer per unit time, Q_d is given by:

$$Q_d = A_c [\alpha \tau I_N - U_L (T_{ai} - T_a)] \quad 4.1$$

Where, Ac= area of transparent cover (m^2)

I_N= incident insulation (W/m^2)

U_L = overall heat loss for the collector (W /0C)

α = solar absorbance

τ = transmittance

Tai = temperature of incoming air

Ta = temperature of ambient air

Since temperature of incoming air is equal to temperature of ambient air, the last term on the right-hand side zero and the rate of energy collection is simply: because the dryer draws the ambient air directly.

$$Q = A_c I \alpha \tau \quad 4.2$$

If the mass of air leaving the dryer per unit time is ma, the heat gained by the air Q_u is:-

$$Q_u = m_a C_{pa} (T_{ao} - T_{ai}) \quad 4.3$$

Where: Cpa= specific heat capacity of air ($KJ/kg\ ^0C$)

Tao = temperature of out-going air

A simplified energy equation for the dryer is $Q_d = Qu$, i.e:

$$Q_d = m_a C_{pa} (T_{ao} - T_{ai}) \quad 4.4$$

Therefore, the required surface area of the transparent cover, which determines the size and dimensions of the dryer, is obtained from:

$$A_c = \frac{m_a * C_{pa}(T_{po} - T_{ai})}{\alpha \tau I N \eta c} \quad 4.5$$

The total energy required for drying a given quantity of coffee beans can be estimated using the basic energy balance equation for the evaporation of water.

$$M_w h_{fg} = m_a C_{pa} (T_{ao} - T_{ai}) \quad 4.6$$

Where, h_{fg} = specific latent heat of vaporization of water from the coffee beans surface (kJ/kg).

M_w = mass of water evaporated from the coffee beans (Kg /s).

The mass of water is estimated from the initial moisture content M_i and the final desired moisture content M_f. The total quantity of moisture to be removed from the coffee beans to bring it to the desired moisture from the initial moisture content is used to determine the total mass flow of air required for drying. The quantity of moisture to be removed (M_w) depends on the coffee parchment and can be found from the following relationship:

$$M_W = m_{cb} \frac{M_i - M_f}{100 - M_f} \quad 4.7$$

$$M_W = 50 \frac{55 - 11.5}{100 - 11.5} \quad 4.8$$

M_w = 22.5Kg water to be removed

Where: Ww = water removed per kg of the air, [kg]

mcb = mass of coffee beans in the dryer chamber, [kg]

Mi = initial moisture content, [present]

Mf = final moisture content, [present]

During drying, water from the surface of the substance evaporates and water in the inner part migrates to the surface to get evaporated. The ease of this migration depends on the porosity of the

substance and the surface area available. Other factors that may enhance quick drying of substances are: high temperature, high wind speed and low relative humidity.

To determine the size of collector and drying bed, it is obvious to know the amount of coffee beans that has gone to be dried.

The total energy required for drying a given quantity of coffee beans items can be estimated using the basic energy balance equation for the evaporation of water is

$$Q_g = M_w h_{fg} \quad 4.9$$

Where: h_{fg} is latent heat of vaporization J/kg which is given by

$$h_{fg} = 4.186 * 10^3 (597 - 0.56 Tp) \quad 4.10$$

Where: Tp -maximum allowable temperature (60^oc)

h_{fg} =2.36MJ/kg

Qg =22.5 kg* 2.36*10^6J/kg

=**53.1MJ/day**

From data which was gathered maximum daily sun shine time in 9 hours

So energy required per second is

Qg = 53.1MJ/9*3600s =1640W

The overall collector efficiencies of solar dryers give in the literature have been shown to vary widely depending on the loading densities and weather conditions. From efficiency collector curves for an air heating flat-plate collector plotted as functions of Ti, Ta and I_T [11].

- $(Ti - Ta)/I_T$ ($m^2\ ^o$c/w) = 0.013

Based the values the collector efficiency is η_c = 42%

$$A_c = \frac{m_a * C_{pa}(T_{po} - T_{ai})}{\eta cIN} = \frac{Mw\ hfg}{\eta cIN} \quad 4.11$$

$$A_c = \frac{1640}{965*0.42} = 4m^2$$

This calculation is done for average maximum values of daily solar radiation and sunshine time in jimma, because, to overcome over size which results in cost reduction.

4.1.3 Sizing the Solar Dryer

The solar air heater serves to provide the primary supply of energy to the dryer. Essentially, the absorber within the air heater converts direct and diffuse solar radiation into heat, which is then transferred to the air flowing through it. Taking the ratio of the length of the air-heater (solar collector) to the width as 3:1, which fulfill the length of the cabinet should be at least three times its width to minimize shading effects of the side panels [16].

A_c= L* w, But L=3*w 4.12

4 = 3w*w Implies that w=1.15m

L= 3.1m.

The breadth of the drying chamber, B, is made equal to the width (W) of the air-heater. Thus, the length of the drying chamber, Ls, is determined from the number of tray in drying chamber, assume three (3), the vertical distance between them is 10cm.

Ls = 3*0.1 + 0.15 = 0.45m

4.1.3.1 Area of Drying Bed

The effective drying bed area Ada is obtained from first principles by relating the solid density of the wet material to its mass and the corresponding volume as:

$$A_{da} = \frac{\mathrm{Mw}}{\rho * h_l} \quad (4.13)$$

$$= 0.45\mathrm{m}^2$$

Where: - M_w is the mass of the coffee bean to be dried,

ρ is the bulk density of the coffee bean on wet basis (421kg/m3),

h_l is the layer drying bed thickness (6cm),

For solar drying of parchment coffee the layer drying bed thickness 6cm can be taken because temperature of drying air much greater the ambient .

Air vent dimensions:

The air vent was calculated by dividing the volumetric airflow rate by wind speed:

Av = Va/Vw

$= 0.044m^2$

Where: Av is the area of the air vent, m^2,

Vw is wind speed, m/s.

The length of air vent, Lv, m, will be equal to the length of the dryer. The width of the air vent can be given by:

$Bv = Av/Lv$

$= 0.036m$

Where Bv is the width of air vent, m

Final or equilibrium relative humidity:

Final relative humidity or equilibrium relative humidity was calculated using sorption isotherms equation for coffee beans as follows:

$aw = 1- \exp[-\exp (0.914+0.5639\ln Mf)]$ 4.14

$= 1- (\exp[-\exp (0.914 + 0.5639 \ln(0.11))]$

$= 0.5122$

Where: aw = water activity, decimal

M = moisture content dry basis, kg water/kg dry solids

$RH_f = ERH = 100 * 0.5122$

$= 51.2\%$

Average drying rate:

Average drying rate, m_{dr}, was determined from the mass of moisture to be removed by solar heat and drying time by the following equation:

$m_{dr} = mw/ td$ 4.15

$= 22.5/9 = 2.46kg/hr$

Mass flow rate of air (m_a):

The mass of air needed for drying was calculated using equation given as follows:

Mass flow rate of air m_a was determined by:

$$m_a = m_{dr} / [w_f - w_i] \quad 4.16$$

Where: wi is initial humidity ratio, 0.014 kg H2O/kg dry air

Wf is final humidity ratio, 0.021 kg H2O/kg dry air

The values of from chart based on the ambient relative humidity and ambient temperature for initial humidity ratio and also the final humidity ratio is based on equilibrium relative humidity and final enthalpy [B.1].

$m_a = 0.05kg/s$

Thus, volumetric flow rate of air V'a = ma/ ρ_a

$$= 0.044m^3/s$$

Drying time (t_d) $= \frac{Mw}{m_a (w_f - w_i)}$

The drying time which get from the meteorological data for average daily sunshine hours is 9hours, depending on this values when change mass flow rate air, the drying time also changes.

4.1.4 Absorbed Radiation

The solar radiation energy incident on the collector surface which is inclined at an angle β to the horizontal, defined in terms of the global radiation G_r, the diffuse radiation D_r, the beam radiation factor R_b and the ground reflectivity factor (ρ =0.2), is given by:[14]

$$I_T = R_b (G_r - D_r) + 0.5(1+\cos\beta) Dr + 0.5\rho (1-\cos\beta) Gr \quad 4.17$$

Where: $R_b = \frac{cos\theta i}{cos\ \theta z}$ 4.18

Θ_i - angle of incident, and

Θ_z - Zenith angle

$$Cos\Theta_i = (\cos\phi \cos\beta + \sin\phi \sin\beta \cos\gamma) \cos\delta \cos\varpi + \cos\delta \sin\varpi \sin\beta \sin\gamma$$
$$+\sin\delta (\sin\phi \cos\beta - \cos\phi \sin\beta \cos\gamma) \quad 4.19$$

$$\cos\Theta z = \cos\phi \cos\delta \cos\varpi + \sin\delta \sin\phi \quad 4.20$$

It is convenient to define an average transmittance-absorbance as the ratio of the absorbed solar radiation, Ic, to the incident solar radiation, I_T.

Thus, the flux collected per unit time is given by:

$$Ic = (\tau_g \alpha_p) \text{ ave } I_T \quad 4.21$$

This is especially convenient when direct measurements are available for I_T.

$$Ic = 0.96*.88*530 w/m^2$$

$$= 448 w/m^2$$

Before calculating let us take some assumption for analysis above formulas as follows: location= Jimma

Latitude (ϕ) = $7.6^o = 8^o$

Collector facing south (γ) = 0^o

From this the unknowns are the hour angle (ϖ), declination angle (δ) and the collector slope (β) which is calculated as follows.

$$\varpi = (ST - 12)*15^o) \quad 4.22$$

$\varpi = -60^o$, Where: ST=solar time

Angle of Tilt (β) of Solar Collector/Air Heater.

It states that the angle of tilt (β) of the solar collector should be

$$\beta = 10^0 + \text{lat } \phi \quad 4.23$$

Where: lat ϕ is the latitude of the collector location, the latitude of Jimma where the dryer was designed is latitude 7.610N.

Hence, the suitable value of β use for the collector:

$$\beta = 100 + 7.10 = l7.610$$

Then the value of the collector slope is assumed as: $\beta = 18^o$

Finally we can find the value of the declination angle for each day of the year starting from day one of the year which is January 1 as n=1.

$$\delta = 23.45 \sin [2\prod (284+n)/365] \quad 4.24$$

$\delta = 2.5^o$

Then substituting the values on the formula:

$Cos\Theta_i = 59^o$

$Cos\Theta z = 60^o$

Based on the allowable maximum of coffee dryer temperature is 60^{o}c and average ambient temperature is 22^{o}c.The mean temperature between them is 41^{o}c, so the air properties on this temperature: Tmean = 314k

ρ (desity of air) = 1.129kg/m^3

C_p (specific heat of air) = 1007KJ/kg*k

K (thermal conductivity) = 0.0266w/m*k

α (thermal diffusivity) = 2.348*10^{-5} m^2/s

ν (kinematic viscosity) = 1.701 *10^{-5}m^2/s

μ (dynamic viscosity) = 1.918*10^{-5} kg/m·s

pr (prandtl number) = 0.726

Top Loss Coefficient:

The top loss coefficient, Ut is evaluated by considering convection and re-radiation losses from the absorber plate in the upward direction.

Convective heat transfer coefficient from the plate to glass cover**:**

$$h_{1c} = N_u \frac{K}{L} \qquad 4.25$$

Where: $N_U = 1 + 1.44[1 - \frac{1708\sin(1.8\beta)^{1.6}}{R_a \cos\beta}]^{+}(1 - \frac{(R_a\cos\beta)^{0.33}}{5830} - 1]^{+}$

$$R_a = \frac{\mathrm{g\ \Delta T\ L^3}}{\mathrm{Tm\ \alpha\ \nu}} \qquad 4.26$$

= 12919.23

L = air gap (distance between plate and glass)

N_U = 2.429

There fore h_{1c} = 2.7w/m^2*k

Convective heat transfer coefficient from glass cover to ambient:

h_{2c} = 2.8 + 3*v

= 10.3w/m^2*k

Radiative heat transfer coefficient from the plate to the cover

$$h_{1r} = \epsilon_{eff}\sigma\{\frac{(T_P+273)^4-(T_c+273)^4}{T_P-T_c}\}$$

Where: $\epsilon_{eff} = (\frac{1}{\epsilon_p} + \frac{1}{\epsilon_g} - 1)^{-1}$

$\epsilon_p = 0.95$

$\epsilon_g = 0.88$

$\sigma = 5.67*10^{-8}$

h_{1r} = 6.633w/m^2*k

Radiative heat transfer coefficient from the glazing cover to the ambient

$$h_{2r} = \epsilon_{eff}\sigma\{\frac{(T_P + 273)^4 - (T_{sky} + 273)^4}{T_P - T_c}\}$$

= 10.5w/m^2*k

The effective heat transfer coefficient from plate to ambient (i.e. the top loss coefficient) is given by:

$$U_t = (\frac{1}{h_{1r} + h_{1c}} + \frac{1}{h_{2r} + h_{2c}})^{-1}$$

= 6.47w/m^2*k

Bottom loss coefficient

$U_b = \frac{K_{in}}{L_{in}}$ = 1.18w/m^2*k

Edge Loss Coefficient

$U_e = U_b\{\frac{A_e}{A_c}\}$ = 0.0479w/m^2*k

The overall heat loss coefficient is the sum of the top, bottom and edge loss coefficient. That is:

$U_L = U_t + U_b + U_e$

= 6.69w/m^2*k

The overall heat lost by the absorber to the ambient per unit area per unit time can be expressed as:

$q_L = U_L (T_c - T_a)$ = 140w/m^2

Then useful energy gained by the collector is expressed as:

$Q_u = \alpha\ \tau\ I_T\ A_c - A_c U_L (T_{co} - T_{ai})$, in watt

$q_u = \alpha\ \tau\ I_T - U_L (T_{co} - T_{ai})$, w/$m^2$

= 0.96 *0.88*530 -140

q_u= 308w/m^2

Equilibrium temperature (T_e):

This temperature is the equilibrium temperature of the drying air and the coffee.

$$T_e = \frac{(1.005+1.88\ Ho)Td+Cpcof\ Tcofo}{L1.005+1.88\ Ho+Cpcof} \quad 4.27$$

Where: T_0=initial temperature, [^{o}k]

T_e=equilibrium temperature of coffee, [^{o}k]

H_0=initial humidity ratio of air, [decimal]

Cp_{cof}=specific heat of coffee, [J, kg^{-1}, k^{-1}]

T_{cof0}=initial coffee temperature, [^{o}k]

4.1.5 Equilibrium moisture content (Emc)

The equilibrium moisture content, Emc, is the moisture content of a product that is in equilibrium with air at a particular mean dry-bulb temperature and relative humidity that would be attained by the grain over in finite time, at a constant value of air relative humidity and temperature. Equilibrium moisture content equation for coffee determined to be: [14]

$$E_{mc} = \{\frac{ln(1-\phi)}{-1.918\ x10-5(Te+51.161)}\}^{0.40898} \quad 4.28$$

4.1.6 Pressure drop

Pressure drops occur at entrances, transitions, exits and elbows due to energy dissipation by eddies and by distortion of velocity profiles. However, the major pressure loss in a dryer is caused by the coffee bed considering the coffee bed as packed bed, the pressure drop through packed beds is the result of frictional losses and inertia characterized by the linear dependence of flow velocity and quadratic dependence of flow velocity respectively as can be seen from the well-known Ergun's Equation [3]

$$\Delta p = \frac{150\mu v_s Y(1-\varepsilon)^2}{D_p^2\varepsilon^3} + \frac{1.75Y\rho_a v_s^2(1-\varepsilon)}{D_p\varepsilon^3} \quad 4.29$$

= 0.0577 +2.01

=2.075pa

Where: Δp is pressure drop

μ is viscosity of air

ρ_a is density of air

ε is porosity

Y is depth of coffee bed (6cm)

D_p is equivalent diameter of the particle

v_s is Superficial velocity

When the air flows through the solar dryer system, due to friction, sudden construction and sudden expansion, the air pressure drops along the length of the flow pipes and channel. Pressure drops along the length of the flow pipes is given below,

$$\Delta p = f\frac{L}{D}\frac{(\rho V^2)}{2} \quad 4.30$$

Reynolds Number (Re) = $\frac{D\rho V}{\mu} = \frac{(\frac{m}{v\tau})DV}{\nu} = \frac{(\frac{m}{v\,A})DV}{\nu} = \frac{(\frac{m}{A})D}{\nu}$ 4.31

For rectangular duct the hydraulic diameter (D) = 4*A/p

D = 0.096m

Re = 4383.4, turbulent flow

4.1.7. Turbulence intensity

Turbulent flow is characterized by random and rapid fluctuations of swirling regions of fluid, called eddies**,** throughout the flow. These fluctuations provide an additional mechanism for momentum and energy transfer. Even when the average flow is steady, the eddy motion in turbulent flow causes significant fluctuations in the values of velocity, temperature, pressure, and even density (in compressible flow). As a result, turbulent flow is associated with much higher values of friction, heat transfer, and mass transfer coefficients [26].

The turbulence intensity, I, referred to as turbulence level, also defined as the ratio of the root-mean-square of the velocity fluctuations, u' to the mean flow velocity, U

$$I = u'/U \quad (4.32)$$

Where: u' is the root-mean-square of the turbulent velocity fluctuations and U is the mean velocity (Reynolds averaged).

When setting boundary conditions for a CFD simulation it is often necessary to estimate the turbulence intensity on the inlets. To do this accurately it is good to have some form of measurements or previous experience to base the estimate on. Here are a few examples of common estimations of the incoming turbulence intensity:

1. High-turbulence case: High-speed flow inside complex geometries like heat-exchangers and flow inside rotating machinery (turbines and compressors). Typically the turbulence intensity is between 5% and 20%.
2. Medium-turbulence case: Flow in not-so-complex devices like large pipes, ventilation flows etc. or low speed flows (low Reynolds number). Typically the turbulence intensity is between 1% and 5%.
3. Low-turbulence case: Flow originating from a fluid that stands still, like external flow across cars, submarines and aircrafts. Very high-quality wind-tunnels can also reach really low turbulence levels. Typically the turbulence intensity is very low, well below 1%.

Fully developed pipe flow:

For fully developed pipe flow the turbulence intensity at the core can be estimated as:

$$I = 0.16\, Re_{dh}^{-1/8} \quad (4.33)$$
$$= 0.16 * 4383.4^{-0.125}$$
$$= 5.6\%$$

Where: Re_{dh} is the Reynolds number based on the pipe hydraulic diameter d_h.

The flow in a circular pipe is laminar for Re equal and below of 2300, turbulent for Re equal and above of 4000, and transitional in between [26].

The based on the value of the friction factor from moody chart, f = 0.025[17].

Where: L is flow channel length (m)

D is pipe diameter (m)

f is friction factor

v is velocity of air

A is area of inlet duct

p is perimeter inlet duct

$\Delta p = (0.025*3.2*1.126*0.64^2) / (2*0.096)$

$= 0.061pa$

Frictional losses are mainly due to flow separation whether it be separation from a sudden expansion or diffusers, vena contracts in a sudden contractions or high angled nozzles, or separation/secondary flows in a pipe bend. Pressure drops by minor losses is given below,

$$\Delta P = \rho K_L \frac{V^2}{2} \quad 4.34$$

Where: K_L is loss coefficient,

For Elbows shape regular 90^o flanged component pipes and ducts the value of loss coefficient is 0.3 [17].

$\Delta P = 1.126*0.3*0.64^2 / 2$

$= 0.069pa$

Then the total pressure drop $\Delta p = 2.205pa$

Fan selection:

Fans provide air for ventilation and industrial process requirements. Fan generate a pressure in move air against a resistance caused by ducts, dampers and others components in a fan system. The fan rotor receives energy from a rotating shaft and transmits it to the air.

For this thesis select the axial flow fan which is single stage compressor of low increasing in pressure rise is used for ventilating. An axial fan uses a propeller to draw the air into the fan and discharges the air the same axial direction.

Velocity air pressure have been established, then velocity can be determined from the equation below:

$$\text{Velocity (v)} = \frac{CP\sqrt{2g*\Delta P*\rho}}{\rho} \quad 4.35$$

Ideal power consumption for fan (without losses) can be expressed as:

$$P_{fan} = \frac{\Delta p*v\prime}{\eta_E \eta_M} \quad 4.36$$

$$= 0.143\text{kw}$$

Where: Pfan is electrical fan power consumption

η_E (80%) is electromotor electric efficiency

η_m (85%) is impeller mechanical efficiency

By using this two values flow rate of air in the duct and total pressure drop in duct from the fan curve the fan power in put P =0.143kw and the speed of the fan = 160rpm [24].

4.2 Performance Evaluation of Dryers

4.2.1 Collector Efficiency (η_c)

Collector efficiency measures the thermal performance, i.e. the useful energy gain of the collector. Not all of the solar radiation from the sun incident on the collector surface is converted to heat. Part of the radiation is reflected back to the sky and the other component is absorbed by the glazing. Once the collector absorbs heat and as a result temperature gets higher than the surrounding, there will also be a heat loss to the atmosphere by convection and radiation.

Collector efficiency (η_c) measures how effectively the incident energy on the solar collector is transferred to the air flowing through the collector and is given as the ratio of the useful energy output (over a specified time period), to the total radiation energy I_T, available during the same period [19]:

$$\eta_c = \frac{m_a*C_{pa}(T_{po}-T_{ai})}{\text{AcIN}} \quad 4.37$$

4.2.2 Drying Efficiency (η_d)

Drying efficiency is the ratio of the energy needed to evaporate moisture from the material to the heat supplied to the dryer. This term is used to measure the overall effectiveness of a drying system. But it may not be used for comparing one dryer with another due to different factors such as the

particular material being dried, the air temperature and mode of air flow may differ for various dryers [19].

Effects of Various Parameters on Dryer Performance

A large number of parameters influence the performance of air heater flat-plate collector. These parameters could be classified as:

- ✓ Design parameters,
- ✓ Operational parameters,
- ✓ Meteorological parameters, and
- ✓ Environmental parameters

The effective total area surface of the dryer for collecting incident radiation is related to the overall system drying efficiency (ηd), which is given by

$$\eta_d = \frac{\mathrm{Mw\ hfg}}{\mathrm{A_c I_t\ t+pfan}} \qquad 4.38$$

Where: A_c is the total area of the dryer receiving incident radiation (the total surface area of the primary and secondary collectors),

t is the total time,

h_{fg} is the latent heat of vaporization and It the intensity of radiation incident on a tilted

P_{fan} is fan power

4.3 Mass and heat transfer of dryer

The drying process coffee parchment involved by two mechanism: the migration of moisture from the interior of an individual material to the surface, and the evaporation of moisture from the surface to the surrounding air. For this design the initial total mass of coffee dryer was 50kg contenting initial moisture content 55% and final moisture content 11.5%. The inlet dry air through the dry chamber 60^{o}c and humidity 0.021 kg H_20/kg dry air and dry air outlet 41^{o}c. The coffee enters at 22^{o}c and with wet bulb temperature was 26^{o}c.

Water content in the coffee feeds = 50kg *0.55 = 27.5kg

Dry coffee in feeds = 50 - 27.5kg = 22.5kg

Water content in product = 22.5 * 0.115 = 2.5kg

Water removed by the drier = 22.5 - 2.5 = 20kg

The migration of moisture from interior of coffee parchment to the surface using conduction (called diffusion). The rate of mass diffusion m_{diff} of a water vapour in a stationary medium (coffee parchments) in the direction y is proportion to the concentration gradient dc/dy in that direction:

$$m_{diff} = -D_{AB} * A * dCA/dy \quad (4.39)$$

Where: D_{AB} is the diffusion coefficient (or mass diffusivity of the water vapour in the coffee parchment)

CA is the concentration of the species in the mixture at that location

The evaporation of moisture from the surface to the surrounding air by using convection. Convection means the mass transfer mechanism between a surface and a moving body fluid that involves both mass diffusion and bulk fluid motion.

$$m_{conv} = h_{mass} Ac(C_s - C_{inf}) \quad (4.40)$$

Where: m_{conv} is the rate of mass convection

h_{mass} is the mass transfer coefficient

As is the surface area and

$C_s - C_{inf}$ is a suitable concentration difference across the concentration boundary layer.

4.3.1 Mass transfer by convection:

From the design system the outlet of air heater (inlet of the dryer chamber) temperature, velocity, and related humidity ration of air are 60^{o}c, 1.4m/s, and 0.014kg H_2O/kg drying air respectively. The above surface coffee drier (that means free stream air condition) the temperature 22^{o}c, pressure 83.3kpa and relative humidity of air 69.15%. The air–water vapor mixture is dilute and thus can use dry air properties for the mixture at the average temperature of 41°C. Noting that the total atmospheric pressure is 83.3/101.3= 0.8280 atm, the properties of dry air at 41°C and 0.8280 atm are:

k = 0.02644 W/m·K, Pr = 0.7262

$\alpha = (2.312 \times 10^{-5}\ m2/s)/0.8280 = 2.545 \times 10^{-5}\ m2/s$

$v = (1.679 \times 10^{-5}\ m2/s)/0.8280 = 1.849 \times 10^{-5}\ m2/s$

The properties of water at 60°C are:

hfg = 2383 kJ/kg and Pv = 12.35 kPa.

Taking the water vapor and the air as ideal gases and noting the total atmospheric pressure is the sum of vapor and dry air pressures, the densities of the water vapor, dry air and their mixture at the water –air interface and far from the surface are determined to be:

At the surface:

$$\rho_{v-s} = \frac{p_{v-s}}{R_v T_S} \qquad 4.41$$

Where: ρ_{v-s} is density of water vapor at the surface

Pv-s is vapor pressure at the surface

Ts is vapor temperature at the surface

Rv is universal constant of vapor = 0.4615kpa/kg k)

$$\rho_{v-s} = \frac{12.35\ kpa}{0.4615\frac{kpa*m2}{kg\ k}\ x\ 323k} = 0.08285 kg/m^3$$

$$\rho_{a-s} = \frac{p_{a-s}}{R_a T_S} \qquad 4.42$$

Where: ρ_{a-s} is density of dry air at the surface.

Pa-s is dry air pressure at the surface

Ts is vapor temperature at the surface

Ra is universal constant of dry air = 0.2875kpa/kg k)

$$\rho_{a-s} = \frac{83.3\ kpa - 12.35\ kpa}{0.287\frac{kpa*m2}{kg\ k}\ x\ 323k} = 0.765 kg/m^3$$

$\rho_s = 0.0285 + 0.765 = 0.848 kg/m^3$

Away from the surface:

$$\rho_{v-inf} = \frac{p_{v-inf}}{R_v T_{inf}} \quad 4.43$$

Where: ρ_{v-inf} is density of water vapor away from the surface.

Pv-inf is vapor pressure away from the surface

Tinf is vapor temperature the free stream

But, $p_{v\text{-}inf} = \phi * p_{sat@}T_{inf}$ = 0.6913 x 3.13kpa = 2.1kpa

$$\rho_{v-inf} = \frac{2.1kpa}{0.4615\frac{kpa*m2}{kg\,k}\ x\ 298k} = 0.0144 kg/m^3$$

$$\rho_{a-inf} = \frac{p_{a-inf}}{R_a T_{inf}} \quad 4.44$$

Where: ρ_{a-inf} is density of dry air away from the surface.

Pa-s is dry air pressure away from surface

Tinf is free stream air temperature

$$\rho_{a-inf} = \frac{83.3\ kpa - 1.98\ kpa}{0.287\frac{kpa*m2}{kg\,k}\ x\ 298k} = 0.9508 kg/m^3$$

$$\rho_{inf} = 0.9508 + 0.0144 = 0.9652 kg/m^3$$

The area of the dryer chamber of the coffee parchment stored is A_s = (1.2 m) (0.65 m) = $0.78m^2$ and its perimeter is p = 2(1.2* 0.65) = 3.7 m.

Therefore, the characteristic length is Lc = As /p = 0.21m

The using upstream velocity and characteristic length for forced convection flow, the Reynolds number is determined to be:

$$Re = v * L_c/\nu \quad 4.45$$

Where: v is free stream velocity

Re = (2.5 * 0.21)/1.848 $x10^{-5}$ = 15909.8, the flow is turbulent

The nusselt number is determined to be:

$Nu = 0.023Re_L^{0.8} pr^{0.4}$ 4.46

Where: Nu = nusselt number

$Pr = \frac{\nu}{\alpha} = 0.722$

Nu = 24.87

The convection heat transfer coefficients are determined to be:

$h_{conv} = NuK/Lc$ 4.48

$= 3.13 w/m^2 k$

The mass diffusivity of water vapor (D_{AB}) in air at the average temperature of 315.5K is determined to be:

$D_{AB} = D_{H20-air} = 1.87 \times 10^{-10} \frac{T^{2.072}}{P}$ 4.49

$= 1.78x10^{-10} (315.5^{2.072}/0.6804)$

$= 4.005 x10^{-5} m^2/s$

The Schmidt number is determined from its definition to be

$Sc = \frac{\nu}{D_{AB}}$ 4.50

Sc = 0.634

The Sherwood number and the mass transfer coefficients are determined to be

$Sh = 0.023(Re_L)^{0.8} (Sc)^{0.4}$ 4.51

= 24.87

$h_{mass} = \frac{S_h * D_{AB}}{L_C}$ 4.52

$= \frac{24.87\ X\ 4.005\ X10-5_1}{0.2108} = 0.0137 m/s$

Then the evaporation rate (mv) become

$m_v = h_{mass} A_s (\rho_{v-s} - \rho_{v-inf})$ 4.53

= 0.0137 * 0.78 * (0.08285 -0.0144)

m_v = 0.00073kg/s = 2.63kg/h

4.3.2 Mass transfer by diffusion:

$m_{diff} = D_{AB}A(\rho_{v\text{-}s} - \rho_{v\text{-}inf})/L$ 4.54

= 4.005×10^{-5} *0.78 (0.08285 – 0.0144)/0.2108

= 1.014×10^{-5} kg/s

Heat transfer during mass transfer:

- ✓ Heat required to raise the product to discharged temperature =

Dry coffee in feed x specific heat of coffee (average temperature of dry air – ambient temperature of coffee inlet) + water content in product (average temperature of dry air – ambient temperature of coffee inlet)

= 22.5 * 1030(41 – 22) + 2.5 (41 – 22)

= 0.44×10^6 J

Heat required to remove the water = 53MJ

Total heat = 53.44MJ

- ✓ Heat required to preheat the feed from inlet to wet bulb temperature (preheating period) =

= 22.5 *1.03kJ (26 -22) + 27.5 (26-22)

= 93.71kJ

- ✓ Heat required to heat product from wet bulb temperature to discharge temperature (heating period)

= 22.5 *1030 (41 – 26) + 2.5 (41 -26)

= 0.43MJ

- ✓ Heat required to evaporate water wet bulb temperature (evaporating period)

  = 53.44 – 0.093 -0.43 MJ

  = 52.9917MJ

Natural convection heat transfer rate becomes:

$Q_{conv} = h_{conv}A_s (T_s - T_{inf})$ 4.55

= 73.37w

CHAPTER FIVE

CFD Simulation of Solar Dryer Using ANSYS FLUENT

Computational fluid dynamics (CFD) is the analysis of systems involving fluid flow, heat transfer and associated phenomena such as chemical reactions by means of computer-based simulation.

Simulation is an important tool for design and operation control. For the design of a drying system, simulation makes it possible to find the optimum design and operating parameters. Also for to control system, simulation provides a means to devise control strategies and to analyze the effects of disturbances [10].

The operation of solar dryer and physical phenomena that take place in it is explained by the three processes of heat transfer and the properties of the solar radiation. Sun energy incident on semi-transparent cover (polycarbonate) of the collector is transmitted in the visible range and is practically opaque to radiation in the longer-wavelength infrared regions of the electromagnetic spectrum. A fraction of solar radiation is reflected by the polycarbonate and the other fraction is transferred to the absorber plate increasing its temperature, transferring heat by convection and radiation into the air causing the greenhouse effect, changing its density, and pushing it by the cooler air into the cabinet and the chimney to induce air flow through the dryer [12]. Considering merits and demerits of different configurations and to minimize the pressure drop throughout the system by using ANSYS15.0.7, different dryer configuration based on pressure drop and uniform air flow distribution have been compared.

Moreover, there are several unique advantages of CFD over experimental-based approaches to fluid systems design.

- Substantial reduction of lead times and costs of new design.
- Ability to study systems where controlled experimental are difficult or impossible to perform. (e.g. very large systems)
- Ability to study systems under hazardous conditions at and beyond their normal performance limits. (e.g. safety studies and accident scenarios)
- Practically unlimited level of detail of results.

In contrast CFD codes can produce extremely large volumes of results at virtually no added expense and it is very cheap to perform parametric studies, for instance to optimize equipment performance [18].

CFD codes are structured around the numerical algorithms that can tackle fluid flow problems. In order to provide easy asses to their solving power all commercial CFD packages include sophisticated user interfaces to input problem parameters and to examine the results. Hence all code contains three main elements:

- Pre-processor
- Solver
- Post-processor

To solve the physical phenomena used the ANSYS-FLUENT 15.0.7 code, and the following steps where applied:

- Design geometry and discretization of the control volume using ANSYS design modeler program.
- Specification of construction material properties and boundary conditions for each system element.
- Solution of the conservation equations in each element of the mesh for each time interval.
- Graphical representation of the results [5].

The overall dimension for solar coffee dryer is 1.2 X 3.33 X 0.05 m^3 of solar air heater with 1.2 X 0.65 X 0.5m dryer chamber. And 0.005m thick glass plate. A sheet of Aluminum with thickness 0.001 m and 1.2 x 3.33 m^2 area with longitudinal fins attached to lower surfaces was used as the absorber plate. The distance between glass and absorber that means air gap is 0.05m. Another wood for insulated part with thick 0.02m.

Table 5.1 material properties which used for ANSYS FLUENT

No-	Thermal conductivity(w/m k)	Density (Kg/m^3)	Specific heat (KJ/kg*k)
Air	0.025	1.069	1007
Aluminum	202.5	2719	871
Glass	1.19	2500	840
Insulated	0.173	700	2310

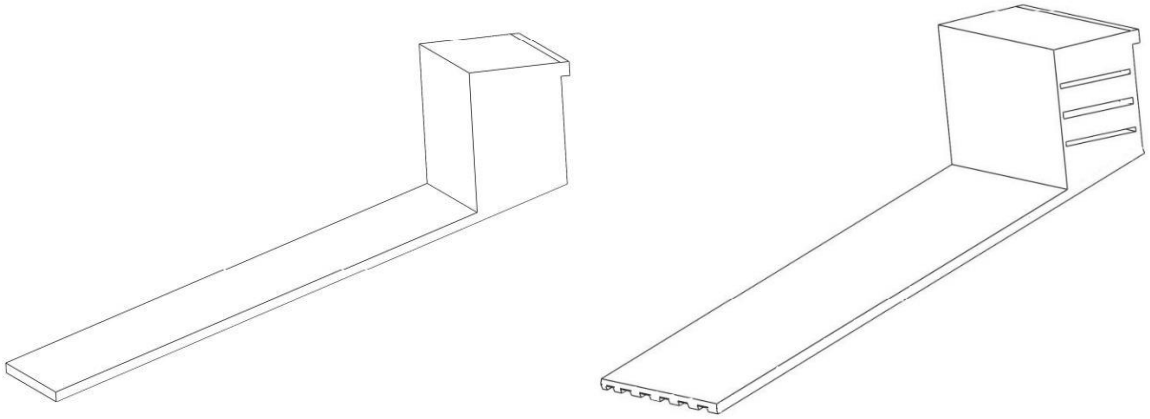

A) Flat plate collector B) Rectangular type of collector

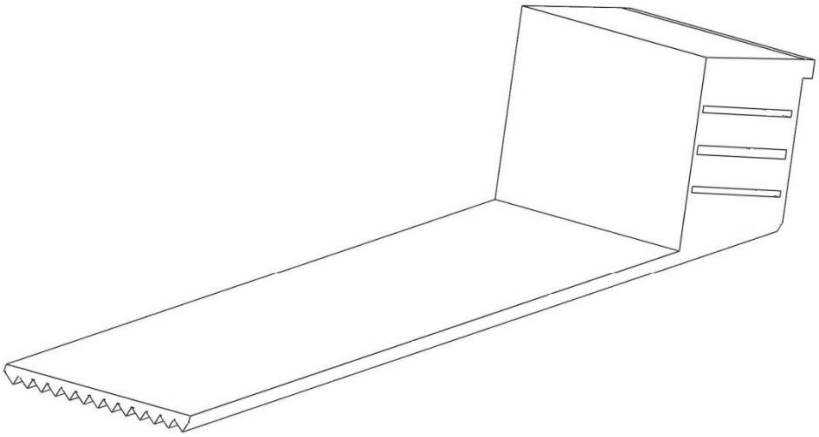

C) v-grooved type of collector

Figure 5.1. Different models of solar dryer based on the collector types using solid work

Table 5.2.Surface area of different type's solar dryer.

Types of dryer	Flat plate collector	Rectangular collector	V-grooved collector
Surface area (m^2)	3	3.25	4.22

The 3D model consisting of the solar air collector involving air inlet, absorber plate, and glass cover plate is modeled by ANSYS Workbench and the unstructured grid was created in ANSYS ICEM. The results were obtained by using ANSYS FLUENT software.

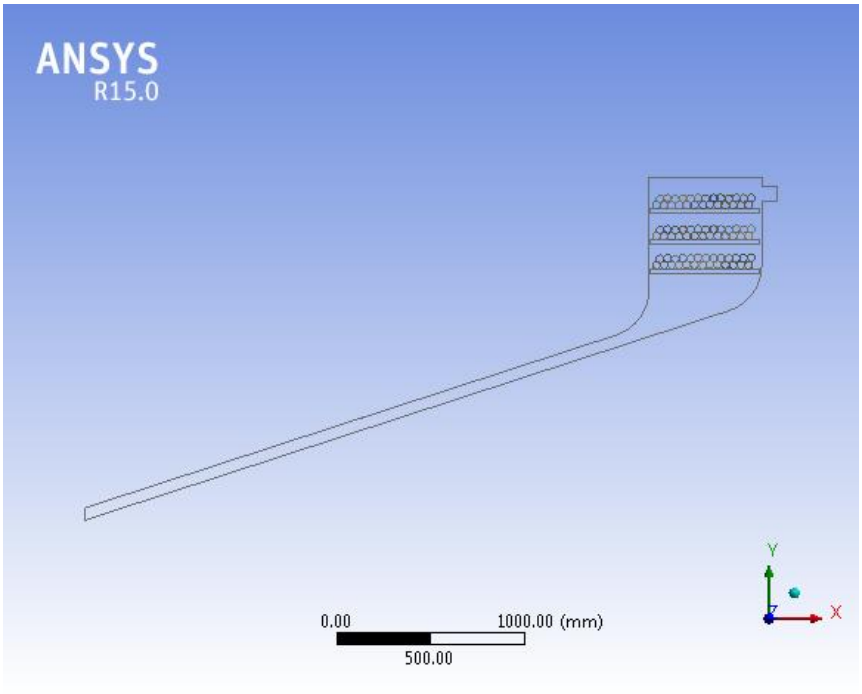

Figure 5.1. 2D drawing of solar coffee dryer using ANSYS

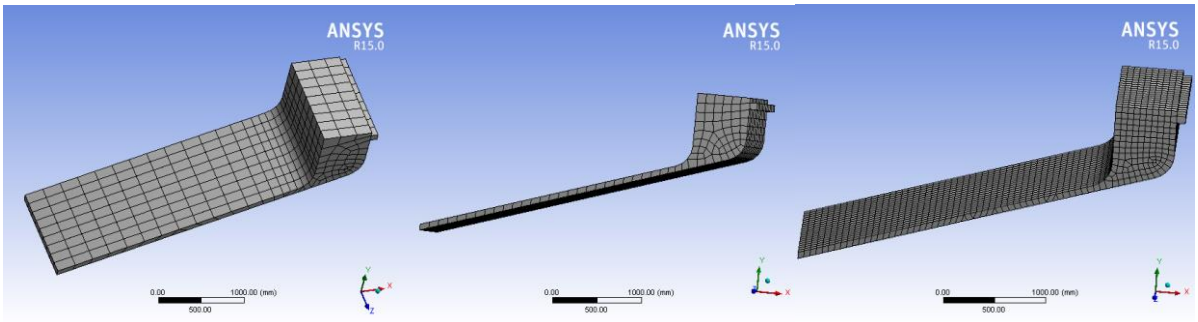

a) Coarse b) medium c) fine

Figure 5.2.Types of meshing by using ANSYS FLUENT

CHAPTER SIX

RESULT AND DISCUSSION

After all stages of this thesis, some results are observed and presented in analytical and simulation results. The analytical results contain the energy required for dyer, moisture to be removed and drying time. The simulation result has been expressed by figure bellows. These figures contain temperature, pressure and velocity profile values of collector, duct shapes, arrangements of trays and direction of air flow between outlet and inlet air heater with solar dryer at same and different mass flow rate. After observing all those results present, there will be some discussion which describes that solar dryer has high efficiency and optimized one.

6.1 ANALYTICAL RESULTS

a) The moisture to be removed

The moisture to be removed with initial coffee mass at fixed initial moisture content 55% in wet basis. It is shown that moisture to be removed is directly proportional to initial coffee mass at fixed initial moisture content which means moisture to be removed increasing with increasing initial coffee mass.

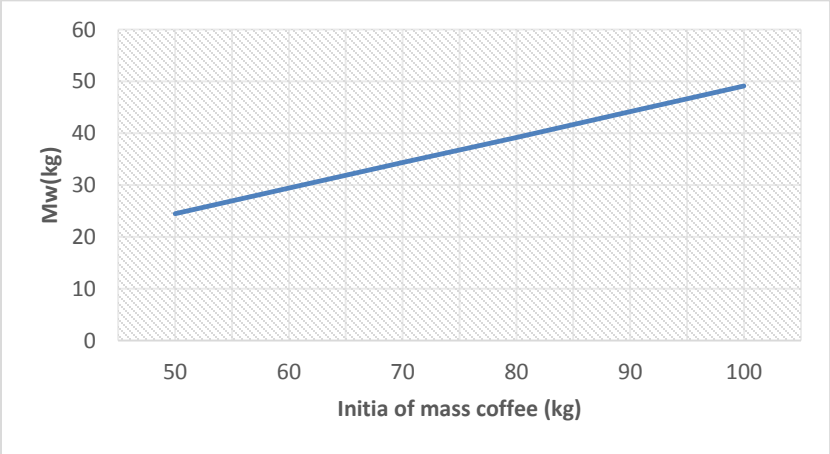

Figure 6.1.The variation of moisture to be removed vs initial coffee mass at fixed initial moisture content (Mi=55%).

b) Drying time

Drying time variation with mass flow rate of air at fixed coffee mass (50kg) and the outlet temperature of solar collector which means dryer inlet temperature (42°c). It is shown that the drying time is a function of mass flow rate of air at fixed inlet condition.

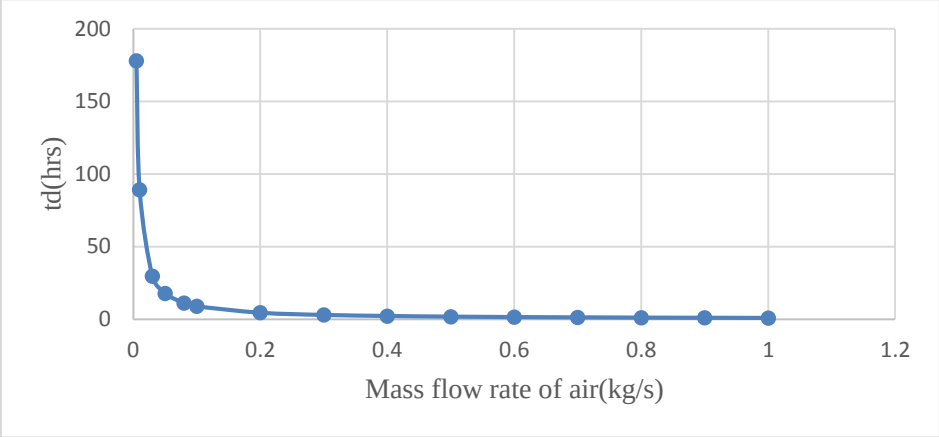

Figure 6.2. Drying time variation with mass flow rate of air at fixed coffee mass (50kg) and dryer inlet temperature (42°c)

c) equilibrium moisture content

Fig.6.3 illustrates the variation of the equilibrium moisture content with the relative humidity of the ambient air. It is shown that the equilibrium moisture content is a function of relative humidity. Equilibrium moisture content increases with increasing relative humidity.

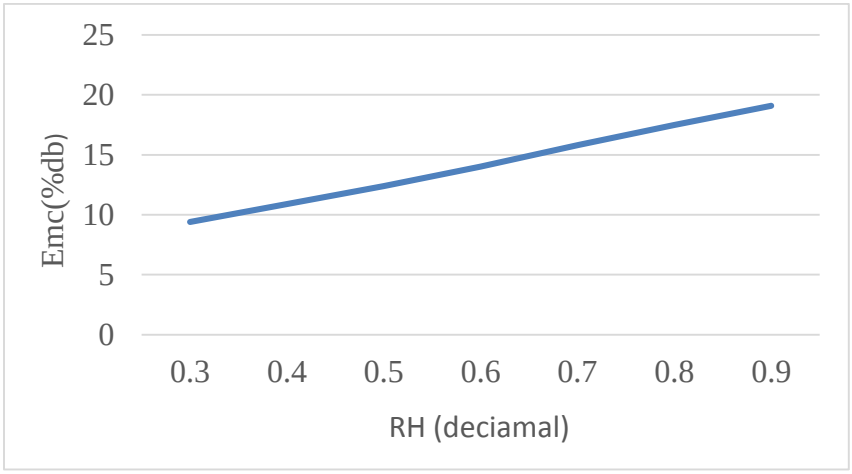

Figure 6.3.Variation of equilibrium moisture content with relative humidity of drying air at fixed temperature

6.2 SIMULATION RESULTS

Here by using ANSYS Fluent 15.0.7 for solving governing equations. To find out best design of the solar coffee dryer should know about the dynamic behavior inside solar dryer. By using fluent can know about the behavior of the air velocity, temperature and pressure inside the dryer. The uniform air distribution inside the dryer is possible with forced convection. So simulation has been done on the whole solar dryer not any part of the solar dryer. The simulation was carried out pressure profiles velocity profiles and temperature profiles inside the solar dryer. The temperature fluctuates throughout the day so soar dryer temperature and pressure are fluctuates respectively as well as air velocity profile also fluctuates throughout the day. The result is analyzed the different models with different and same parameter shown at figure bellows.

Table 6.1 grid sensitivity study

Types mesh	Number of element	Number of nodes	Output temperature (^{o}c)	Pressure drop (pa)	Max. Velocity (m/s)	(%) change of T_{out}	(%) Change pressure
Coarse	585	960	45	0.129	0.252	0.66	3.4
Medium	1068	1768	45.3	0.138	0.261	0.43	6.7
Fine	3572	5220	45.5	0.142	0.311	0.65	0.95
fine	3610	5240	45.8	0.144	0.314	0	0

For the (0.05kg/s) uniform inlet temperature in solar collector, simulated result showed a smooth increase in output temperature and velocity magnitude, but for mesh size finer than coarse, the temperature rising and velocity fluctuation did not detect. Therefore, the coarse mesh with 585 cells was selected for simulation analysis. Also the pressure drop of coarse mesh for solar dryer was lower than the three others mesh. A detail view of the mesh domain for solar dryer has been presented in fig 5.2.

6.2.1 Simulation results for different types of solar collector dryer.

The simulation results were within the same flow (laminar flow), duct shape type (smooth curve) and when air flow was passed above the absorber plate of the collector dryer. Those simulation results shows the effect of different types of collector on the temperature outlet of air, pressure drop and velocity flows.

A) Smooth flat plate collector

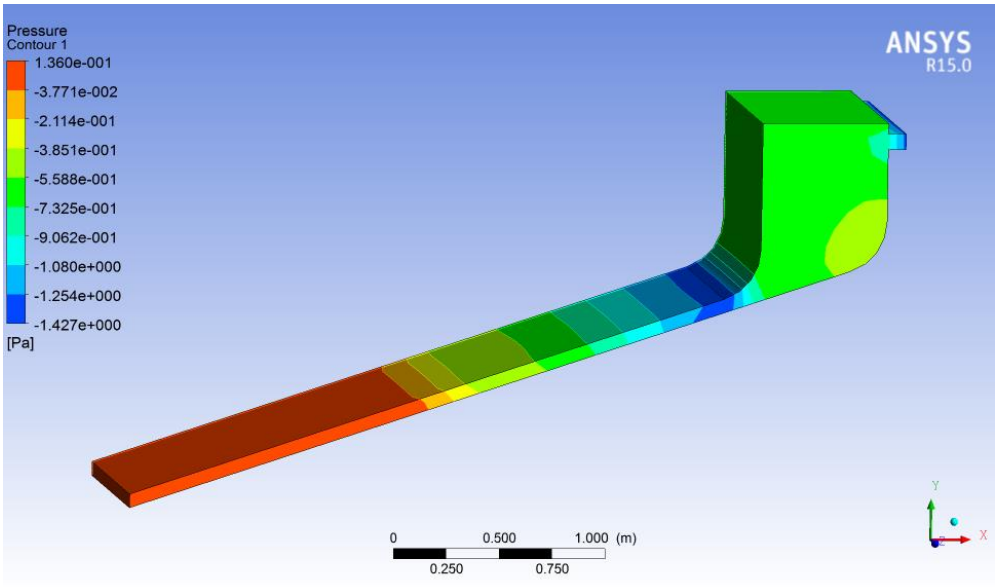

Figure 6.4. Pressure contour for smooth flat plate collector

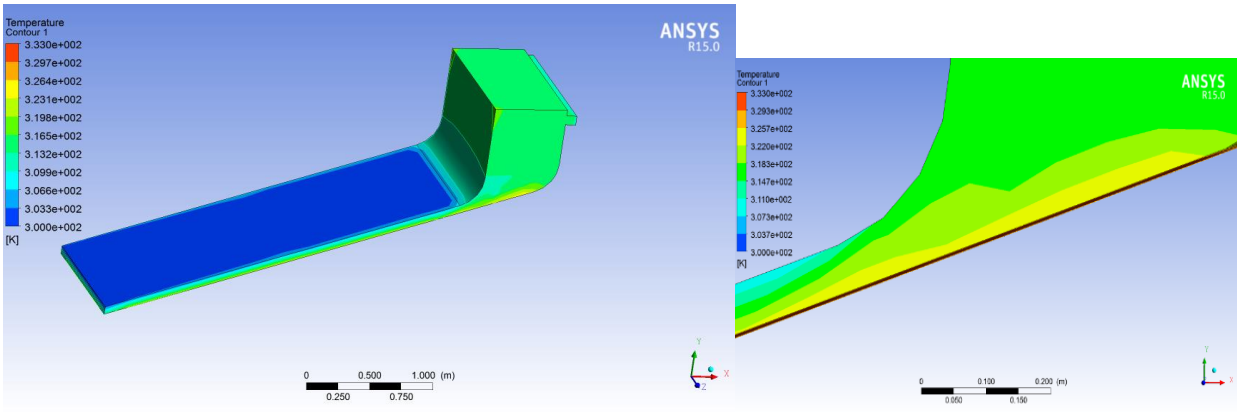

Figure 6.5. Temperature contour for smooth flat plate collector

The above figures from (6.4-6.5) shows the pressure contour and temperature contour on smooth flat plate collector. From those figures at (0.05kg/s) mass flow rate inlet to the collector of the dryer outlet temperature of air from collector which enter in to the solar dryer chamber is 43^{o}c and average pressure drop 0.35pa.

B) Rough flat plate collector when air flow above absorber plate

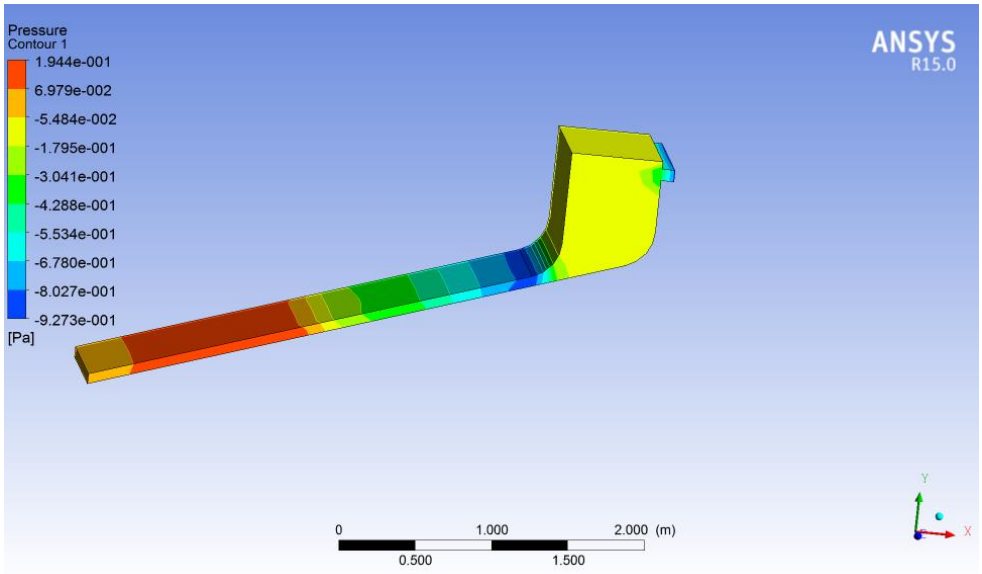

Figure 6.6. Pressure contour rough flat plate collector

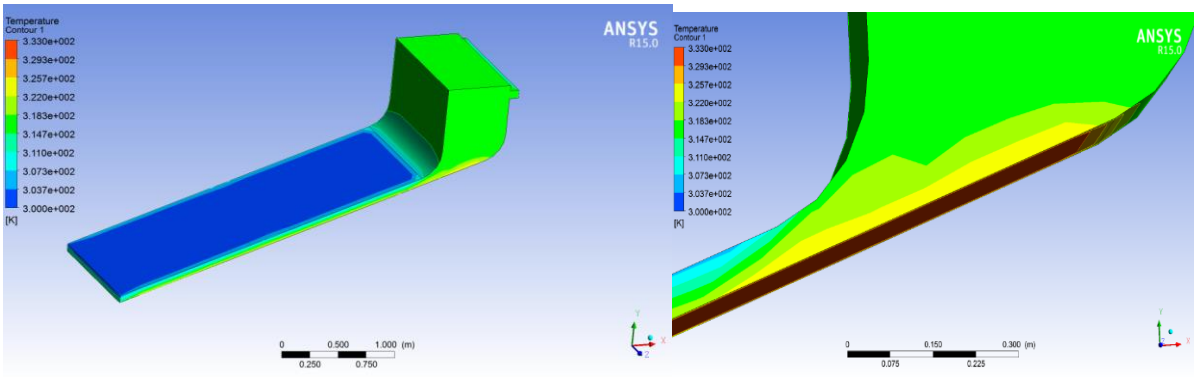

Figure 6.7.Temperature contour rough flat plate collector

The above figures from (6.6-6.7) shows the pressure contour and temperature contour on roughen flat plate collector when air flow above absorber plate of the solar dryer. From this dryer at (0.05kg/s) mass flow rate inlet to the collector, the dryer outlet temperature of air from flat plate collector which enter in to the solar dryer chamber is 43.5^{o}c and pressure drop 0.207pa.

C) V-groove type of collector plate.

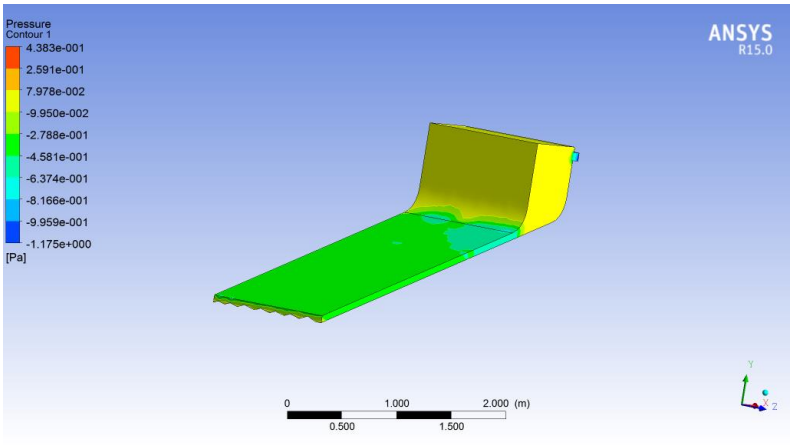

Figure 6.8. Pressure contour V-groove type of collector

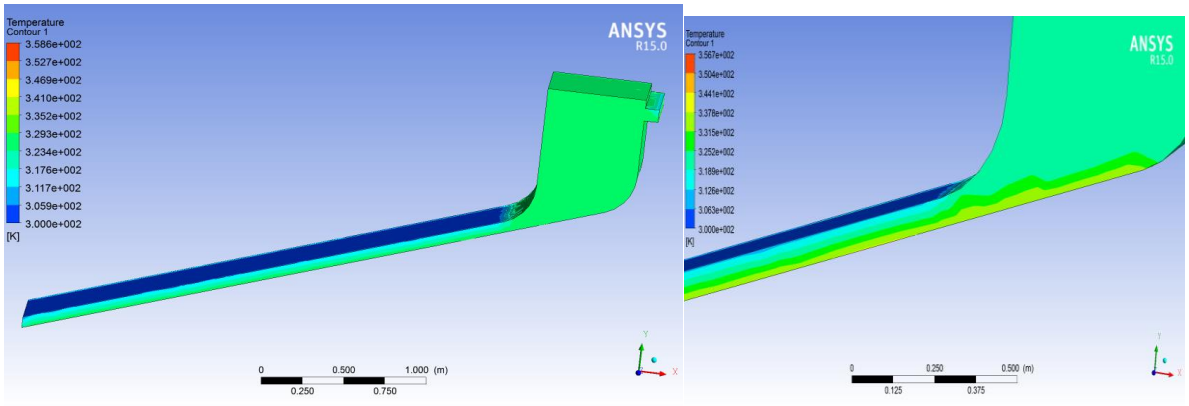

Figure 6.9. Temperature contour V-groove type of collector

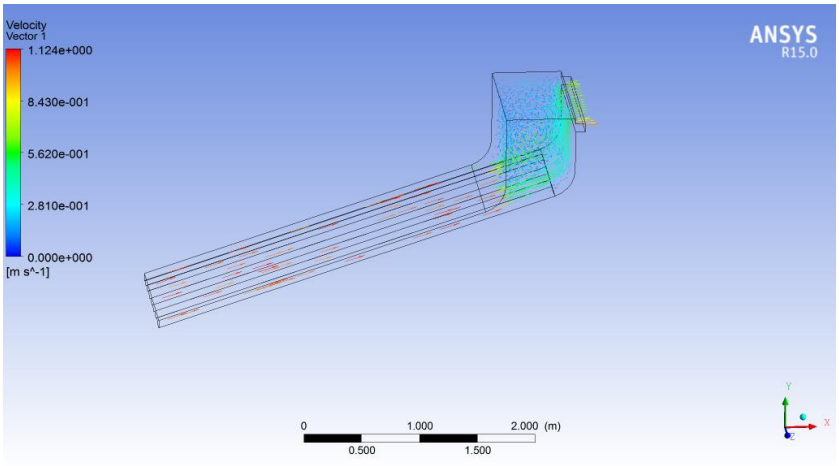

Figure 6.10. Velocity vector profile V-groove type of collector

The above figures from 6.8 – 6.10, shows the pressure contour, temperature contour and velocity profile on V-groove type of collector when air flow above the absorber plate of the solar dryer. From this mode at (0.05kg/s) mass flow rate inlet to the collector, the outlet air from v-grooved type collector temperature which enter to the solar dryer chamber is 46.5^{o}c and pressure drop 0.225pa

D) Rectangular type of collector plate

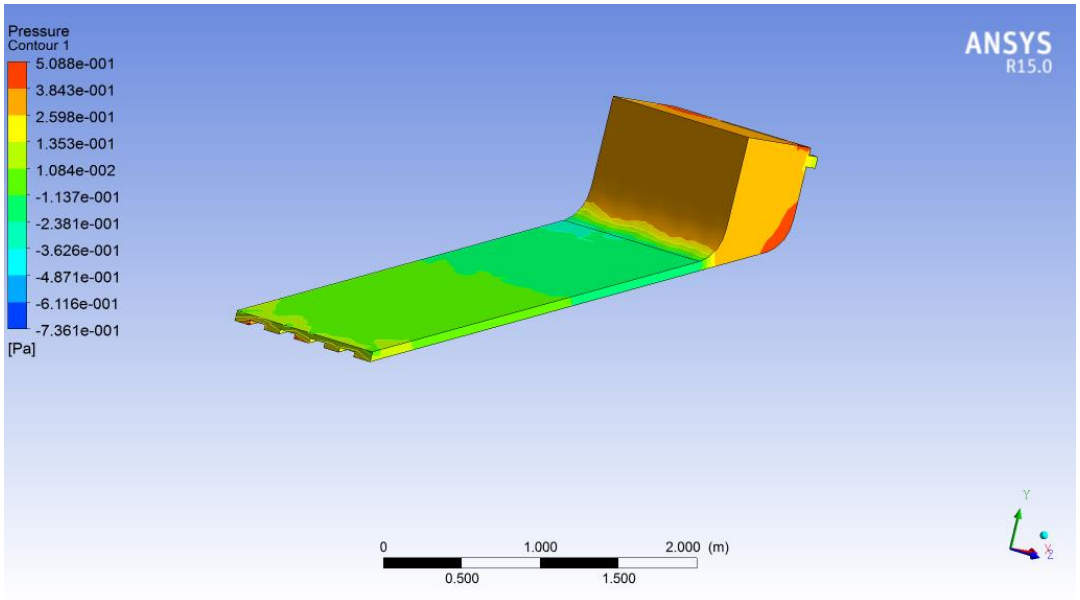

Figure 6.11. Pressure contour rectangular type of collector plate

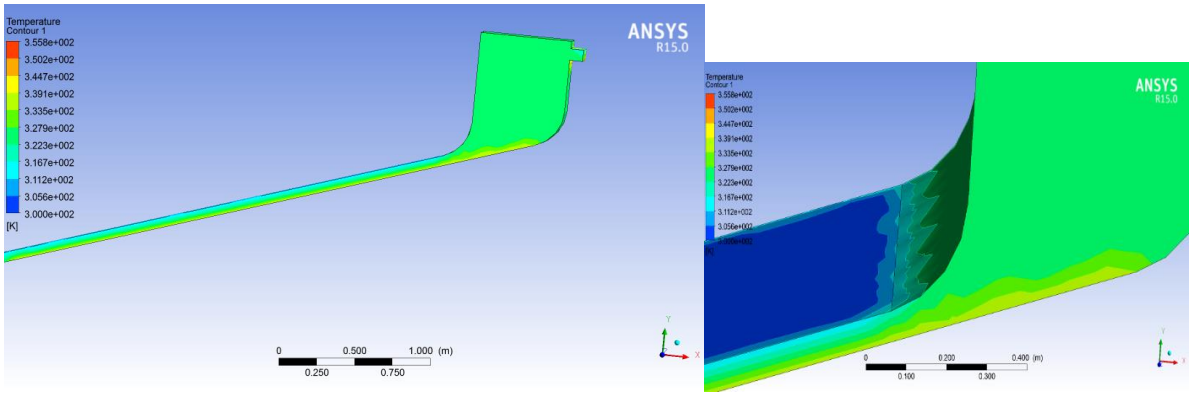

Figure 6.12. Temperature contour rectangular type of collector plate

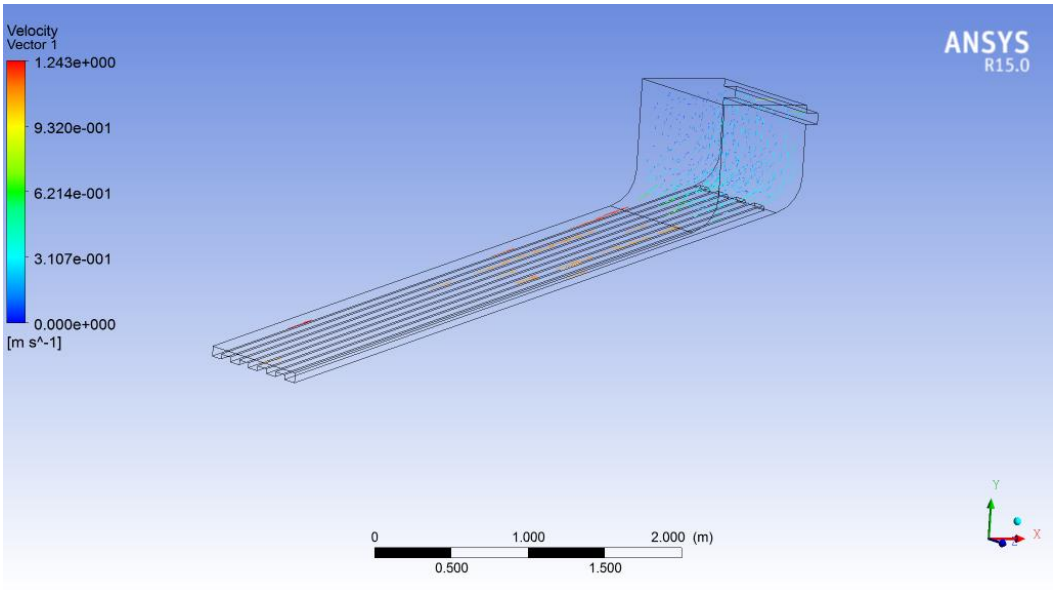

Figure 6.13. Velocity vector profile rectangular type of collector plate

The above figures from 6.11 – 6.13, shows the pressure contour, temperature contour and velocity profile on rectangular type of collector when air flow above the absorber plate of the solar dryer. From this types collector at (0.05kg/s) mass flow rate inlet to the collector, the outlet air from rectangular collector of temperature which enter to the solar dryer chamber is 44^{o}c and pressure drop 0.195pa.

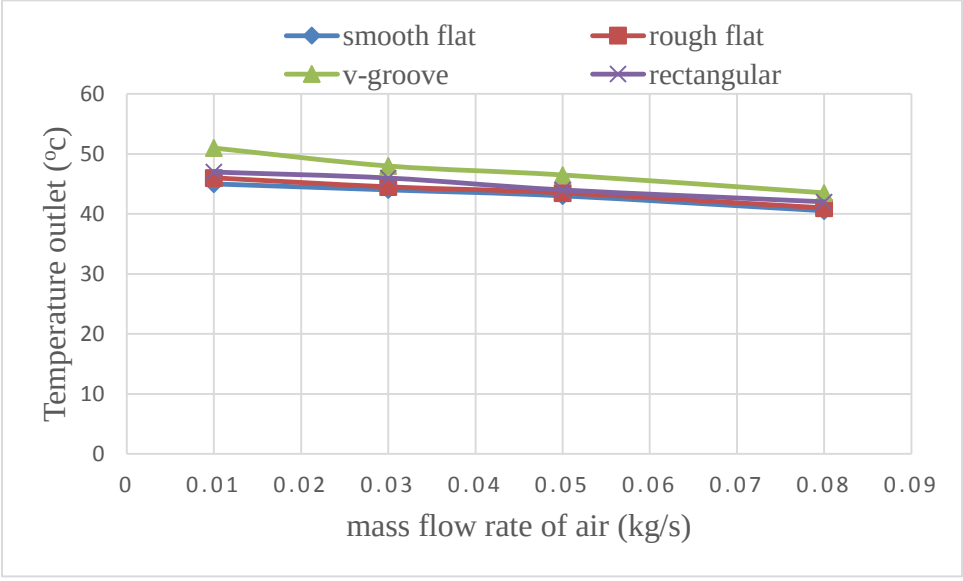

Figure 6.14. Variation of outlet temperature with mass flow rate at different geometry

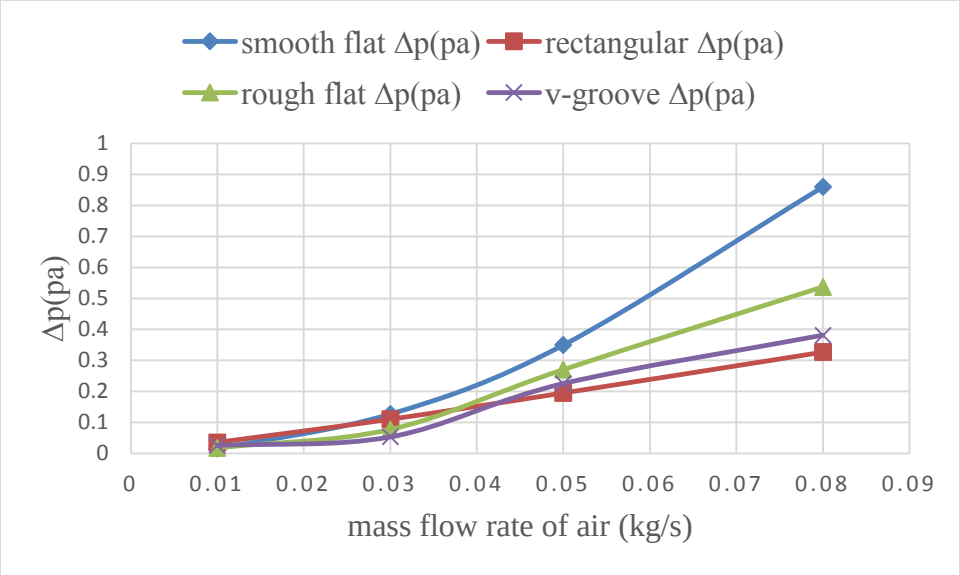

Figure 6.15. Comparing different geometry by pressure drop with mass flow rate.

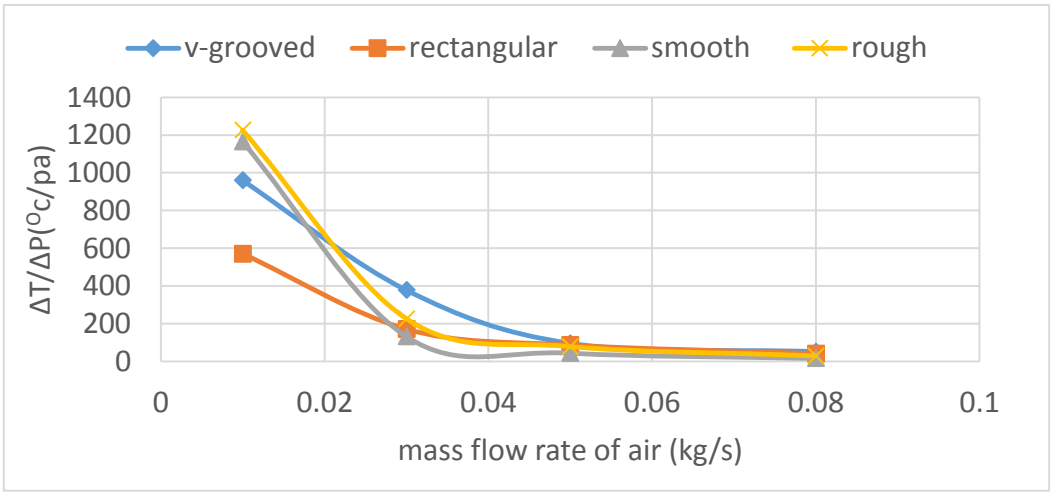

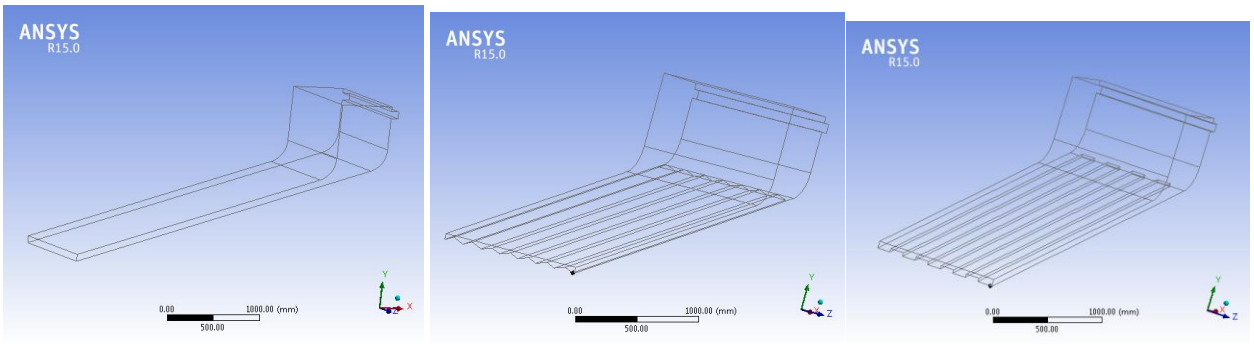

A, smooth flat plate B, v-grooved shape C, rectangular shape

Figure 6.16. Comparing different geometry by unit change outlet temperature per unit change pressure drop with mass flow rate.

Comparing the above results based on temperature outlet of solar air heater (temperature inlet of solar dryer chamber) quantitatively, v-groove types of solar collector when air flow above the absorber plate of solar dryer has higher temperature outlet than any other three solar collector configuration shown in fig 6.14. By velocity stream line and vector comparing the four dryer configuration qualitatively, velocity stream line for rough flat plate of collector dryer connection with guide vanes is better than any other dryer configuration type. Comparing based on pressure drop quantitatively, v-grooved collector dryer configuration has small pressure drop when mass flow rate was small than any other three dryer configuration and rectangular collector dryer configuration has small pressure drop when mass flow rate at maximum value shown in fig 6.15.

Finally it was concluded from the above result figure 6.16 that the unit change temperature outlet per unit change pressure drop when mass flow rate of air very small rough flat plate collector is more acceptable and at mass flow rate of air is above 0.02kg/s v-grooved collector type of solar dryer is optimized.

6.2.2. Simulation results of different duct and shapes solar dryer

I) Smooth curve when air flow above absorber plate with collector diffuser.

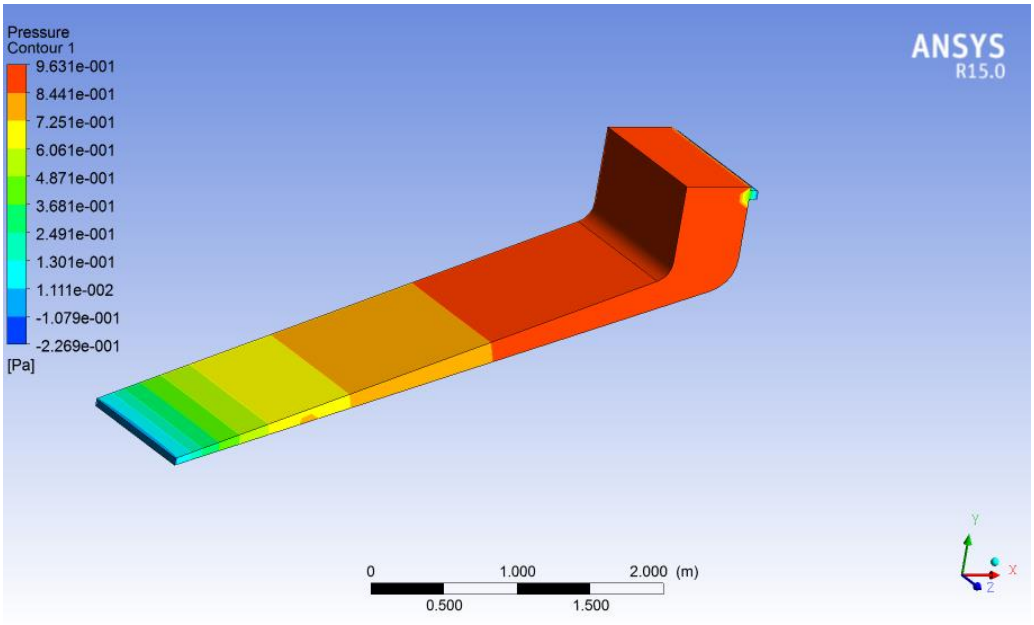

Figure 6.17. Pressure contour for smooth curve with collector diffuser connection with dryer chamber.

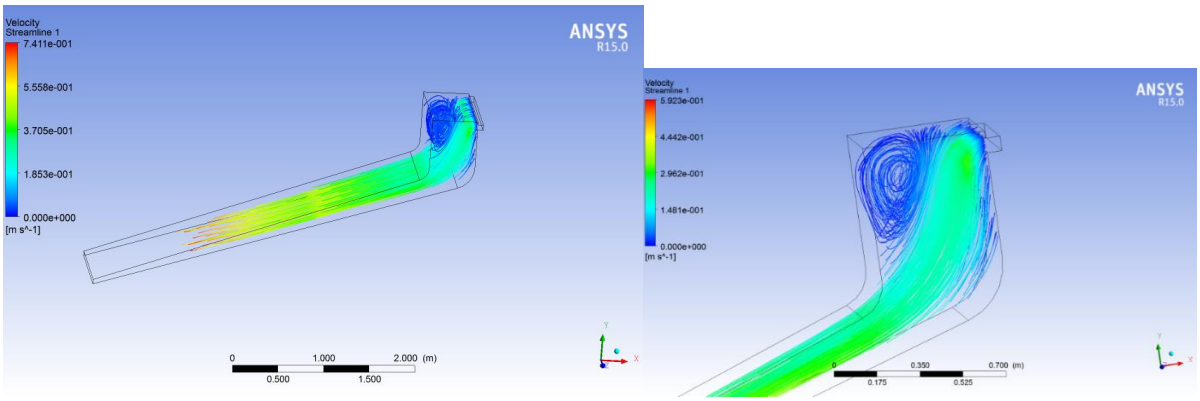

Figure 6.18. Velocity stream profile for smooth curve with collector diffuser outlet connection with dryer chamber.

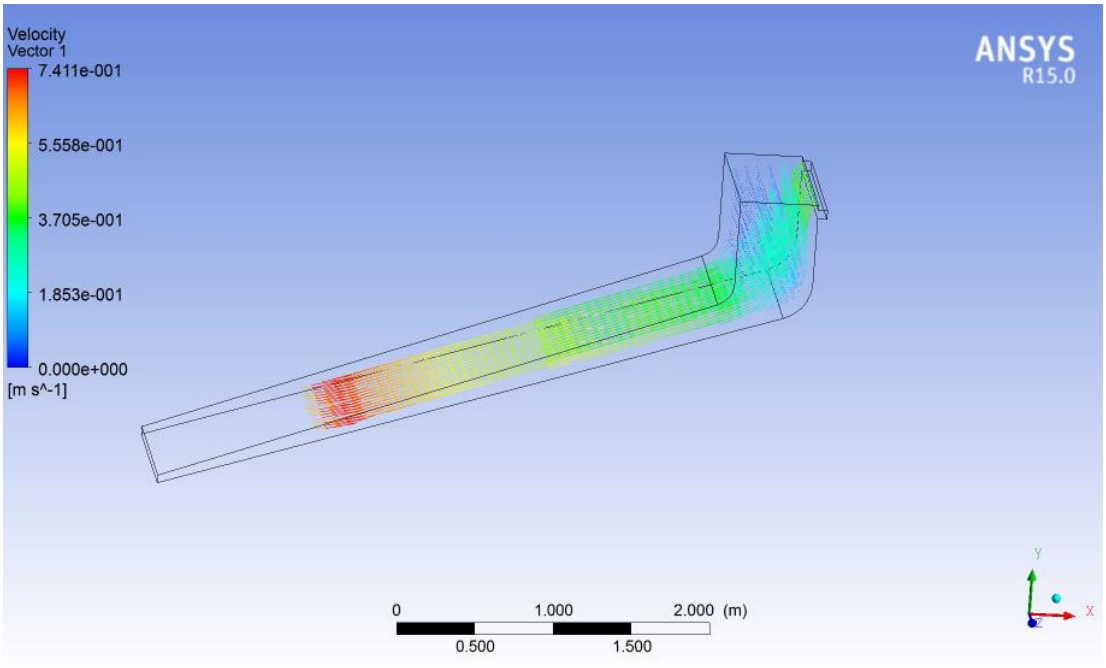

Figure 6.19 velocity vector profile for smooth curve with collector diffuser outlet connected with dryer configuration.

The above figures from 6.17-6.19. Shows the pressure contour, temperature contour and velocity profile smooth flat plate collector when air flow above absorber plate with smooth curve duct with collector diffuser. From this type at (0.05kg/s) mass flow rate inlet to the collector, the outlet air from flat plate collector of temperature which enter to the solar dryer is 43.5^{o}c, pressure drop 0.06pa and velocity stream flow 0.361m/s.

II) Sharp edge

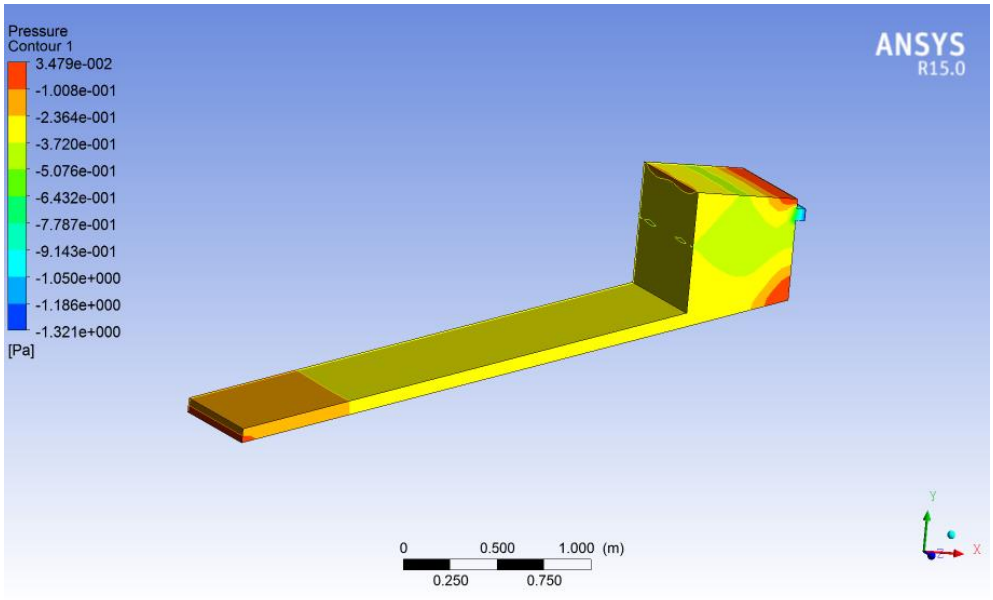

Figure 6.20. Velocity stream line profile for sharp edge connection with dryer chamber.

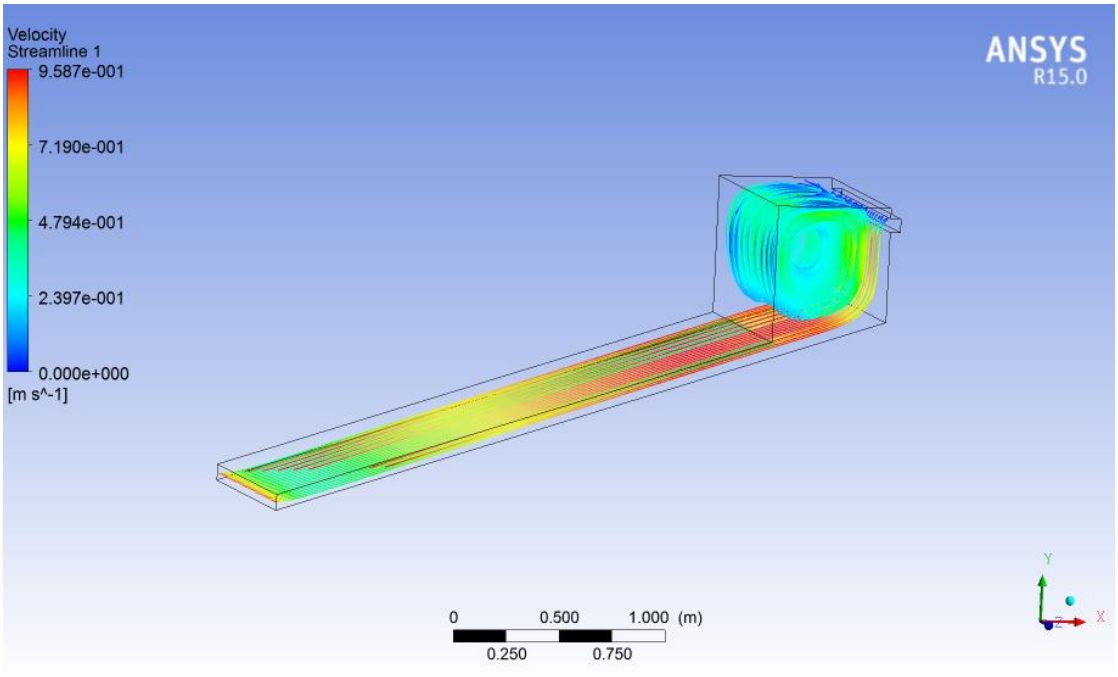

Figure 6.21. Velocity stream line profile for sharp edge connection with dryer chamber

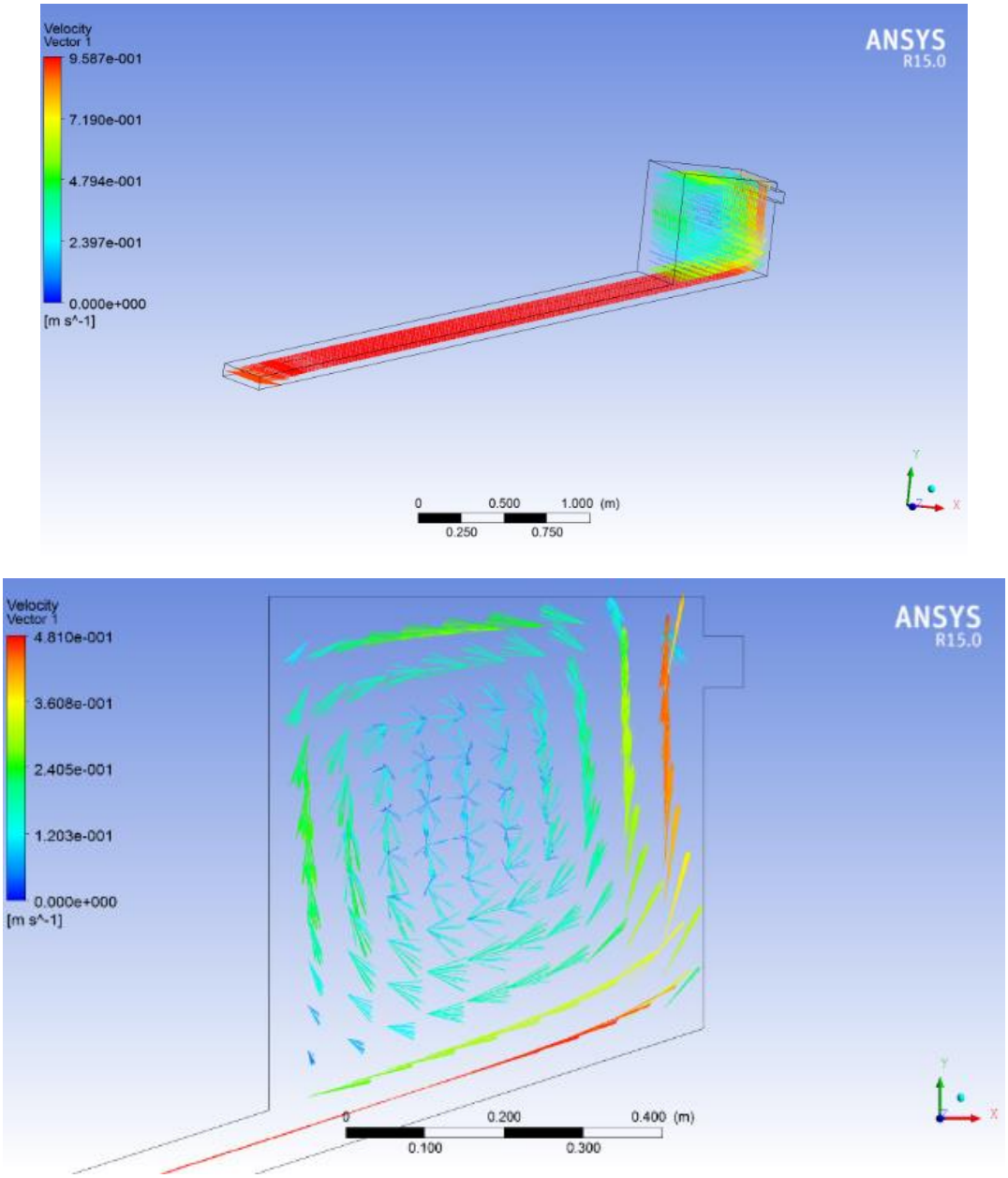

Figure 6.22. Velocity vector profile for sharp edge connection with dryer chamber

The above figures from 6.20-6.22 shows the pressure contour and velocity profile for sharp edge when air flow above absorber plate. From this simulation result type at (0.05kg/s) mass flow rate inlet to the collector, the sharp edge pressure drop and velocity profile has 0.318pa and maximum 0.48m/s respectively.

III) Smooth curve with diffuser

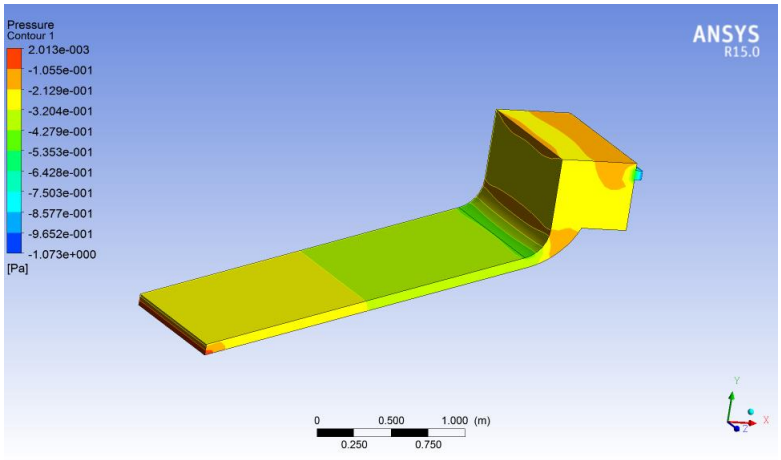

Figure 6.23. Pressure contour for smooth curve with diffuser

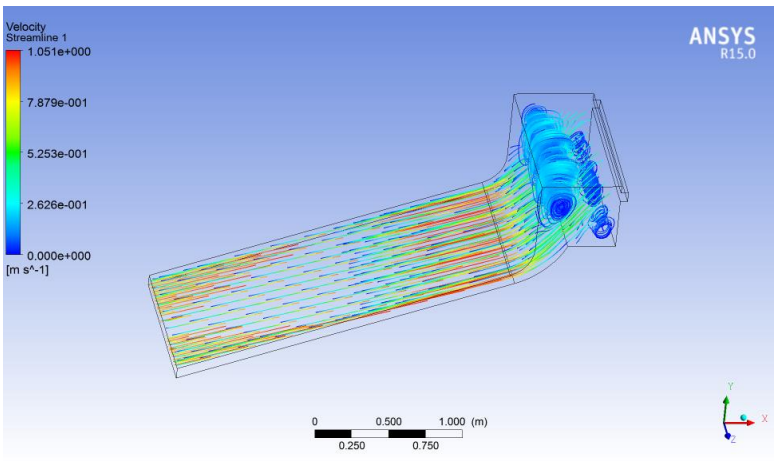

Figure 6.24. Velocity stream profile for smooth curve with diffuser.

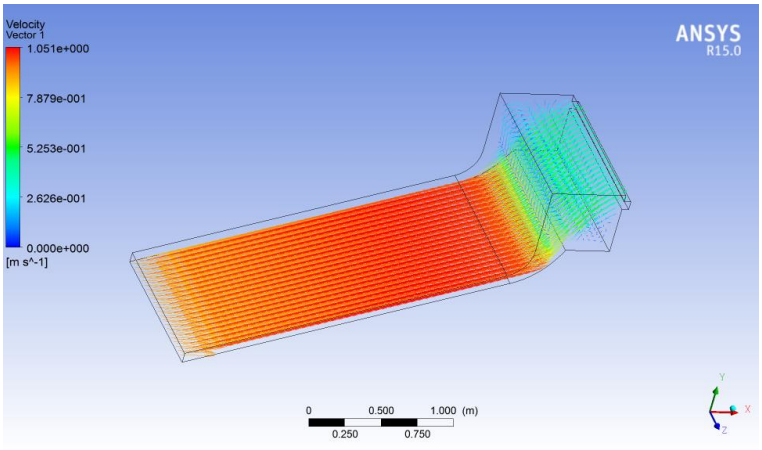

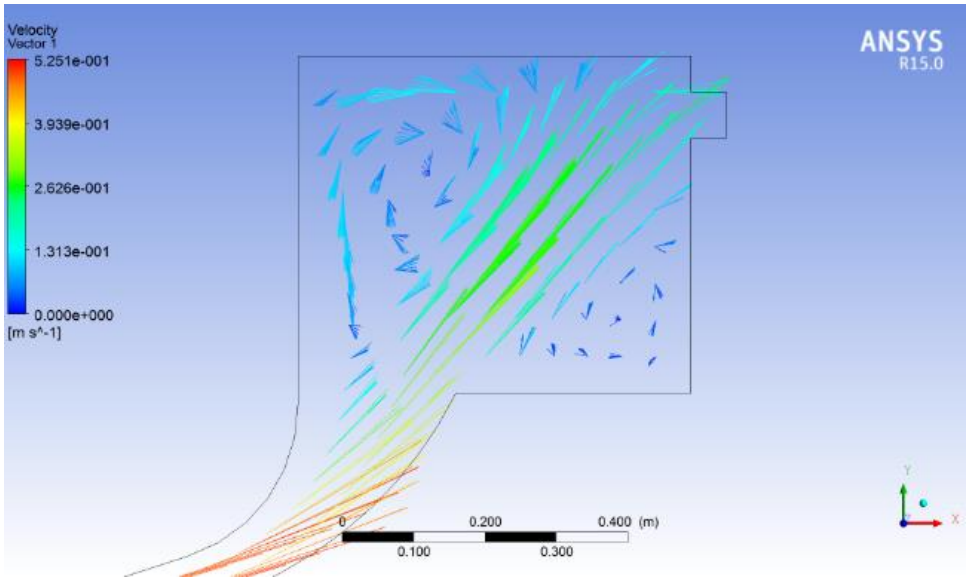

Figure 6.25. Velocity vector profile for smooth curve with diffuser

The above figures from 6.23-6.25 shows the pressure contour and velocity profile smooth curve with diffuser of duct type when air flow above absorber plate. From this type of duct the simulation result at (0.05kg/s) mass flow rate inlet to the collector, the average pressure drop and velocity profile has 0.25pa and maximum 0.48m/s respectively.

IV) Smooth curve when air flow above absorber plate.

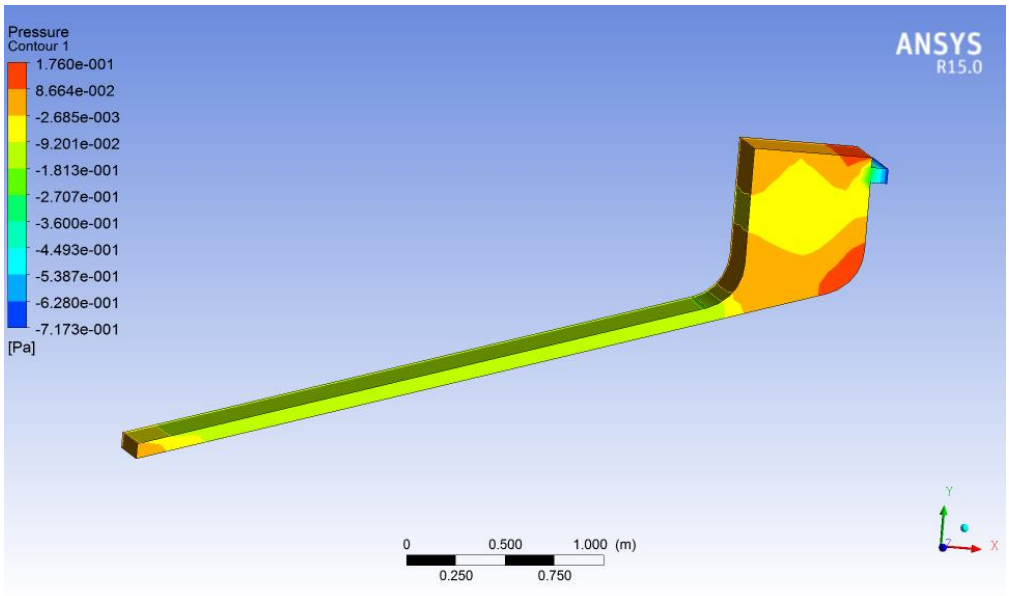

Figure 6.26. Pressure contour for smooth curve when air flow above absorber plate.

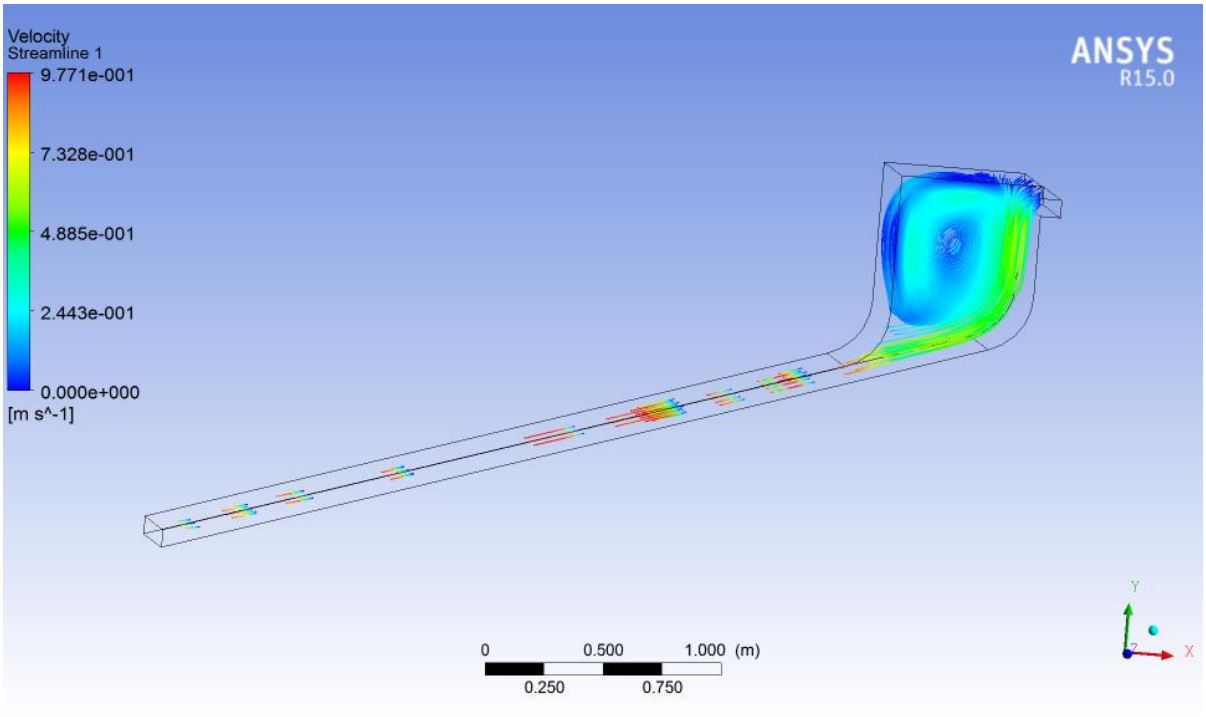

Figure 6.27. Velocity stream profile for smooth curve when air flow above absorber plate.

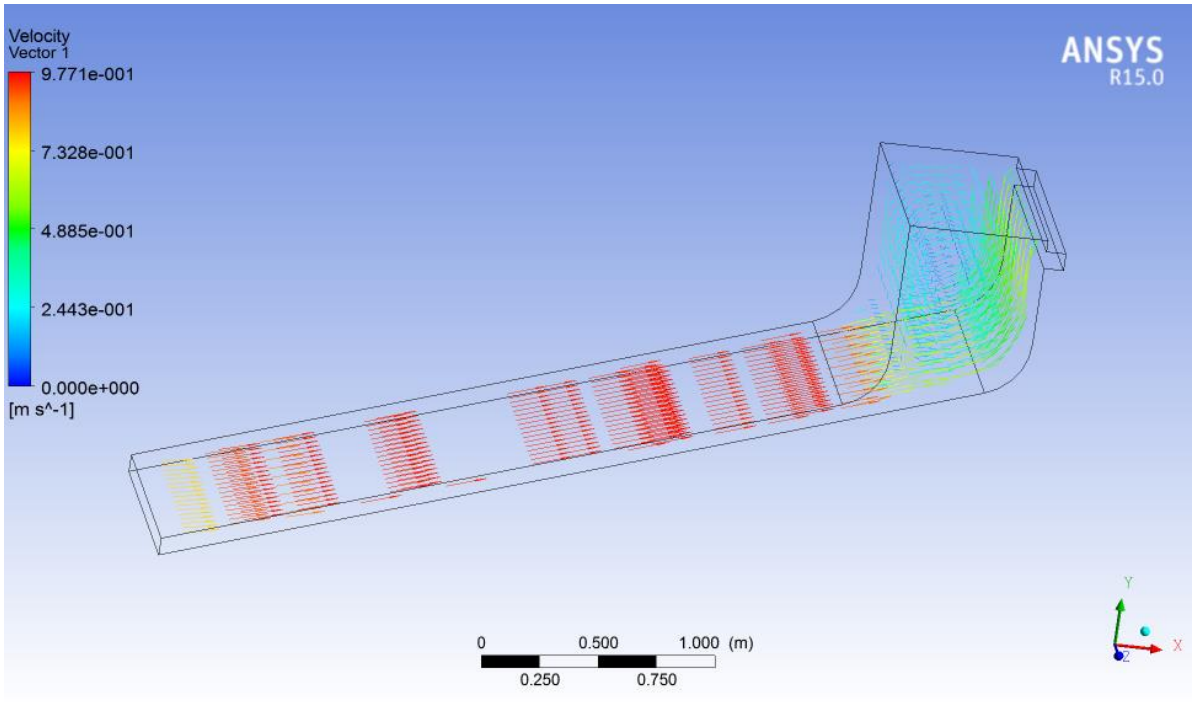

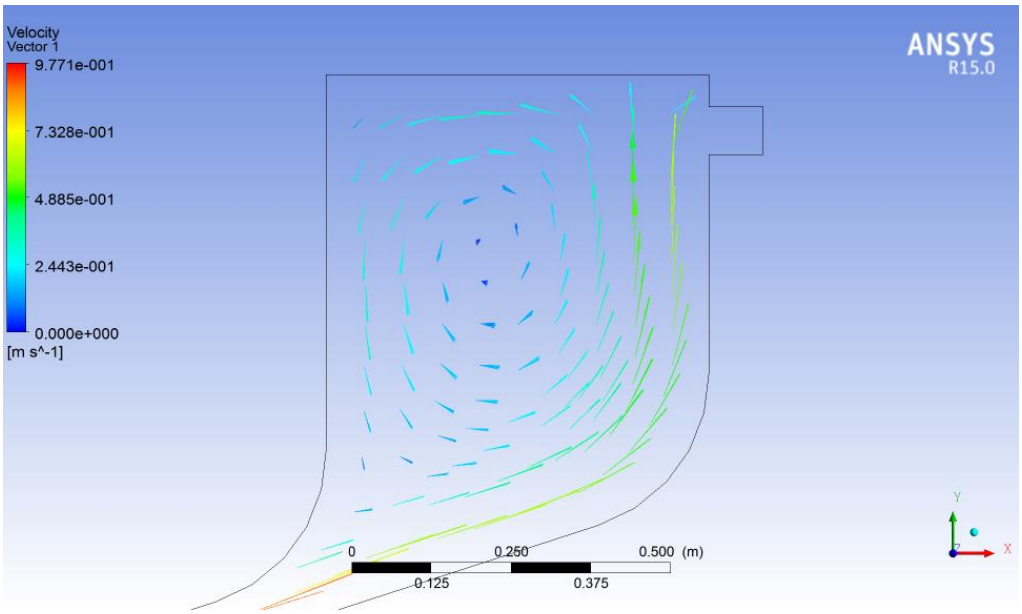

Figure 6.28. Velocity vector profile for smooth curve when air flow above absorber plate.

From figures 6.26-6.28 the pressure contour and velocity profile smooth curve duct when air flow above absorber plate. From those simulation of duct types at (0.05kg/s) mass flow rate inlet to the collector, average pressure drop and velocity profile has 0.35pa and 0.208m/s respectively.

v) Smooth curve connection with guide vanes

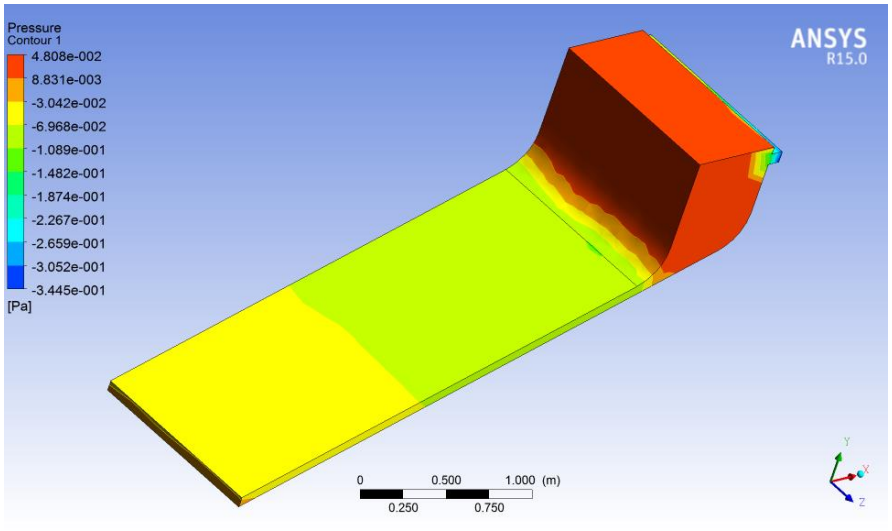

Figure.6.29. pressure contour for smooth curve connection with guide vanes

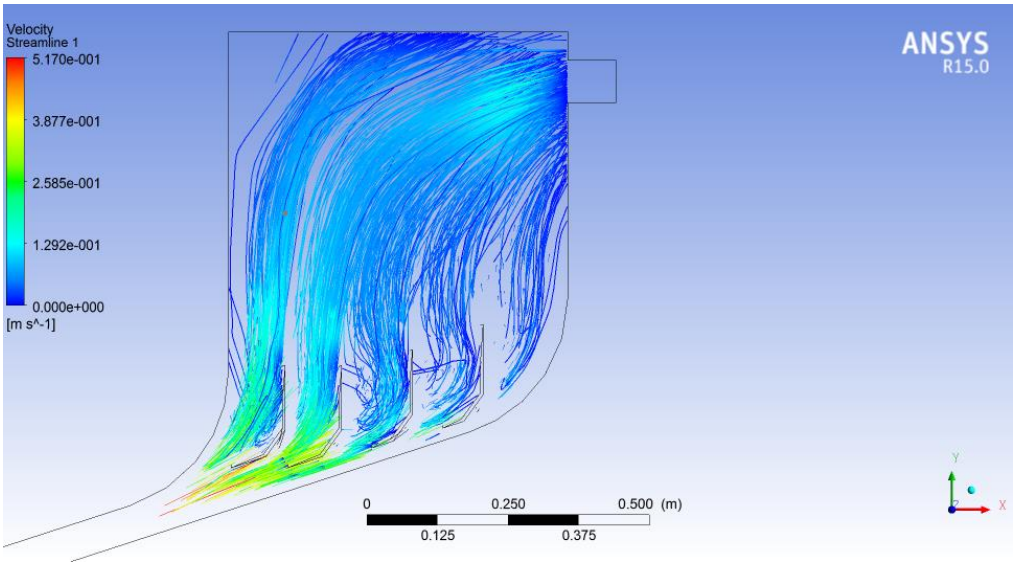

Figure 6.30. Velocity streamline for smooth curve connection with guide vanes

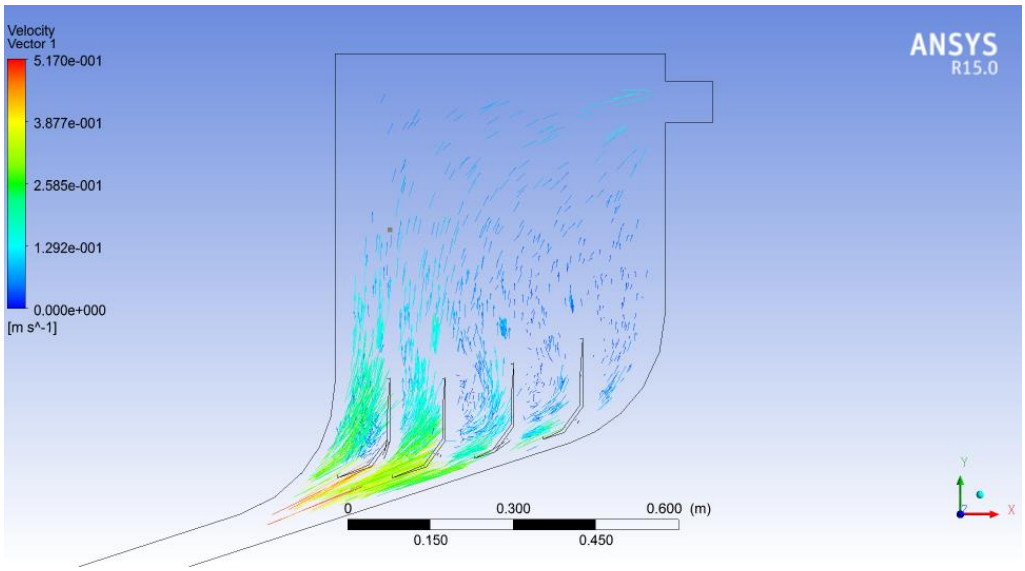

Figure 6.31. Velocity streamline for smooth curve connection with guide vanes

The figures from 6.29-6.31 shows the pressure contour and velocity profile smooth curve connection with guide vanes. From this type at (0.05kg/s) mass flow rate inlet to the collector, the smooth curve pressure drop and velocity mean profile has 0.1636pa and 0.518m/s respectively.

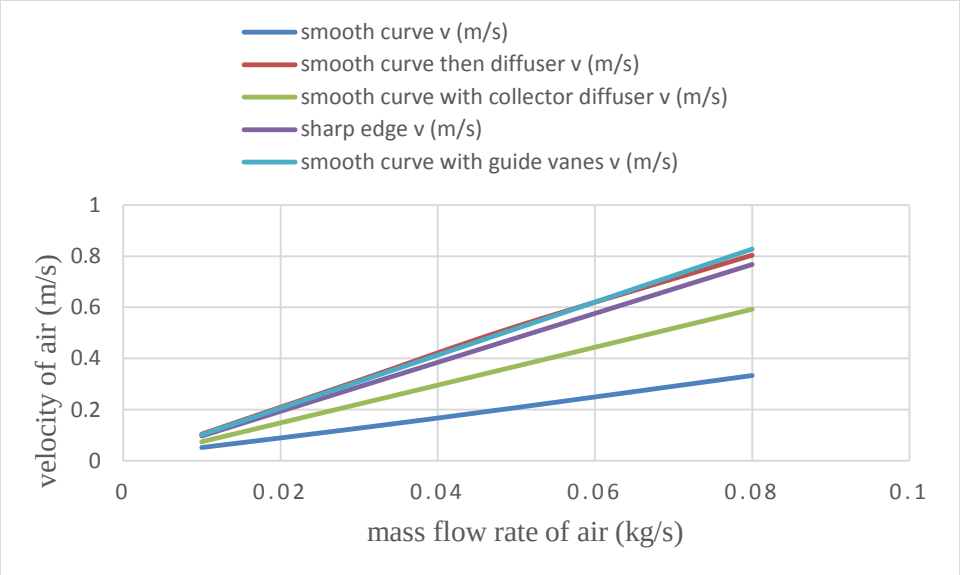

Figure 6.32.Comparing different geometry duct by velocity back flow at different mass flow rate

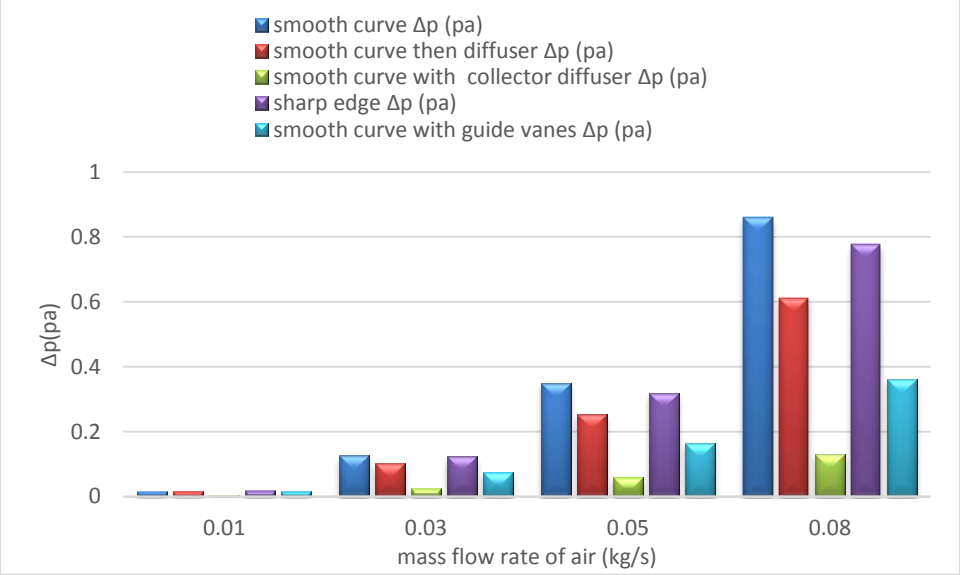

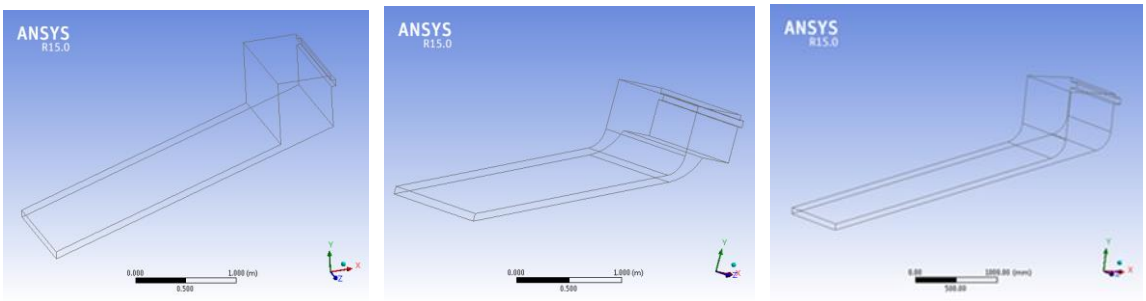

A) Shape edge B) smooth curve then diffuser C) smooth curve

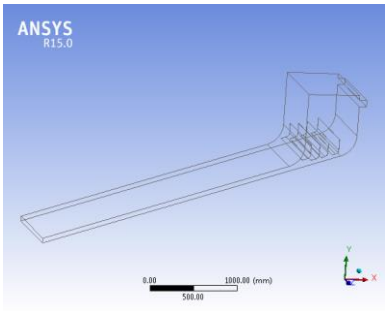

D) Smooth curve guide vanes

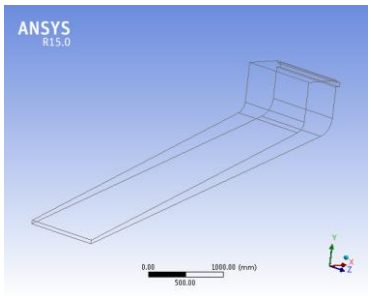

E) Collector diffuser with smooth curve

Figure 6.33 .Comparing different geometry duct dryer by pressure drop at different mass flow rate

Comparing the result duct shapes of solar dryer based on pressure drop quantitatively uniform smooth curve, smooth curve with collector diffuser, uniform smooth edge then diffuser, smooth curve with guide vanes and Sharp edge connected with dryer. Smooth curve with collector diffuser has small pressure drop than the others. But sharp edge has higher than others. Velocity stream lines shows for both sharp edge connected dryer and smooth curve connected dryer configuration have high recirculation flow in the side of dryer cross section. The recirculation flows makes non uniform drying rate for coffee parchments.

Finally, comparing dryer configuration through five different ducts based on pressure drop and temperature smooth curve with collector diffuser connection with dryer better than any other four configuration types (smooth sharp edge, smooth sharp edge with diffuser guide vanes and smooth curve connected dryer configuration). And smooth curve guide vanes has small back flow velocity than any other four dryer configuration.

6.2.3. Simulation results with different arrangements of trays dryer chamber

1) Smooth flat plate collector when air flow above absorber plate when trays was allayment.

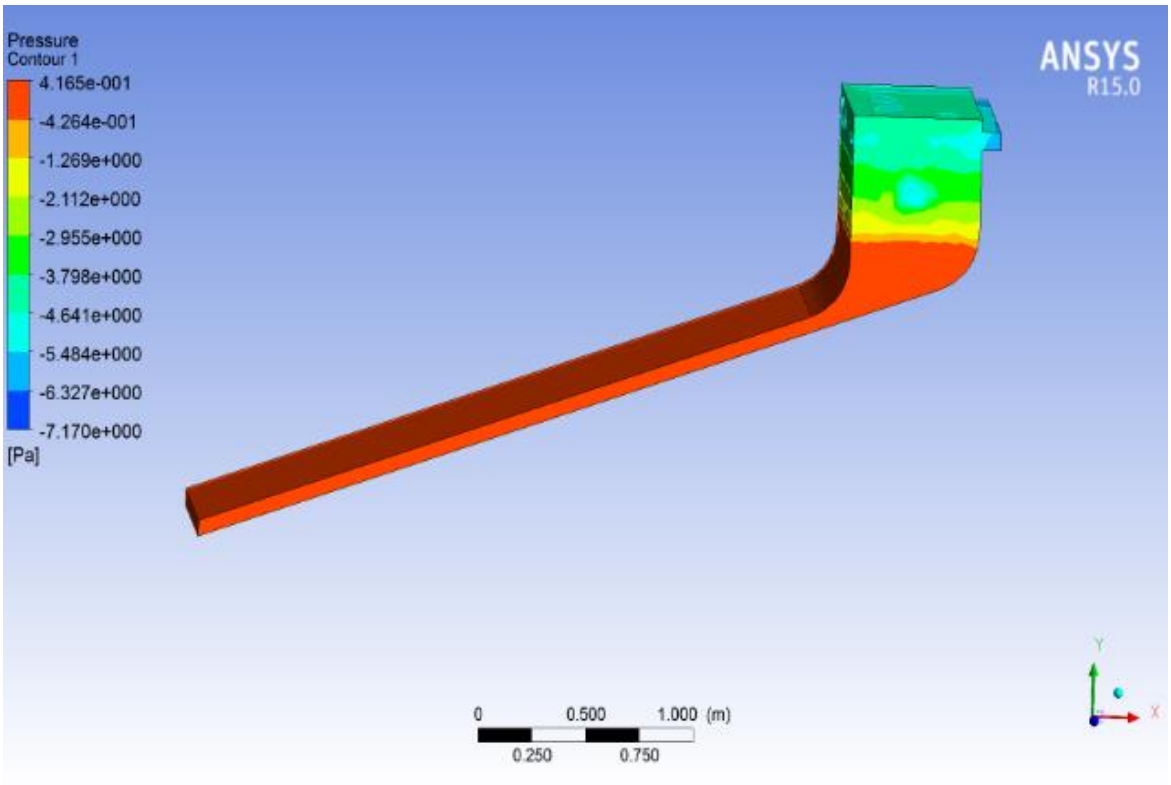

Figure 6.31. Pressure contour smooth flat plate collector when trays was allayment.

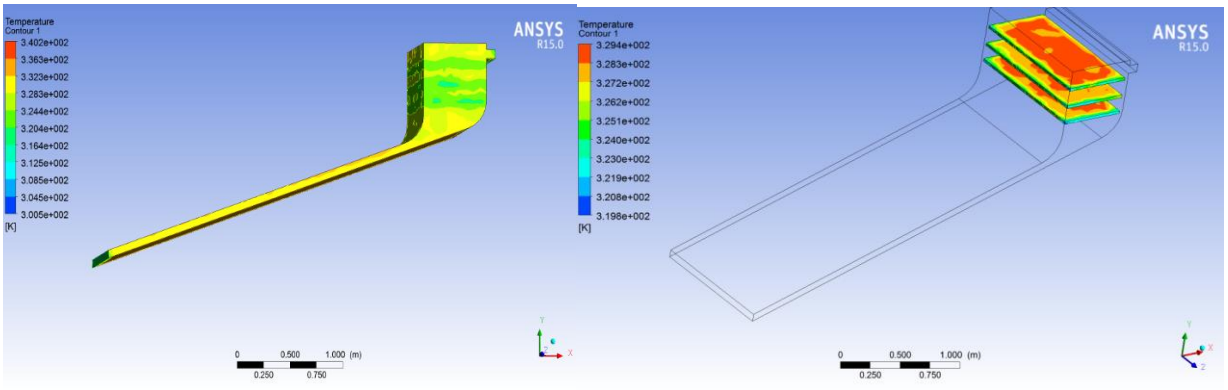

Figure 6.32. Temperature contour smooth flat plate collector when trays was allayment.

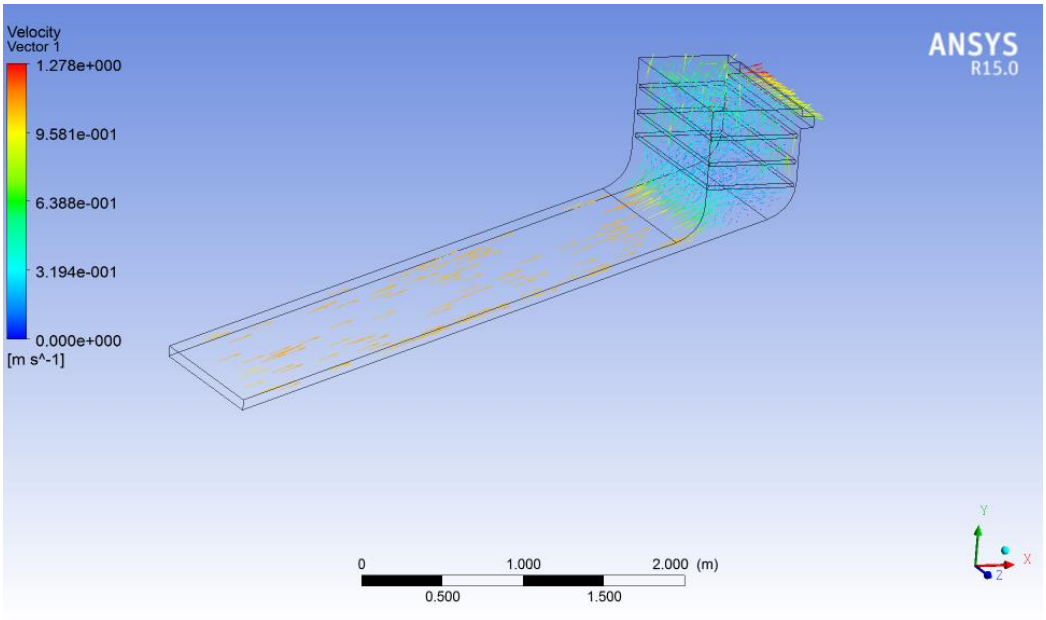

Figure 6.33. Velocity vector profile smooth flat plate collector when trays was allayment.

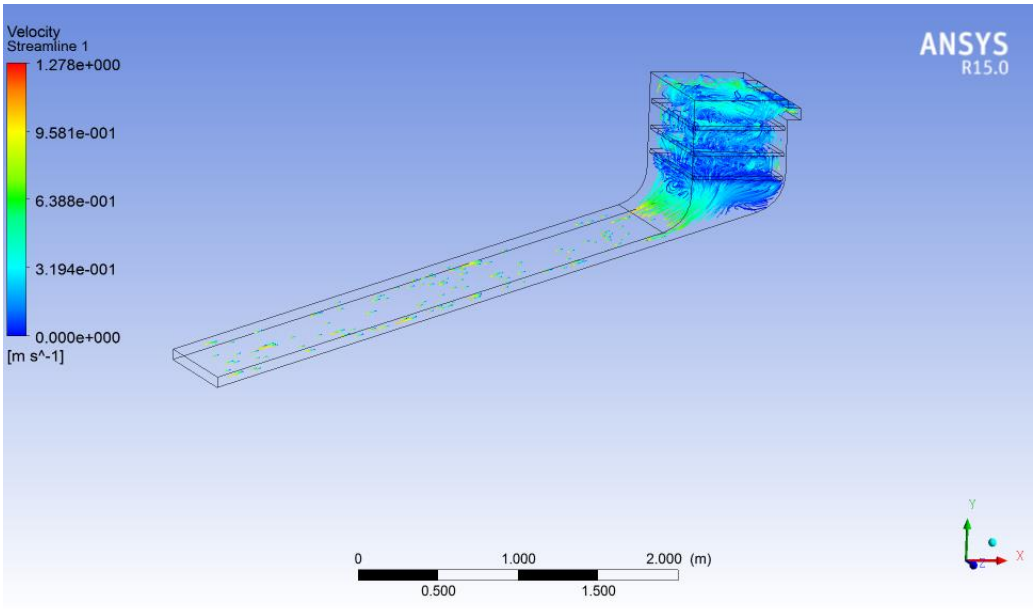

Figure 6.34. Velocity stream profile smooth flat plate collector when trays was allayment.

The above figures from 6.32-6.34 shows the pressure contour, temperature contour and velocity profile smooth flat plate collector when air flow above absorber plate with trays was alignment of dryer chamber. From this type at (0.05kg/s) mass flow rate inlet to the collector, the maximum velocity of air 0.647and pressure drop 2.342pa.

2) Smooth flat plate collector when air flow above absorber plate when trays has different distance with width dryer chamber.

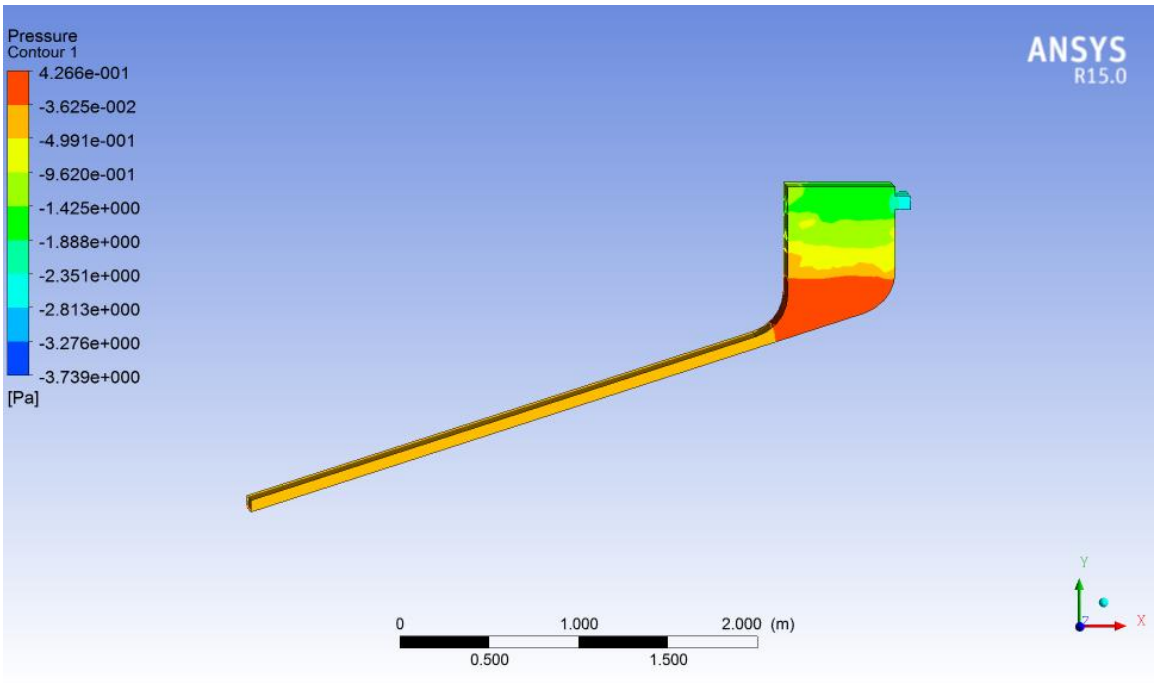

Figure 6.35. Pressure contour smooth flat plate collector when trays has different gap.

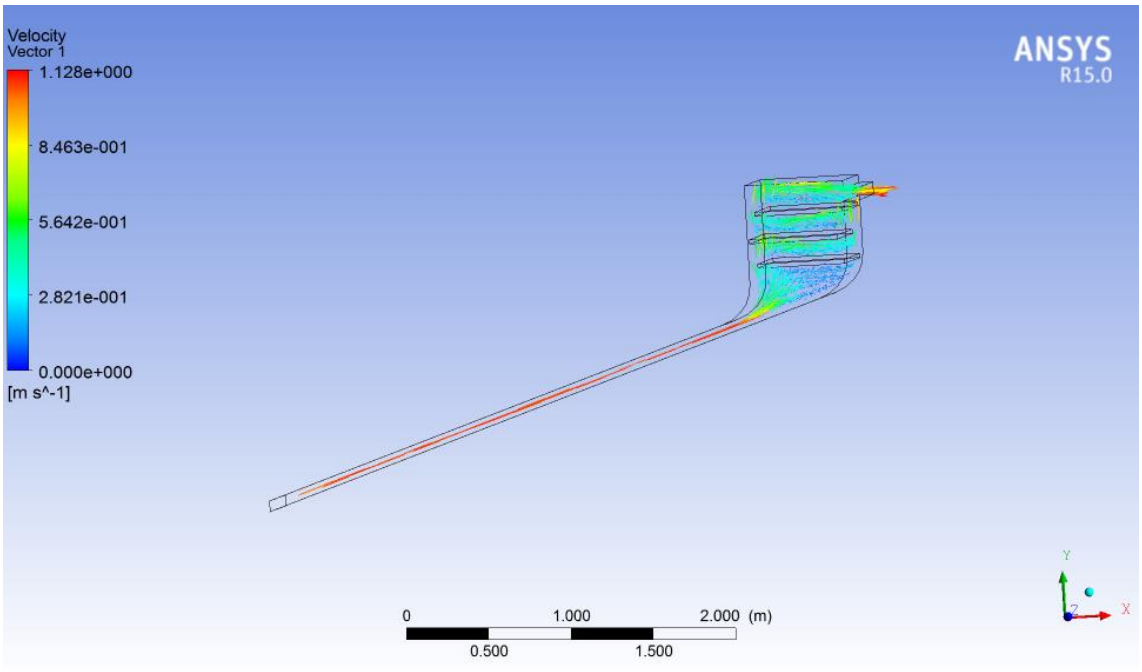

Figure 6.36. Velocity vector smooth flat plate collector when trays has different gap.

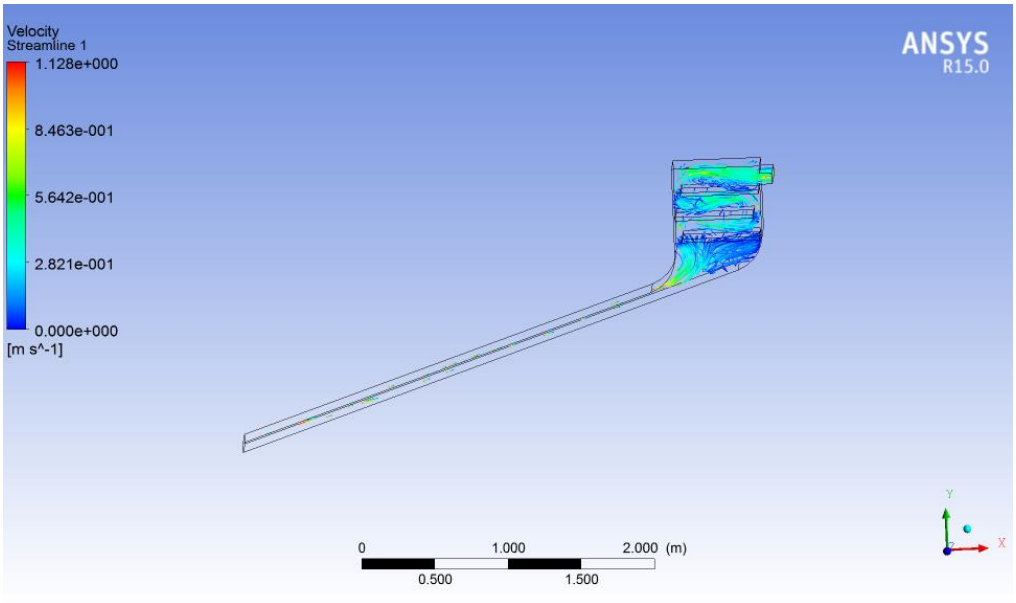

Figure 6.37. Velocity stream profile smooth flat plate collector when trays has different gap.

The above figures from 6.35-6.37 shows the pressure contour, and velocity profile smooth flat plate collector when air flow above absorber plate with trays has different distance with width dryer. From this type at (0.05kg/s) mass flow rate inlet to the collector, the pressure drop 0.977pa and maximum back flow velocity stream is 0.612m/s.

3) Smooth flat plate collector when air flow above absorber plate with hole trays of dryer chamber.

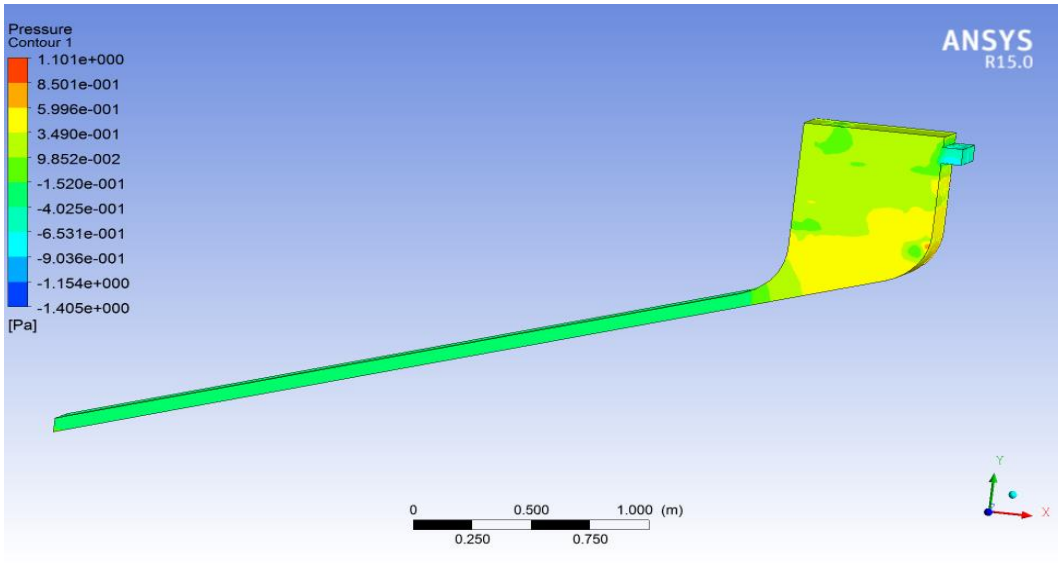

Figure 6.38. Pressure contour smooth flat plate collector with hole trays of dryer chamber.

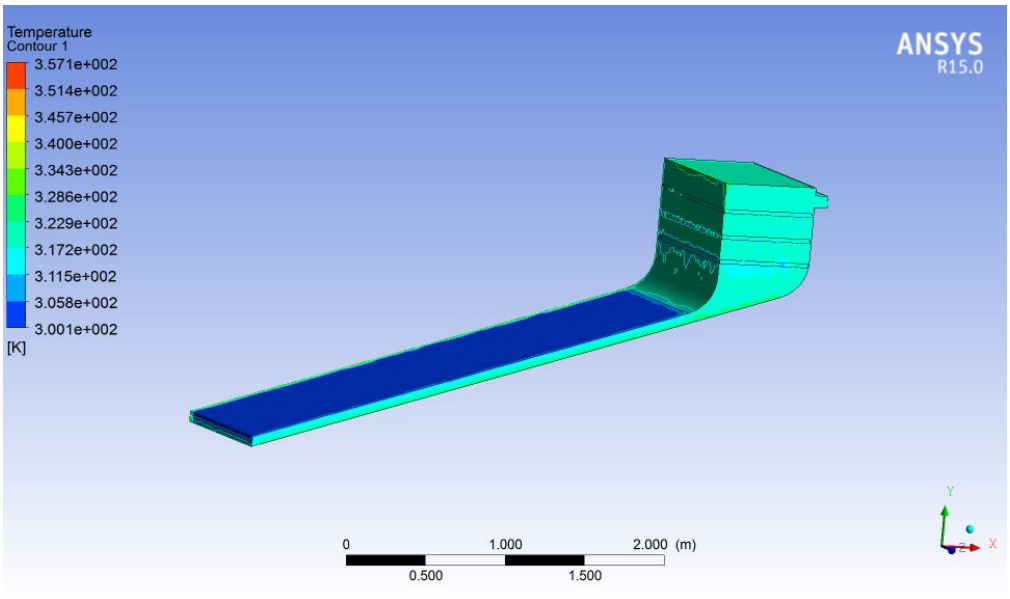

Figure 6.39. Temperature contour smooth flat plate collector with hole trays of dryer chamber.

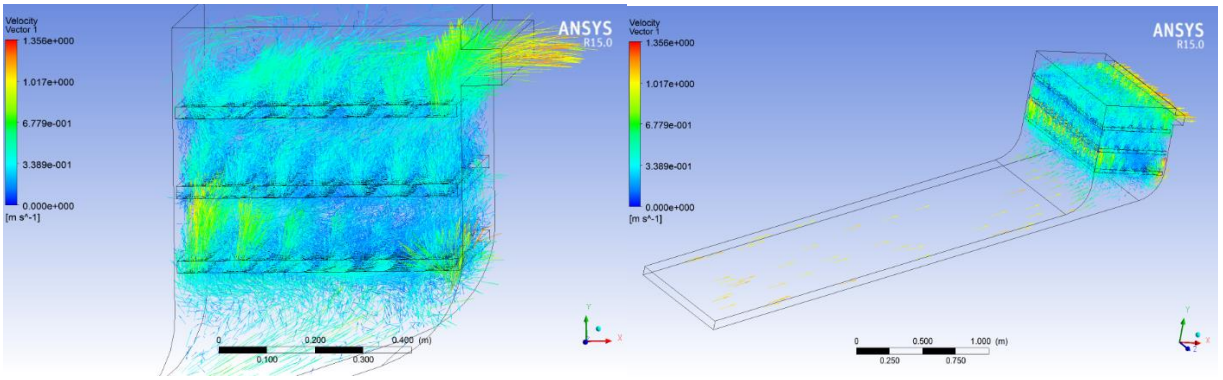

Figure 6.40. Velocity vector profile smooth flat plate collector with hole trays of dryer chamber.

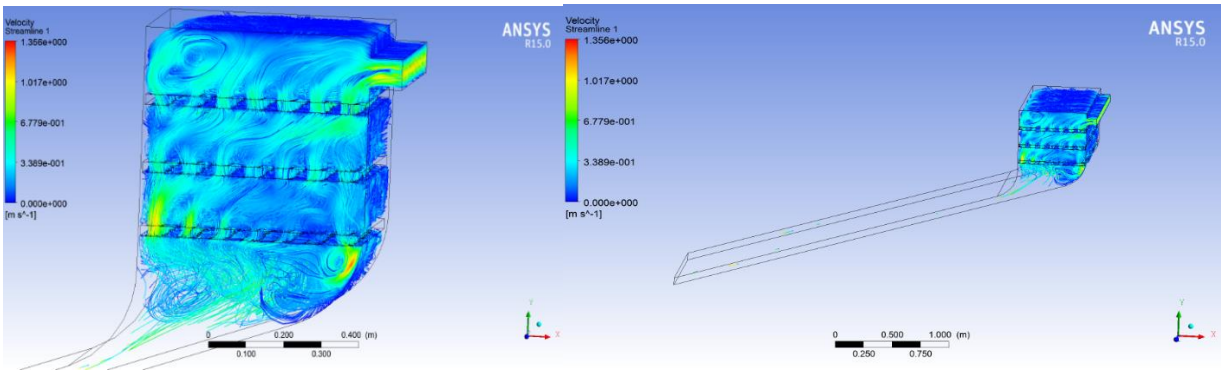

Figure 5.41. Velocity stream profile smooth flat plate collector with hole trays of dryer chamber.

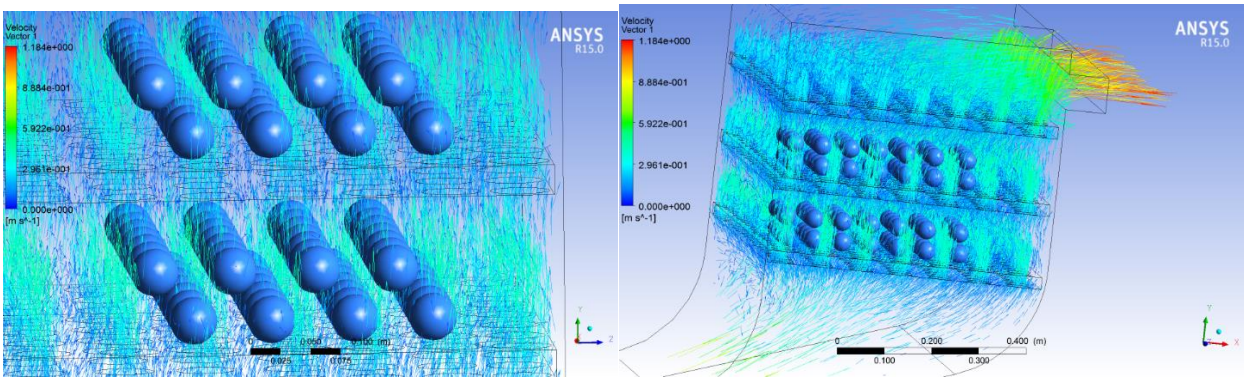

Figure 6.42.Velocity stream profile of sample coffee preachment through in dryer chamber

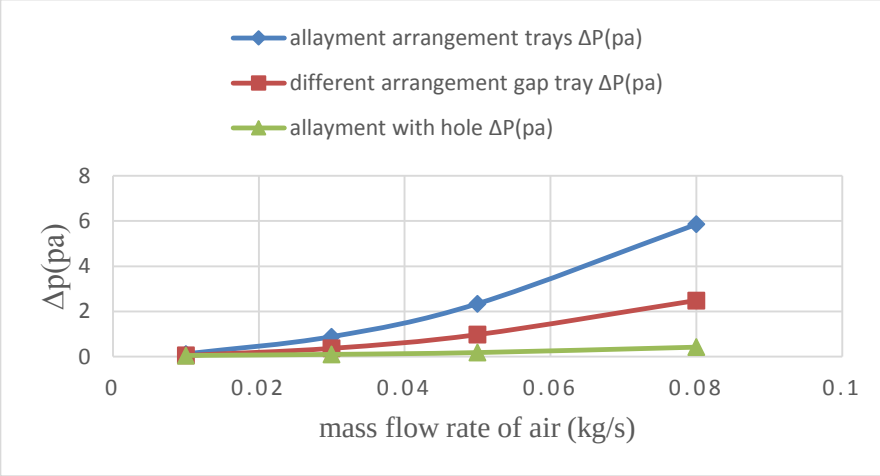

Figure 6.43. Comparing different pressure drop types of trays dryer chamber at different mass flow rate.

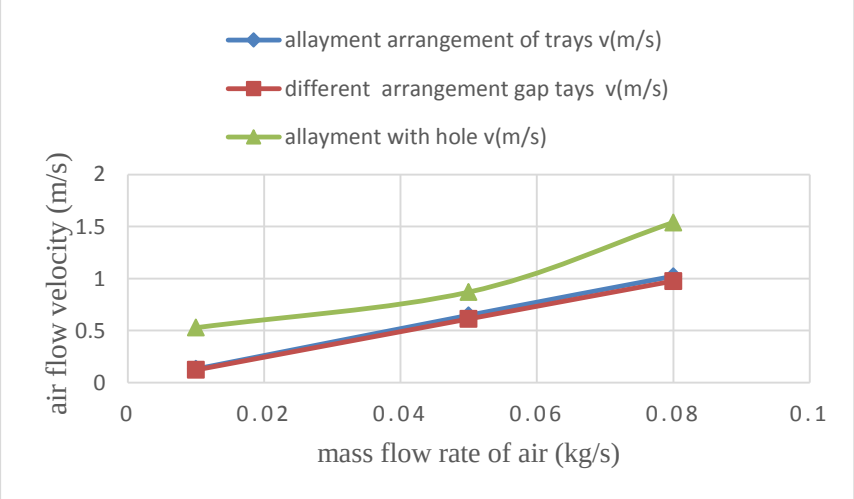

Figure 6.44. Comparing different maximum velocity of type's trays dryer chamber at different mass flow rate.

From figures 6.42 to 6.43 concluded that the pressure drop and velocity stream variations through trays dryer chamber, which different arrangement gap trays has small pressure than the allayment arrangement with in the different mass flow rate of air. Comparing the three results the trays which different gap arrangement has low pressure drop and high uniform flow velocity stream than the other one. From the simulation it can be more acceptable when the trays chamber with holes.

6.2.4 Simulation results different air flow direction through smooth flat plate collector.

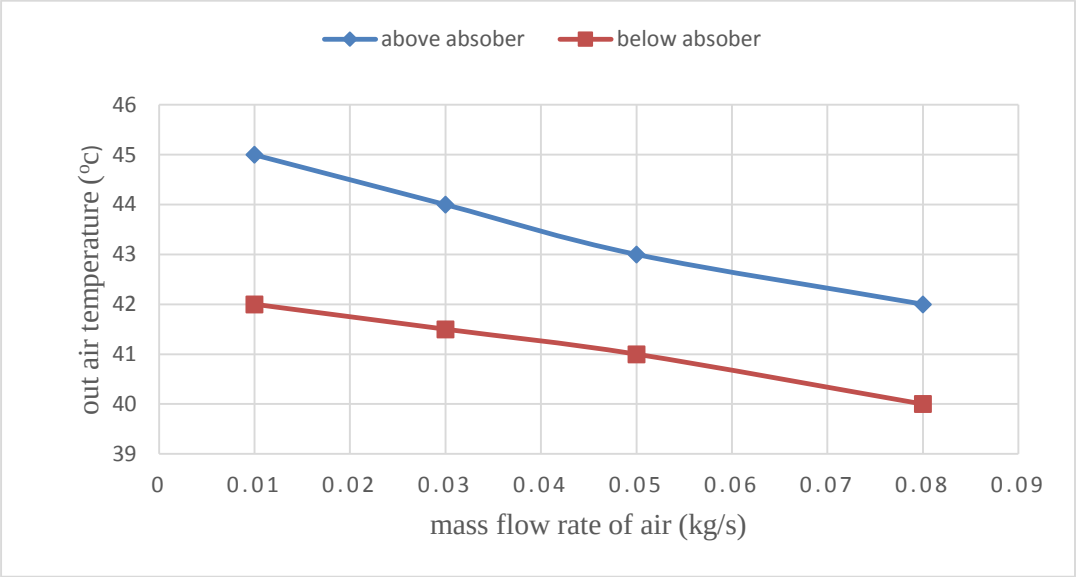

Figure 6.45. Variation of outlet temperature at different flow of air through absorber with mass flow rate

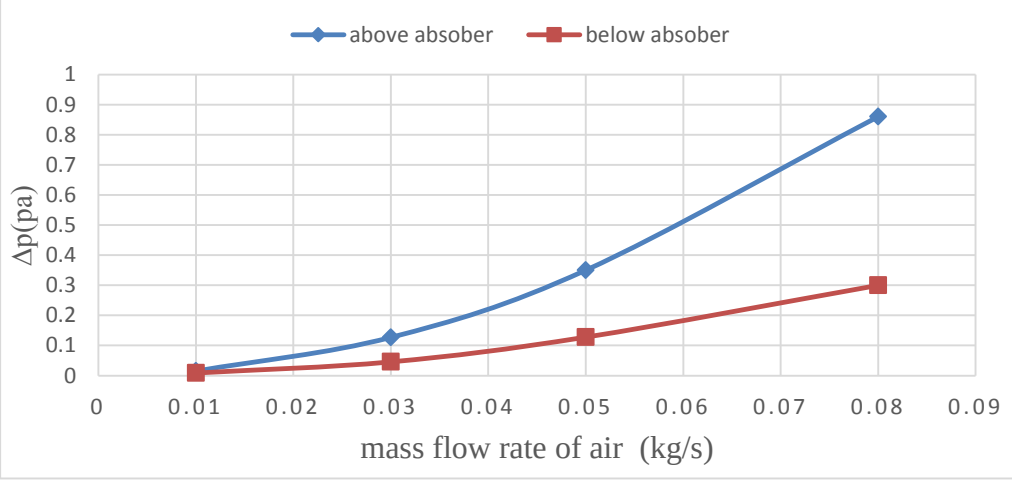

Figure 6.46. Variation of pressure drop at different flow of air through absorber with mass flow rate.

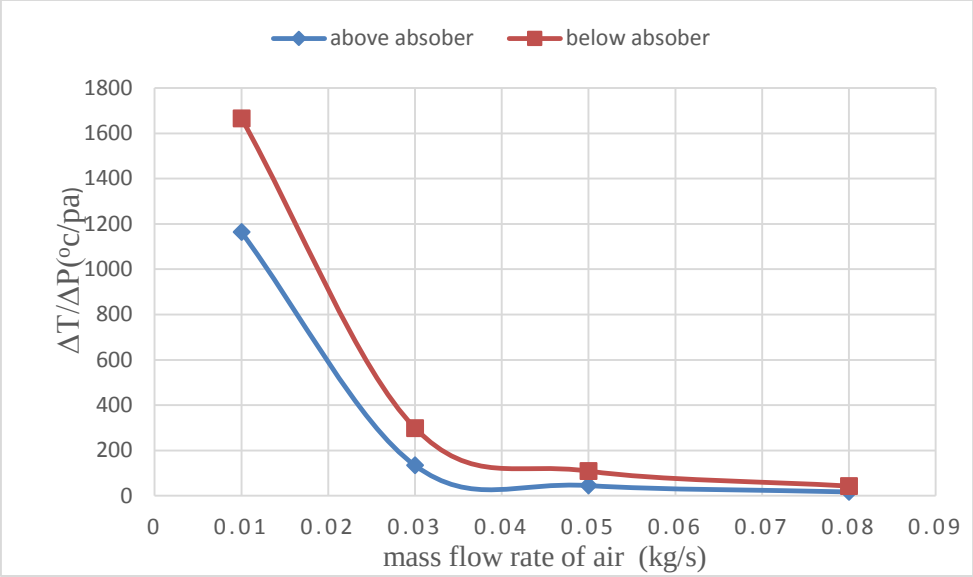

Figure 6.47. Variation of outlet temperature over pressure drop at different flow of air through absorber with mass flow rate.

From figures 6.45 to 6.47 it can be concluded that the pressure drop and maximum outlet temperature variations through different flow direction of air through absorber, when above and below absorber plate at different mass flow rate of air results. Comparing the two directions results, when air flow direction above absorber plate has high pressure drop and outlet temperature than the below one. The unit change of outlet temperature at unit change of pressure drop, air flow direction below the absorber plate is higher than the above flow direction. Finally, from simulation results air flow direction below the absorber plate was more acceptable one.

6.2.5 Simulation results at different air gap through smooth flat plate collector.

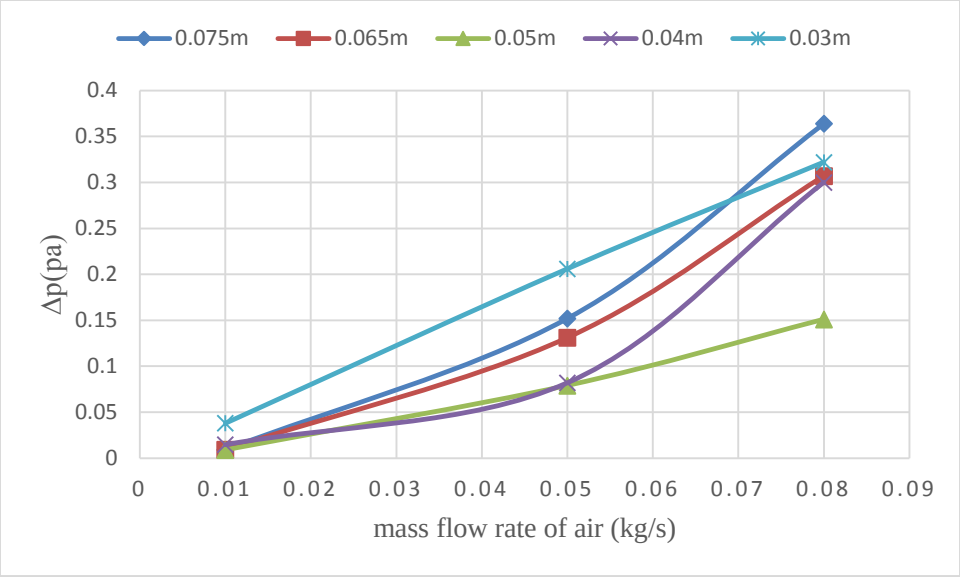

Figure 6.48. Variation of pressure drop through different air gap with mass flow rate of air

.

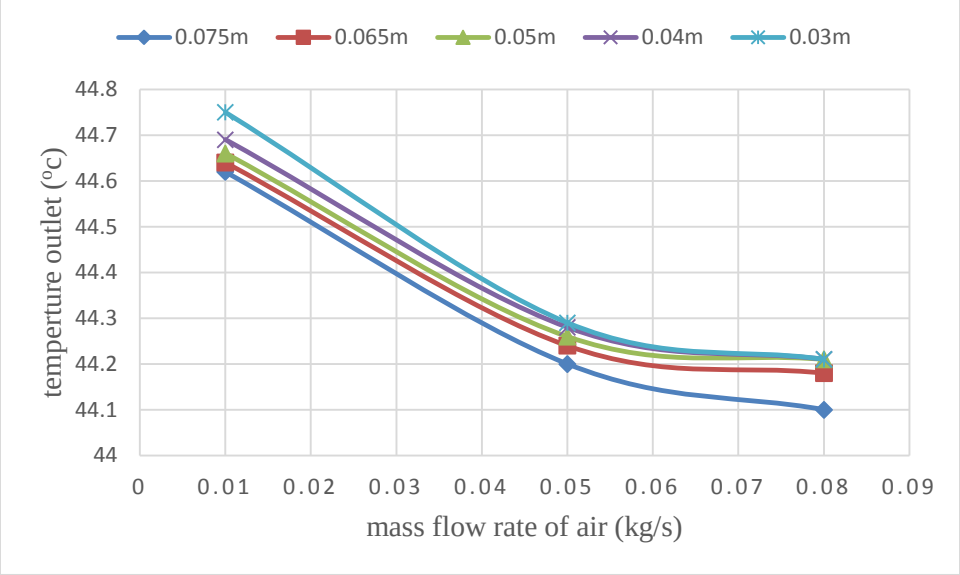

Figure 6.49. Variation of temperature outlet through different air gap with mass flow rate of air.

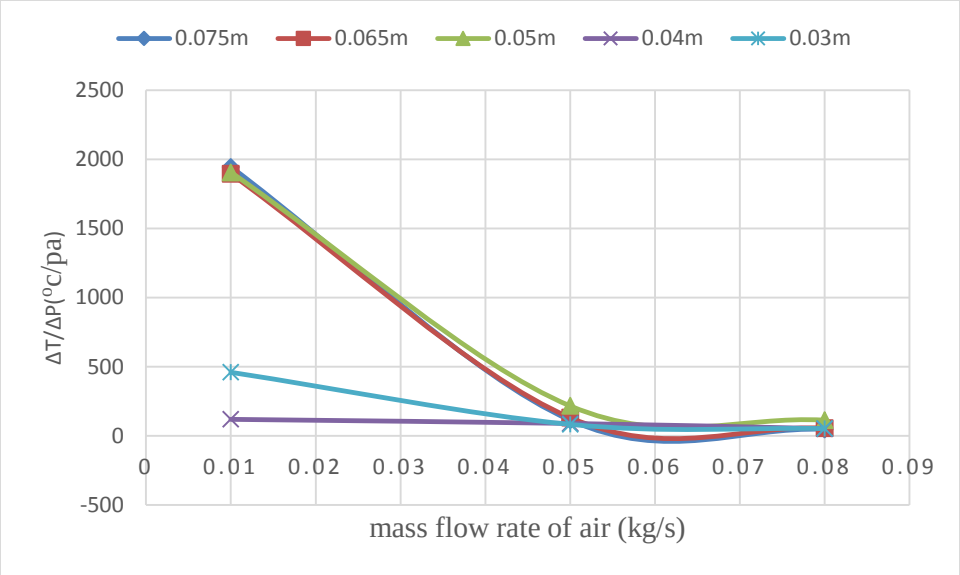

Figure 6.50. Variation of ΔT/ΔP of through different air gap with mass flow rate of air.

Comparing the results of different air gap through same profile shape of solar dryer at different mass flow rate of air based on temperature outlet air and pressure drop quantitatively 0.03m, 0.04m, 0.05m, 0.065m, and 0.075m air gap. From figures 6.48 to 6.49 it can be concluded that the air gap 0.05m has small pressure drop than the others air gap and air gap 0.03m has maximum temperature outlet air higher than the others air gap. From figure 6.50 comparing the results the based on unit change of temperature outlet at pressure drop air gap 0.05m more acceptable than the others air gap results.

6.2.6 Simulation results of different present of turbulence intensity flow with mass flow rate of air through smooth flat plate collector.

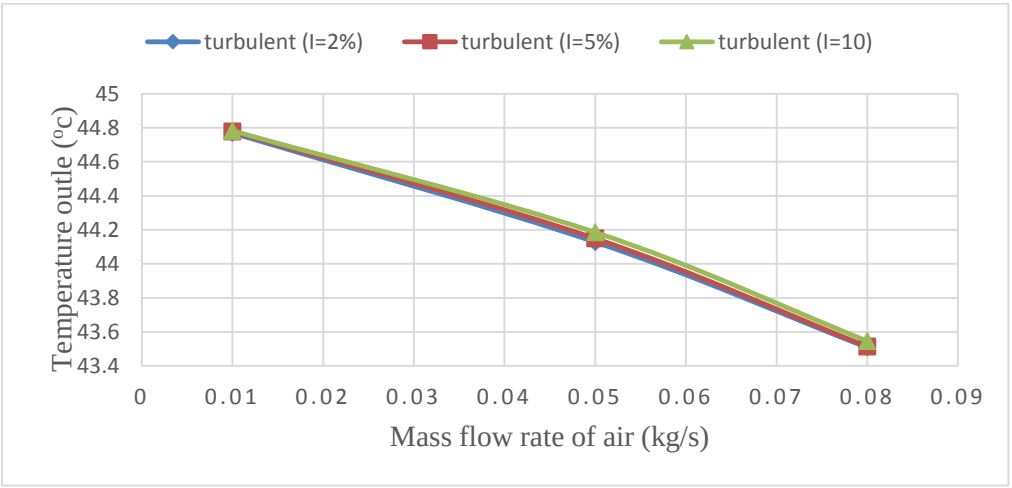

Figure 6.51. Variation of temperature outlet through different turbulence intensity flow with mass flow rate of air.

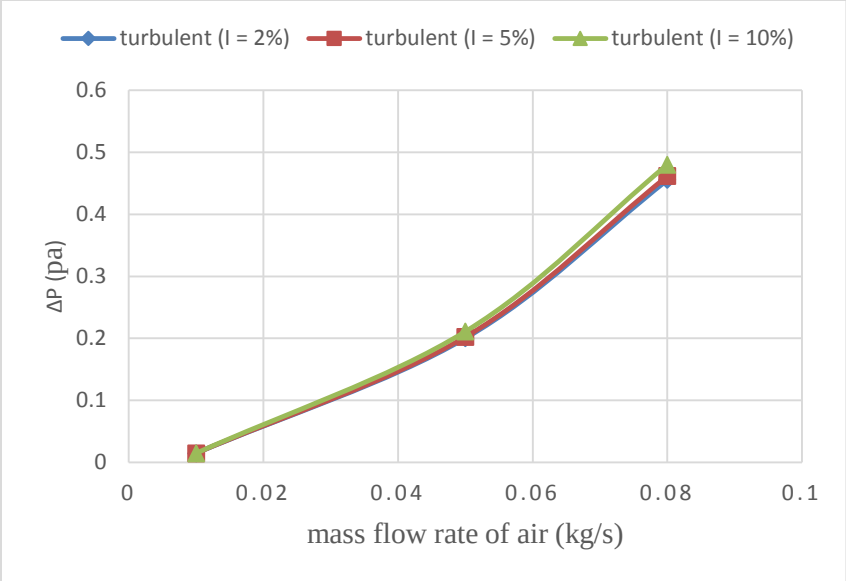

Figure 6.52. Variation of pressure drop through different turbulence intensity flow with mass flow rate of air.

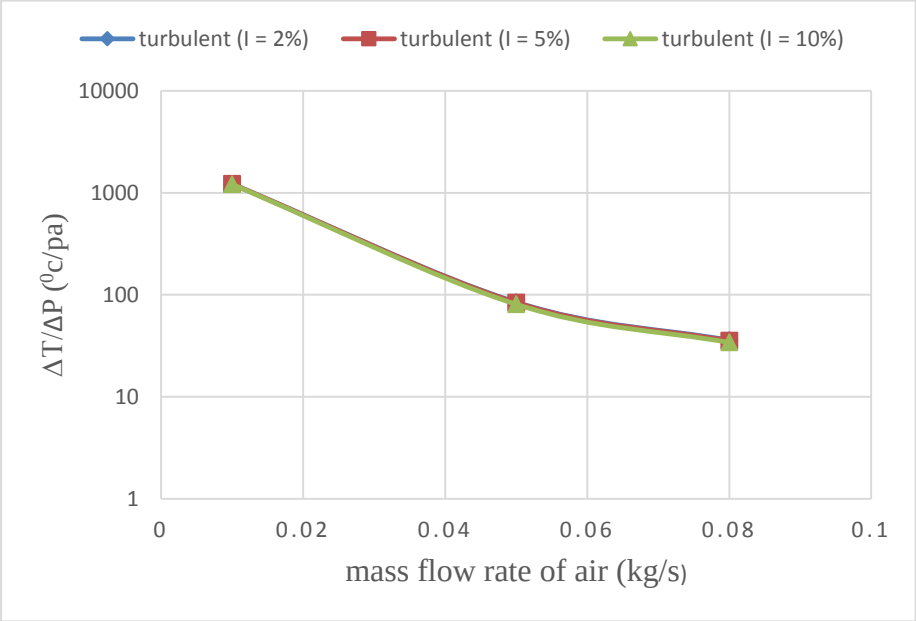

Figure 6.53. Variation of ΔT/ΔP through different turbulence intensity flow with mass flow rate of air.

The above results show that different turbulence intensity flow through same profile shape of solar dryer at different mass flow rate of air based on temperature outlet air and pressure drop quantitatively 2%, 5%, and 10% of turbulence intensity flow. Finally it was concluded the temperature is increased upraise through present of turbulence intensity flow and also pressure drop (increase). The maximum temperature outlet air and pressure drop were obtained when turbulence intensity is 10% and the minimum were obtained when the turbulence intensity is 2%.

From figure 6.53 comparing the results based on unit change of temperature with a unit pressure drop, low turbulence intensity more acceptable than the higher turbulence intensity flow.

6.2.7. Simulation results of different turbulence flow and laminar flow with mass flow rate of air through smooth flat plate collector.

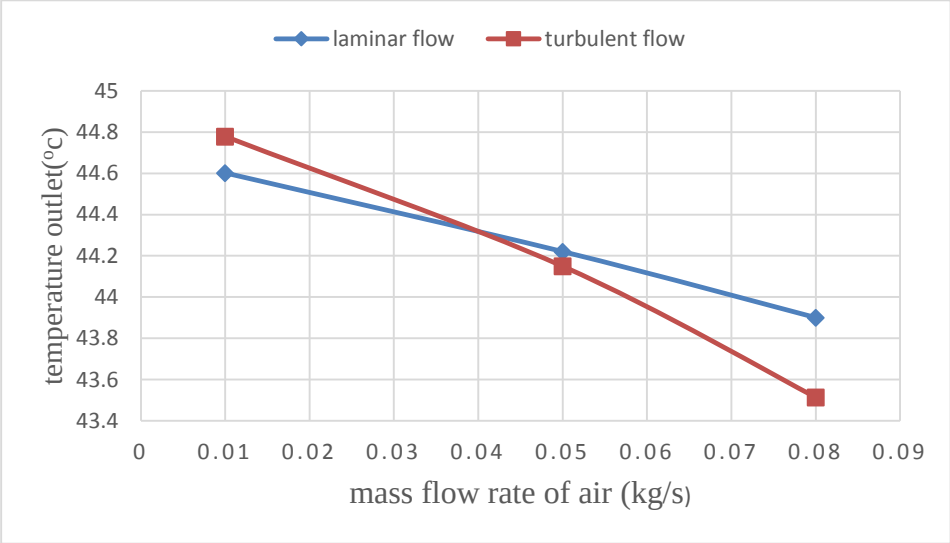

Figure 6.54. Variation of temperature outlet through turbulence intensity flow and laminar flow with mass flow rate of air.

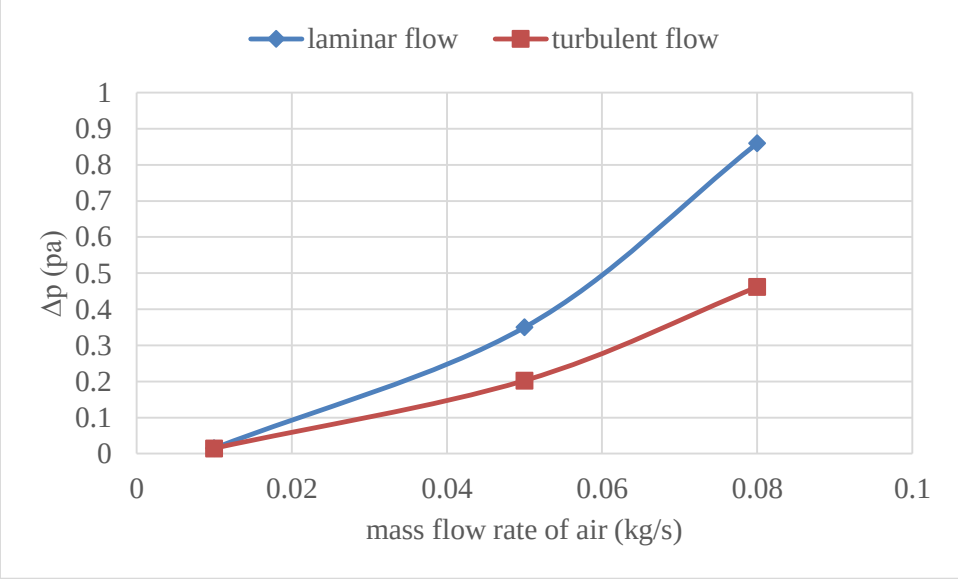

Figure 6.55. Variation of pressure drop through turbulence flow and laminar flow with mass flow rate of air.

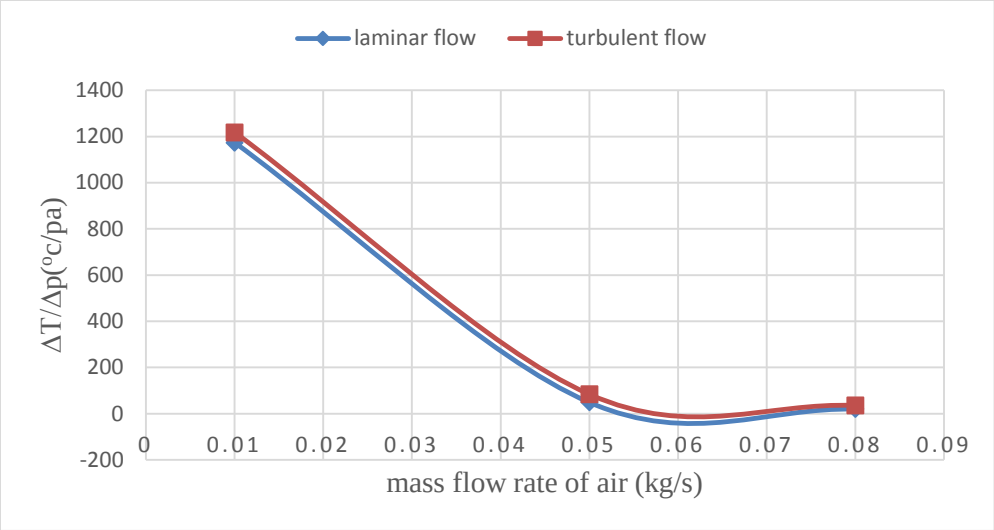

Figure 6.56. Variation of ΔT/ΔP through different turbulence intensity flow with mass flow rate of air.

Figure.6.54.temperature outlet comparing the two flows qualitatively, temperature outlet for turbulent flow is better than laminar flow type when mass flow rate of air was small. When mass flow rate of air was high laminar flow is better than the turbulent flow. Figure .6.55. Shows pressure drop, for laminar flow is smaller than turbulent flow. Figure 6.56. both temperature outlet and pressure drop at unit change comparing the two flows, then turbulent flow is more than laminar flow, so turbulent flow was more acceptable.

6.2.7. Dryer performance analysis.

6.2.7.1 Collector efficiency

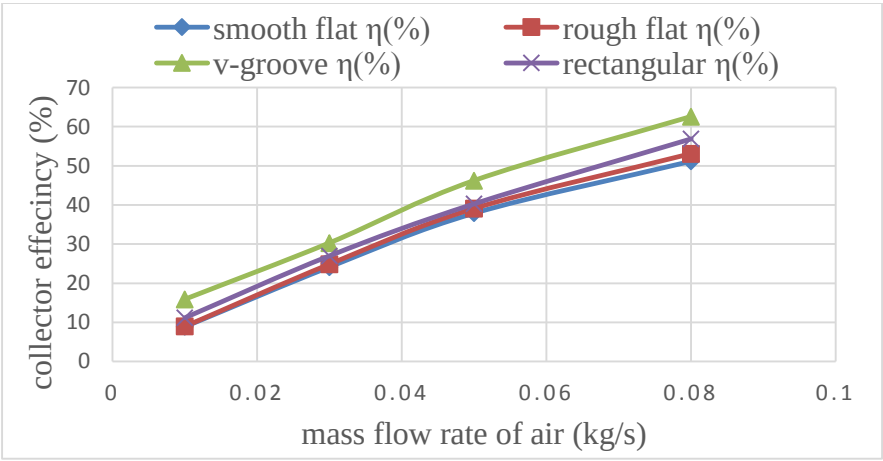

Figure 6.57. Comparing different geometry efficiency of the collectors with mass flow rate.

The efficiency of the collector could be seen from difference in temperature of the exit at the same inlet temperature of the air to the solar collector. In those dryer, by fully opening the inlet and the exit of the dryer, and different inlet of mass flow rate of the air a temperature within 10-25^{o}C higher than the ambient air temperature was recorded from the simulation results. However, for drying of the coffee the temperature was increased by increasing mass flow rate of the inlet air at different geometry of the dryer. Comparing figure 7.44 results based on collector efficiency quantitatively, V-groove collector has higher collector efficiency than any three collector dryers, and it was optimized collector.

The performance analyzed for a year through clear sunshine day has found the system average thermal efficiency of the dryer was determined to be 71%.

6.2.8. Validation

Table. 6.2. Experimental validation of collector

One cover flat plate collector	Experimental result reported [11]	% deviation
46.2 %	42%	9

Validation and verification focus on the comparison between the experimental results reported [11] and the CFD simulation results for solar flat plate collector. An output from the CFD solar absorber plate simulation has been run according to the same absorber configuration. A great agreement has been observed between the experimental results and the CFD collector efficiency predicted output with a deviation 9 %.

CHAPTER SEVEN

CONCLUSION AND RECOMMENDATION

7.1 CONCLUSION

An indirect forced type solar dryer to dry coffee parchment was designed and simulated. From the analytical result the thermal efficiency, moisture to be removed, drying time of solar drying system was affected by the properties of drying material, which is humidity and mass flow rate of air. A detained mathematical model derivation for the flat plate collector cross section (cover, air gap, absorber plate, air flow and insulation) was presented.

A CFD simulation to predict the effect of different parameters on solar collector dryer system to optimized thermal performance, pressure drop and back flow velocity air for different type of plate collector has been conducted. Thermal performance of the solar air heater was simulated at different air flow rates on four different types of flat plate collector configurations. From this collectors the v-grooved (corrugated) absorber plate collector was optimized. The maximum outlet air temperature of 52^{o}c and 44^{o}c was obtained from the v-grooved absorber plate collector for lowest (0.01kg/s) and highest (0.08kg/s) air flow rates, respectively.

The pressure drop and mean flow velocity of the solar air heater was simulated at different air flow rate on four different duct shape for the similar smooth flat plate collector configuration. The minimum pressure drop 0.0052pa and 0.1316pa was obtained from the diffuser collector with smooth curve for lowest (0.01kg/s) and highest (0.08kg/s) air flow rates, respectively. The pressure drop and recirculation flow velocity for smooth curve with collector diffuser and smooth curve with guide vanes configuration has lower than the other duct shape respectively. The dryer chamber pressure drop and recirculation velocity variations through trays chamber arrangement which has different gap has low pressure drop and back flow velocity stream than the allayment arrangement. It was more improve performance of solar dryer.

The effect of different air gap on the temperature outlet and pressure drop of different air flow rate for flat plate collector has been conducted. At air gap 0.05m the unit change of temperature outlet with pressure drop was more accepted. The direction of air flow through the collector was evaluated with in air flow pass above and below absorber plate collector. The maximum unit

change of temperature outlet with pressure drop is when the air flow pass below absorber plate of the collector.

The turbulence intensity effect on temperature outlet and pressure drop was simulated using the 2%, 5% and 10% with in the same flow rate of air and dryer profile. A better turbulence intensity was obtained when the unit change of temperature outlet air with pressure drop is high, that is when turbulence intensity was 2%. When predicted output compared with the CFD results a great agreement has been observed between the CFD and experimental predicted output.

7.2 Recommendations

- For prototype (construction) investigation of v-grooved type collector and smooth curve with guide vanes duct is more efficient for solar coffee dryer.
- The flow of air should be below the absorber plate collector and the arrangement of trays should different gap, then performance of dryer is more efficient and it possible for construction of dryer.

Reference

[1]. Berhanu.Ts, et.al; Effect of Sun Drying Methods and Layer Thickness on Quality of Selected Natural Arabica Coffee Varieties at Jimma, South west Ethiopia; Discourse Journal of Agriculture and Food Sciences,Vol. 3(9): pp, September, 2015

[2]. Tesfaye Meseret, Solomon T/mariam, and Muhidin Seid; Solar Tunnel Dryer Mathematical Modeling and Simulation for Coffee Drying in Harar, Research Gate, Conference Paper · 08 January, 2016.

[3]. Tefera Abera, and Prof. Dr.A. Venkata Ramayya, Simulation and Experimental Investigation on Active Solar Coffee Dryer, pp, 2013.

[4]. Visavale, G.L., Principles, Classification and Selection of Solar Dryers. In solar drying: Fundamentals, Applications and Innovations, Ed. Hii, C.L., Ong, S.P., Jangam, S.V. and Mujumdar, A.S., published in Singapore, pp, 2012,

https://www.researchgate.net/publication/264510127

[5]. Tiruwork Berhanu Tibebu, Design, construction and evaluation of performance of solar dryer for drying fruit, thesis, September 2015.

[6]. Feyza Akarslan. Solar-Energy Drying Systems, Modeling and Optimization of Renewable Energy Systems, Dr. ArzuŞencan (Ed.), InTech, Available from: http://www.intechopen.com /books/modeling-and-optimization-of-renewable-energy-systems/solar-energydrying-systemsand-applications, 2012

[7]. Umesh Toshniwal, S.R Karale. Review paper on Solar Dryer, International Journal of Engineering Research and Applications (IJERA), Vol. 3, pp, March -April 2013.

[8]. R. Vidya Sagar Raju et al. Design and Fabrication of Efficient Solar Dryer, International Journal of Engineering Research and Applications, Volume. 3, pp, Nov-Dec 2013.

[9]. Sandeep. P et al.; Design, Construction and Testing of Solar Dryer with Roughened Surface Solar Air Heater, paper, volume 7, July 2013.

[10]. A.S.Mujumdar, Handbook of Industrial Drying, [book], fourth edition Inc. New York and Basel, pp, 2015.

[11]. John A. Duffie,William A. Beckman Solar; Engineering of Thermal Processes [book],Fourth Edition, 2013.

[12]. Baloraj Basumatary, Mrinmoy Roy and, Dhwrwm Basumatary, Design, Construction and Calibration of Low Cost Solar Cabinet Dryer, International Journal of Environmental Engineering and Managemnt, Volume 4, pp. 351-358, Number 4 (2013).

[13]. Pranav C. Phadke et al. A review on indirect solar dryers, ARPN Journal of Engineering and Applied Sciences, vol. 10, no. 8, may 2015.

[14]. Aschenaki T**.** Feasibility Study and Performance Evaluation (Simulation) of Solar Dryer Hand Tools Share Company Molding Sand Drying Mechanism. Addis Ababa Institute of Technology (AAiT), thesis, 2011.

[15]. Abdulelah. A. et al .Design and Construction of a solar drying system for food preservation, senior project, 2014.

[16]. Ahmed Abed Gatea; Design, construction and performance evaluation of solar maize dryer; University of Baghdad, Iraq. March 2010; pp. 039-046.

[17]. Oguntola J. et.al Design and Construction of a Domestic Passive Solar Food Dryer, Leonardo Journal of Sciences, pp. 71-82, January-June 2010.

[18]. V. Chandrasekar; R. Viswanathan, Physical and Thermal Properties of Coffee, J. Agric. Engng Res. pp, 1909.

[19]. Tiruwork .B , Design, construction and evaluation of performance of solar dryer for drying fruit, thesis , Kwame Nkrumah University of Science ,September 2015.

[20]. Rona Niña, the bubble that dries, Rice today, International research institute vol. 13, no.1, January-march 2014.

[21]. Assefa .T et al., Performance Evaluation of Solar Tunnel Dryer for Ginger Drying, Journal of the 19th Annual Conference March, 2015**.**

[22]. S.Vijayan, and T.V.Arjunan, Performance Study of an Indirect Forced Convection Solar Dryer for Potato**,** International Journal of Applied Engineering Research, pp No.50, 2015.

[23]. Chabane F et al., Experimental study of heat transfer and thermal performance with longitudinal fins of solar air heater, Journal of Advanced Research, articles press (2013), http://dx.doi.org/10.1016/j.jare.2013.03.001

[24]. Bagheri, N. et al., Simulation and control of fan speed in a solar dryer for optimization of energy efficiency. Agricultural Engineering International: CIGR Journal, 14(1): 57－62. 2012.

[25]. Megha S. Sontakke and Prof. Sanjay P. Salve, Solar Drying Technologies: A review, International Refereed Journal of Engineering and Science (IRJES) Volume 4, PP.29-35, April 2015.

[26]. Yunus A. Cengel, John M. and Cimbala McGraw-Hill, Fluid Mechanics: Fundamentals and Applications, 2nd Edition, 2010.

[27]. Aklilu Tesfamichael; Experimental Analysis for Performance Evaluation of Solar Dryer, Addis Ababa University School of Graduate studies Department of Mechanical Engineering.

Appendix A

Raw data of the design and simulation

Table A.1. Raw data gathered from meteorological agency

No years	Maximum. Temperature (^{o}c)	Minimum temperature (^{o}c)	Relative humidity (%)	Radiation (w/m^2)	Sun shine hours (hrs)	Wind speed (m/s)
2012	27.75	11.71	68.13	543	8.75	2.37
2013	27.87	12.47	67.80	554.14	8.85	2.94
2014	27.28	11.75	73.01	509.87	8.89	2.44
2015	27.39	12.19	72.13	521.76	8.84	3.1
2016	27.56	11.85	67.78	504.87	9.53	3.1
Average	27.57	12.17	69.77	530.05	8.99	2.56

Appendix B

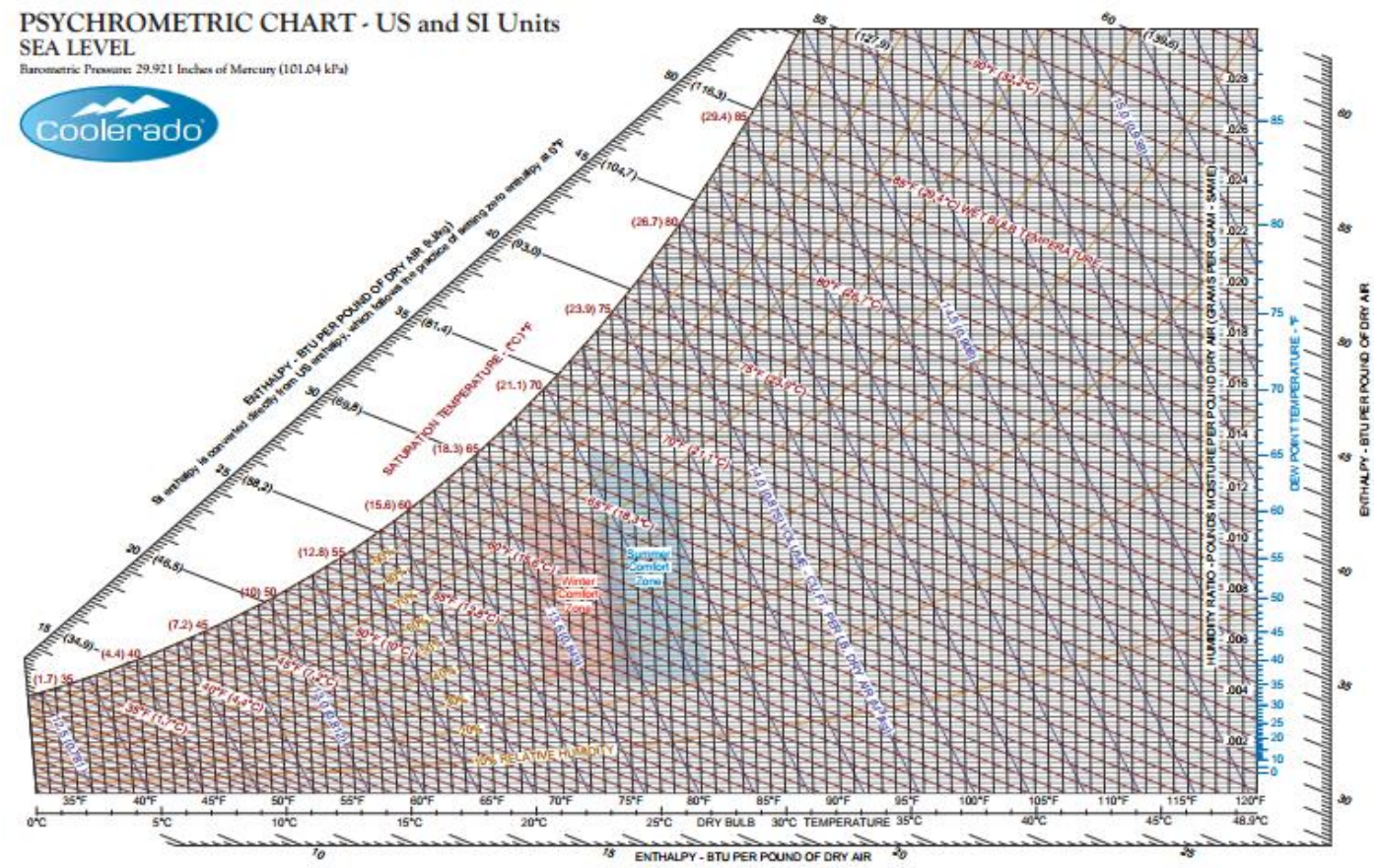

Figure B.1: Psychometric chart at 1 atm total pressure